Helices and Hamburgers from the Assembly of Linear ABC Triblock Copolymers in Block-Selective Solvents

by

JOHN ALBERT CHARLES DUPONT

A thesis submitted to the Department of Chemistry

in conformity with the requirements for

the degree of Doctor of Philosophy

Queen's University

Kingston, Ontario, Canada

April, 2010

Abstract

This Ph.D. thesis reports the discovery and study of several morphologies of ABC triblock copolymer assemblies in block selective solvents. One block copolymer self-assembled into helices (mostly double and some triple helices), and the other block copolymer formed a mixture of structures resembling hamburgers and striped cylinders.

The helices, biomimmetic structures which are unusual from block copolymer self-assembly, were prepared from the triblock copolymer poly(*n*-butyl methacrylate)-*block*-poly(2-cinnamoyloxyethyl methacrylate)-*block*-poly(*tert*-butyl acrylate) (PBMA-*b*-PCEMA-*b*-PtBA). They were formed spontaneously in several binary solvent mixtures including dichloromethane/methanol, tetrahydrofuran (THF)/methanol, and chloroform/methanol. They were formed in the composition ranges where the mixtures were good for the PtBA block, poor for the PCEMA block, and marginal for the PBMA block. The structure was studied and established by TEM, AFM, DLS and ^{1}H NMR and by TEM tomography. The mechanism and kinetics of helix formation was examined.

The Hamburger and striped cylinder structures were produced from poly(*tert*-butyl acrylate)-*block*-poly(2-cinnamoyloxyethyl methacrylate)-*block*-poly(succinated glyceryl monomethacrylate) or (PtBA-*b*-PCEMA-*b*-PSGMA) in mixtures of THF, (-)-sparteine and 1- or 2-propanol. Here THF solubilized all the blocks of the copolymer, while propanol was a precipitant for the middle block

(PCEMA), and the chiral amine, (-)-sparteine, complexed with PSGMA and made it insoluble. Within the Hamburger-like structure, the “filling” was made of the complexed PSGMA chains and the "buns" were made of PCEMA. The striped cylinders were made of stacking alternating PCEMA and PtBA stubs. The PtBA chains were located on the outer surfaces of both of these structures. With the hamburger structures, after PCEMA crosslinking, we were able to remove the chiral amine by dialysis and make the PSGMA chains soluble again in solvents such as *N*, *N*-dimethylformamide. The hamburgers were thus separated into two halves, with each half existing as a Janus particle, which had PtBA chains on one side and PSGMA chains on the other side. The Janus particles might have interesting applications, such as in Pickering emulsion stabilization.

Acknowledgements

I wish to express my sincere appreciation to Dr. Guojun Liu for all of his guidance, support and patience over the last several years without which I would not be where I am today. I appreciate all the hard work and direction that he has provided, as well as for his taking a chance on someone who may not have been the best candidate for the job.

I would also like to thank all of the post-docs that have helped contribute to my development over the years: Dr. Xiaohu Yan, Dr. Ronghua Zheng, Dr. Gabriel Njikang, Dr. Kyoungmoo Koh and Dr. Dehui Han. I would also like to express my thanks to all of the other Liu Group graduate students who have helped contribute ideas and support: Zhihan Zhou, Scott Curda, Nan Wang, Gao Yang, Xiaoyu Li, Qiliang Peng. I would like to also express my appreciation for my lab benchmate Heng Hu. I also would like to express my appreciation for Jian Wang and all the other group members not mentioned here.

I would also like to thank my sister, Andrea for all of her help in editing and all her encouragement while she is following her dreams. I would also like to express my appreciation for my parents, Chris and Margaret, for all their loving help and support and my brother Dave for the example he has set. I really could not have done it without my family.

I would like to express my appreciation for Irene Kwan for all her support. I would like to thank Ian Wyman for his help with final editing. Finally I would like to thank my friends and all the graduate students, faculty and support staff in the Department of Chemistry for their support along the way.

Statement of Co-Authorship and Originality

All the results presented in this thesis, *Helices and Hamburgers from the Assembly of Linear ABC Triblock Copolymers in Block-Selective Solvents*, were conducted by the author under the supervison of Professor Guojun Liu. All results are the product of orginial research, with the exception of the TEM tomography results and associated measurements on the helices in Chapter 2 which were made by **Ken-ichi Niihara** and **Hiroshi Jinnai** of the Department of Macromolecular Science & Engineering, Graduate School of Science & Engineering*, Kyoto Institute of Technology, Matsugasaki, Kyoto, Japan*. The specific contributions made in this thesis are outlined below:

1. The preparation and study of block copolymer multihelices produced by the use of a mixed solvent system (Chapter 2).

2. The determination of the exact structure of a block copolymer helix (Chapter 2).

3. The preparation and study of Hamburger and striped cylinder aggregates produced by amine complexation in a mixed solvent system (Chapter 3).

4. The use of Hamburger-like aggregates as a template for the formation of Janus-type particles (Chapter 3).

Table of Contents

List of Tables

List of Figures

List of Schemes

List of Abbreviations

^{1}H NMR	proton NMR
1-Pro	1-propanol
2-D	two dimensional
2-Pro	2-propanol, isopropanol
3-D	three dimensional
Å	ångstrom (1 Å = 10^{-10} m)
Ac	acetyl group
AFM	atomic force microscopy
CA	chiral amine ((-)-sparteine)
$CHCl_3$	chloroform
COOH	carboxylic acid
d-DCM	deuterated dichloromethane (CD_2Cl_2)
d-MeOH	deuterated methanol (CD_3OD)
DCM	dichloromethane
d_h	hydrodynamic diameter
DLS	dynamic light scattering
dn_r/dc	specific refractive index increments
d_{TEM}	TEM diameter
e.g.	example
eV	electron volt
f_{MeOD}	fraction of deuterated methanol
f_{MeOH}	fraction of methanol
f^*_{MeOH}	critical methanol fraction
f_{Pro}	fraction of 1- or 2-propanol
f^*_{Pro}	critical fraction of 1- or 2-propanol
HCl	hydrochloric acid
ie	in example
I_X	relative peak intensity
kV	kilovolt
kHz	kilohertz
LS	light scattering
M	mol / litre
MA	micelle-like aggregate
MAs	micelle-like aggregates
MeOD	deuterated methanol
MeOH	methanol
mg	milligram
MHz	megahertz
mL	millilitre
mol%	molar percent
MPa	megapascal

M_w/M_n	polydispersity index
η	viscosity
nm	nanometre (1 nm = 10^{-9} m)
NMR	nuclear magnetic resonance
n_r	refractive index
OsO_4	osmium tetraoxide
PBMA	poly(n-butyl methacrylate)
PBMA-*b*-PCEMA-*b*-PtBA	poly(n-butyl methacrylate)-*block*-poly(2-cinnamoyloxyethyl methacrylate)-*block*-poly(*tert*-butyl acrylate)
PCEMA	poly(2-cinnamoyloxyethyl methacrylate)
PCEMA-*b*-PtBA	poly(2-cinnamoyloxyethyl methacrylate)-*block*-poly(*tert*-butyl acrylate)
PGMA	poly(glyceryl methacrylate)
ppm	parts per million
PS-*b*-PAA	poly(styrene)-*block*-poly(acrylic acid)
PSGMA	poly(succinated glyceryl monomethacrylate)
PSMA	poly(solketal methacrylate)
PtBA	poly(*tert*-butyl acrylate)
PtBA-*b*-PCEMA-*b*-PSGMA	poly(*tert*-butyl acrylate)-*block*-poly(2-cinnamoyloxyethyl methacrylate)-*block*-poly(succinated glyceryl monomethacrylate)
PTFE	poly(tetrafluoro ethylene)
r	molar ratio
RuO_4	ruthenium tetraoxide
RT	room temperature (typically 20 ^oC)
SMAs	spherical micelle-like aggregates
SEC	size-exclusion chromatograph
TEM	transmission electron microscopy
THF	tetrahydrofuran
µm	micrometer (1 µm = 10^{-6} m)
$UO_2(Ac)_2$	uranyl acetate
UV	ultraviolet
vol%	volume percent
vs	versus
W	watt
wks	weeks

Chapter 1 – Introduction

This thesis studies the assembly of linear ABC triblock copolymers in block-selective solvents. These block copolymers assemble to make interesting structures on the nano-scale. Chapter 2 will discuss the self-assembly of an ABC triblock copolymer to form double and triple helices in block-selective solvents. The assembly of an ABC triblock copolymer under the influence of a diamine to form Hamburger and striped cylinder aggregates will be the subject of discussion in Chapter 3. This chapter will introduce some relevant background material for the research. Included is the definition of block copolymers, block copolymer aggregation (and the uses of block-selective solvents), assembly (self-assembly and directed assembly), and chemical modification.

1.1 Block Copolymers

Block copolymers are macromolecules made of two or more distinct polymers that are covalently joined together. Linear triblock copolymers are polymers that have three such blocks joined linearly in a head-to-tail fashion (see Scheme 1.1).

Block copolymers can be made with different architectures. These include linear, branched, star, *mikto*-arm and graft. Block copolymers can also be made with varying numbers of blocks: diblock (2), triblock (3), tetrablock (4), for example.

Block copolymers can be used for a number of possible applications including self-assembly to make nanosized objects,[1-2] creation of membranes,[3] and for

drug delivery systems.[4-5] The self-assembly of block copolymers can yield a variety of architectures including nanospheres, nanofibers, nanotubes, among other structures.[1-2] Block copolymers can also be used to make membranes that have pores on the nanoscale. Finally, block copolymers can be used in drug delivery applications, to either supply a drug at a steady rate, or to a specific location inside the body of the patient.

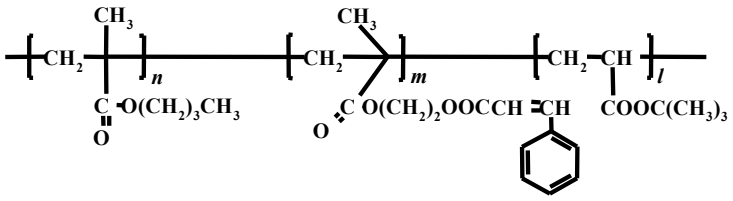

Scheme 1.1. Structure of a linear ABC triblock copolymer (PBMA-*b*-PCEMA-*b*-PtBA), used in Chapter 2.

1.2 Block Copolymers in Block-Selective Solvents

1.2.1 Solvent Quality

Many polymers readily dissolve in liquid media. If a significant amount of a polymer dissolves in a solvent it is said to be good for the polymer. Better solvents will dissolve larger amounts of the polymer. Conversely, poor solvents do not dissolve significant amounts of a given polymer, and can cause precipitation of the polymer if the poor solvent is added to a polymer solution. Marginal solublility conditions are defined as the point where a given polymer starts to precipitate from a given polymer solution. For example, when you dissolve a polymer in a good solvent and then slowly add a poor solvent under vigorous stirring, the point at which precipitation starts to occur is said to be marginal.

1.2.2 Diblock Copolymers in Block-Selective Solvents

Block copolymers have been seen to self-assemble to form aggregates with a number of different morphologies in block-selective solvents.[6-8] In order to form dispersed aggregates, the copolymer is dissolved in a solvent that is a good solvent for all blocks, and then a poor solvent for one of the blocks is added. This causes one block to aggregate, while the other block remains well solvated and keeps the structure dispersed.

The simplest and most commonly studied block copolymers are AB diblock copolymers. The most common morphologies of micelles formed from AB diblock copolymers (Figure 1.1) are spherical micelles, cylindrical micelles, and vesicles.[6] In these systems, typically, solvent mixtures are used that constitute a good solvent for one block and a poor solvent for the second block. Eisenberg *et al.*[6-8] have done extensive work on these systems. They have found that poly(styrene)-*block*-poly(acrylic acid) (PS-*b*-PAA) can form a number of different morphologies as the relative block lengths are changed under different conditions. As the soluble block is shortened to a fixed length relative to the insoluble block, the morphology changes from spheres (Figure 1.1A), to cylinders (Figure 1.1B), to vesicles (Figure 1.1C), and finally to large compound micelles (Figure 1.1D). This morphology change is due to the change in the size ratio of the insoluble and soluble block. Similar morphological changes have been seen

due to factors such as solvent composition changes, polymer concentration, ion content, among others.[8]

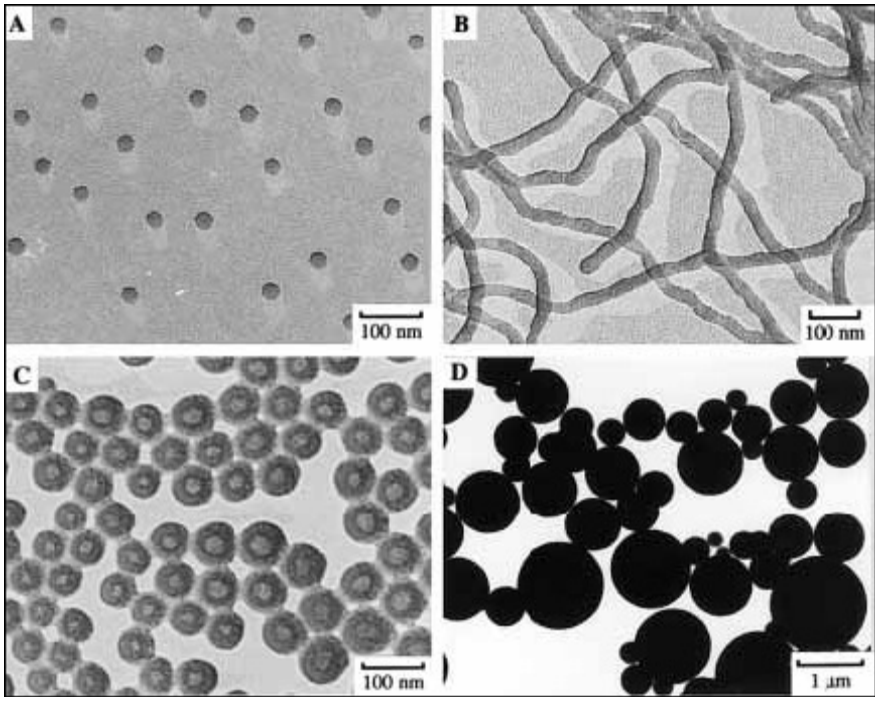

Figure 1.1. Common morphologies produced by an AB diblock copolymer (taken from reference 8):[8] (A) spheres from PS_{500}-*b*-PAA_{58}, (B) rod-like micelles from PS_{190}-*b*-PAA_{20}, (C) vesicles from PS_{410}-*b*-PAA_{20} and (D) large compound micelles from PS_{200}-*b*-PAA_{4}.

1.2.3 Linear ABC Triblock Copolymers in Block-Selective Solvents

ABC triblock copolymers have more complexity in their structure than diblock copolymers because they contain three distinct blocks. Since this thesis focuses on linear ABC triblock copolymers, other polymers (ABA, *mikto*-arm or star) will not be discussed here. Linear ABC triblock copolymers can form a much larger diversity of morphologies compared to AB diblock copolymers, which are facilitated through solvent choice.

Table 1.1 lists some possible block-selective solvent combinations for linear ABC triblock copolymers. The triblock copolymers in solvent systems 1, 2, 4, and 5 produce most likely core-shell-coronal structures with similar characteristics to AB diblock copolymers. Solvent system 3 leads to either phase separated coronal chains if the blocks are highly incompatible, or mixed coronal chains if the solvated blocks are compatible.

Table 1.1. Linear ABC triblock copolymer, block-selective solvent combinations.

Solvent System	Block A	Block B	Block C
1	Poor	Good	Good
2	Good	Good	Poor
3	Good	Poor	Good
4	Good	Poor	Poor
5	Poor	Poor	Good
6	Poor	Good	Poor

The use of solvent system 6 will lead to micelles with a looped central block tethered at both ends to the core.[9] The insoluble blocks should phase separate to form the core of these particles. At high concentrations, the A and C blocks can be incorporated into different micellar cores, resulting in a network structure.[9]

It is also possible with ABC triblock copolymers to target solvent systems where one of the blocks is marginally soluble, by changing the ratio of good to poor solvents in the solvent system. The use of marginally soluble blocks is interesting, because solvent composition can be used to control the degree of swelling (by tuning the solvent composition) of this marginally soluble block and this can be used to control the collapse of this marginally soluble block.[10]

Table 1.2 lists some possible linear ABC triblock copolymer-solvent combinations where at least one block has marginal solubility. In these systems the poorly soluble block should form the core of the aggregates, while the well solvated block should serve to stabilize these structures. The marginally soluble block of the copolymer may be located at the interface between the poorly soluble block and the well solvated block depending on the system. The self-assembly of an ABC triblock copolymer in solvent system 12 was studied and it was discovered that the copolymer self-assembled into helices in this solvent system. This system will be discussed in Chapter 2.

Table 1.2. Possible linear ABC triblock copolymer marginally soluble block combinations.

Solvent System	Block A	Block B	Block C
7	Poor	Marginal	Good
8	Good	Marginal	Poor
9	Poor	Good	Marginal
10	Marginal	Good	Poor
11	Good	Poor	Marginal
12	Marginal	Poor	Good
13	Good	Marginal	Marginal
14	Marginal	Marginal	Good
15	Marginal	Good	Marginal
16	Poor	Marginal	Marginal
17	Marginal	Marginal	Poor
18	Marginal	Poor	Marginal

The cases where two blocks are marginally soluble (solvent systems 13-18) are included for completeness in Table 1.2. However, either the aggregates of these systems will not have a well structured core (lacking a poorly soluble block), or they will not be readily dispersed (lacking a well solvated block). This last case may be impractical because without a soluble block the polymer may precipitate.

In practice all possibilities with two marginally soluble blocks might have limited application in linear ABC triblock systems, because most polymers have different solubility limits, depending on solvent systems. Similar solubilities are possible when using ABA triblock copolymers in place of ABC triblock copolymer systems.

1.2.4 The Use of Complexing Agents in Block Copolymer Aggregation

Complexing agents (such as amines) can be used in block copolymer systems to induce aggregation in a system where it would not otherwise occur. Aggregation may be due to different forces (including electrostatic, charge complex formation, or other forces) and is typically reversible unless covalent bonds are formed.

Complexation has occurred between metal ions and polyacids, to prepare aggregates of approximately 100 nm.[11] Polyamines have been combined with DNA to make micelle-like aggregates (MAs).[12-13] Block copolymers containing polyamines have been combined with block copolymers containing polyacids to make MAs by complex formation.[14-15] Block copolymers containing polyamines and polyacids have also been combined with synthetic homopolymers (either polyacid or polyamine) to form MAs by complex formation.[16]

1.2.5 The Use of Complexing Agents in AB Diblock Copolymer Aggregation

Complexation in AB diblock systems can lead to MA formation. This is the most studied type of complexation among block copolymers, because AB diblock copolymers are the simplest type of block copolymer. Complexation of AB

diblock copolymers will form a number of different morphologies, including spherical MAs, cylindrical MAs, and vesicles.[17]

1.2.6 The Use of Complexing Agents in Linear ABC Triblock Copolymer Aggregation

Complexation can also be used in linear ABC triblock copolymer systems to produce MAs of different types. Complexation can also introduce another degree of control when working with these block copolymer systems. Aggregate formation by complexation can be reversible if a method exists that allows the reversible disintegration and formation of the complexes.

Table 1.3. Possible linear ABC triblock copolymer solvation conditions where one block is complexed.

Solvent System	Block A	Block B	Block C
20	Complexed	Good	Good
21	Good	Good	Complexed
22	Good	Complexed	Good
23	Complexed	Poor	Good
24	Good	Poor	Complexed
25	Good	Complexed	Poor
26	Poor	Complexed	Good
27	Complexed	Marginal	Good
28	Good	Marginal	Complexed
29	Good	Complexed	Marginal
30	Marginal	Complexed	Good

In linear ABC triblock copolymer systems, one can use both state of solvation (good, poor or marginal) and complexation to form aggregates (see Table 1.3). Similar to aggregate formation in block-selective solvents, one block of the copolymer should remain soluble, so that the newly formed aggregates remain well dispersed in the system. Complexation can be done either before or after

the addition of the poor solvent to the system. This may allow for the formation of different architectures in the same system when producing nanoaggregates.

Aggregate formation becomes more complicated when block-selective solvents are used as well as complexation. It is possible to produce structures that will exhibit phase separation in the core of the aggregates due to the collapse of multiple blocks (solvent systems 23-26). Chapter 3 will discuss examples of morphologies of a linear ABC triblock copolymer dispersed in solvent system 24.

Aggregate formation by complexation can also include the use of a marginally soluble block (solvent systems 27-30). In these systems the complexed block should form the core of the aggregates, while the marginal block should be at the interface, with the soluble block stabilizing the structures. This may lead to some interesting structures that have some tunable properties due to the marginal solubility of that block.

1.3 Chemical Modification in Block Copolymer Nanostructures

Chemical modification can transform block copolymer nanostructures into new and interesting structures by changing the molecular properties of the block(s). Chemical modifications can include: the creation of permanent structures (through block cross-linking),[18-19] sculpted structures (through block degradation),[20] the creation of hybrid structures (introduction of inorganic materials into templates),[21] double assembly[22] and the coupling of different nanostructures.[23] Using chemical processing, we can create patterned

structures including Janus particles and membranes with nanochannels among other structures.[24-26]

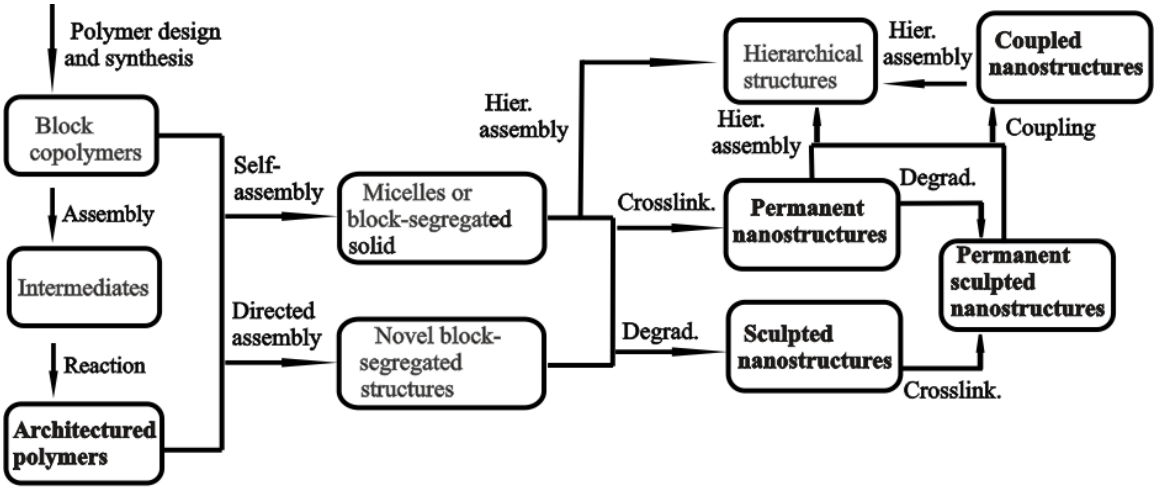

Scheme 1.2. Methodology showing assembly techniques using block copolymers that prepare various nanostructures.[27]

Permanent structures are created from previously prepared structures using various chemical and/or photochemical methods by the cross-linking of one block of the copolymer.[18-19] Block copolymer degradation through block degradation can be used to make sculpted nanostructures including nanotubes,[20] hollow nanospheres[20] and the nanopatterning of a surface.[28] Hybrid nanostructures can be created by the incorporation of different inorganic materials into template block copolymer nanostructures.[21] Hierarchical-assembly involves the assembly of previously created nanostructures (including double assembly).[22] Coupling can also be used to create new nanostructures by combining two or more structures to make a new one.[23] The creation of patterned nanostructures of block copolymer systems, including Janus particles and membranes with nanochannels, have been created using self-assembly and other techniques.[24-26]

Scheme 1.2 shows the methodology mentioned above. All of these structures can be further modified to make more complex structures.

1.3.1 The Creation of Permanent Block Copolymer Nanostructures

Typically, block copolymer nanostructures are formed by self-assembly in solution or in bulk phase. These structures can be used as created, or their properties (chemical nature, properties or other features) may be changed for their final application. It is useful to create permanent nanostructures from self-assembled transient structures, so that post-production modification can be done. This allows for the use of solvents and other reactants that would otherwise degrade the transient nanostructures. One popular method is to cross-link one block of the copolymer in these structures to stabilize or lock in the structure.[18-19] This crosslinking can be done by chemical,[29] photochemical,[18-19] or other methods.

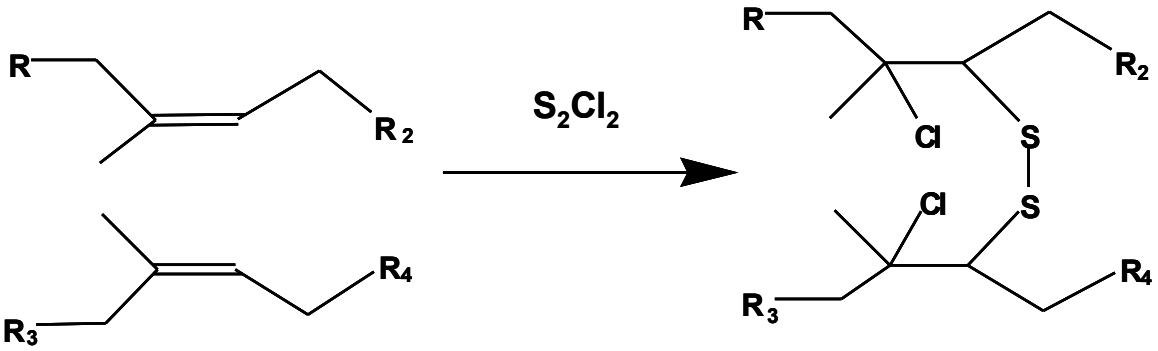

Scheme 1.3. Crosslinking reaction of polyisoprene by sulfur monochloride to form a sulfide bridge, an example of chemical cross-linking.[30]

Chemical cross-linking can be done by the cross-linking of isoprene with sulfur monochloride (Scheme 1.3) to form a sulfide bridge, which can stabilize the desired nanostructures.[30]

Permanent nanostructures can also be made by photochemically cross-linking one of the blocks (Scheme 1.4),[18-19] which is a convenient way to produce structures that may degrade if they are exposed to harsh chemicals before cross-linking. Photochemical methods will be used in Chapter 3 to make a permanent nanostructure, which will then be further chemically modified.

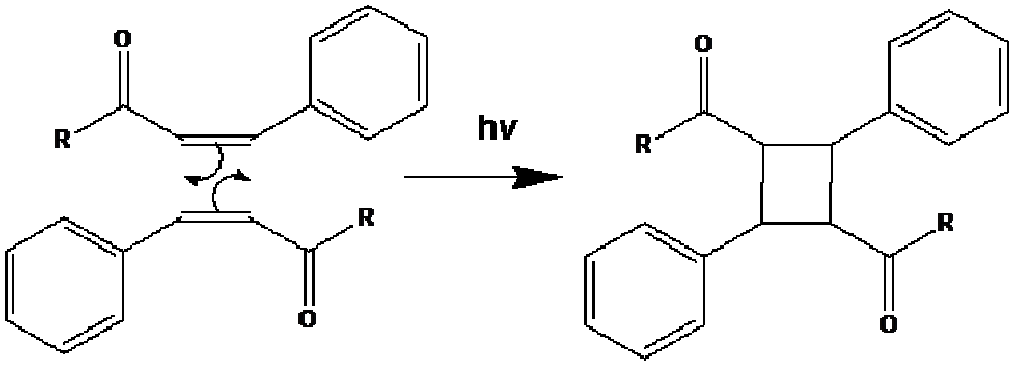

Scheme 1.4. Photochemical dimerization of poly(2-cinnamoyloxyethyl methacrylate) to form a cross-linked structure after exposure to UV light.

1.3.2 The Sculpting of Nanostructures through Block Degradation

Block copolymer nanostructures that have been created by self-assembly can be sculpted by the degradation of one of the blocks of the copolymer. This is usually done after block cross-linking. Block copolymer degradation can be used to make nanotubes,[20] hollow nanospheres[20] and nanopatterned surfaces.[28]

One method for nanosculpting is the degradation of the poly(isoprene) block by ozonolysis to remove the block from the nanostructure. This has been used by Liu *et al.* to make hollow nanotubes and nanospheres.[20] Block degradation can also be used to provide a nanopattern on a surface. Boker *et al.* thermally degraded fluorinated side chains that provided a laterally patterned surface.[28]

1.3.3 The Creation of Patterned Block Copolymer Nanostructures

Patterned block copolymer nanostructures can be created by various methods. Recent advances have allowed the production of different types of particles including Janus particles,[24] membranes with nanochannels,[25] patched particles,[26] patterned surfaces,[31] and vesicles with different interior and exterior functionality.[32]

One type of patterned nanostructure produced from block copolymers is patched particles, which includes spheres with patched surfaces.[26] A second type of patterned structure is patterned surfaces.[31] Several groups have synthesized vesicles with varying interior and exterior functionality.[32-34] Njikang *et al.* have studied the partitioning of different chains on the surface of vesicles.[32-34] Janus-type particles are an interesting type of patterned nanostructure that has been synthesized by various groups.[24] A new synthetic route to the production of Janus particles is shown in Chapter 3.

1.3.4 The Creation of Hybrid Block Copolymer Nanostructures

Block copolymers combined with inorganic materials create hybrid materials. The creation of hybrid nanostructures of block copolymers can involve the reaction of block copolymer nanostructures with inorganic nanoparticles,[21] or the use of block copolymer structures to template the formation of nanostructures.[21]

Hybrid nanostructures are made by the combination of block copolymer structures with other nanostructures. Inorganic particles, including cobalt or iron oxide nanoparticles, can be made using block copolymers as surfactants to produce magnetic spheres.[35-36] Inorganic particles can also be incorporated into the domains of block copolymer morphologies, such as nanospheres or nanotubes.[37-40] Block copolymers can also be used to template the formation of inorganic structures by the use of patterned surfaces to produce inorganic patterned surfaces,[41] or by pyrolysis to produce nanoporous carbon.[42]

1.3.5 Composite Structures from Block Copolymer Nanostructures

Block copolymers have also recently been used to create more complex structures by various methods. These methods include: hierarchical-assembly (double assembly to form cage-type structures),[23] coupling of multiple nanostructures together (to form a new and more complex structure),[22] and the complexation of block copolymers with various agents[17] (as discussed previously in sections 1.2.4, 1.2.5 and 1.2.6).

Hierarchical-assembly includes double assembly, which initially involves the assembly of one structure, followed by the further assembly to form a more complex structure. This type of assembly has been used to make cage-type structures.[23] It is also possible to make different types of nanostructures, and then couple them together by reaction of the functional groups on their surfaces. Coupling techniques can be used to functionalize different nano-objects.[22] These coupled structures can also be used to further assemble into larger and more complicated structures, such as super micelles.[43]

1.4 Thesis Objectives

This thesis will examine two different morphologies that were found during the examination of two different block copolymers that were dispersed in different solvent systems. One system that was studied produced a helical morphology from a linear ABC triblock copolymer. This system will be discussed in Chapter 2. The second system that will be discussed produced both a Hamburger-type and striped cylinder morphology, also from a linear ABC triblock copolymer. This second system will be discussed in Chapter 3.

The objective of the first phase of the project was to study a helix formed by an ABC linear triblock copolymer. The helix morphology was obtained using poly(*n*-butyl methacrylate)-*block*-poly(2-cinnamoyloxyethyl methacrylate)-*block*-poly(*tert*-butyl acrylate) (PBMA-*b*-PCEMA-*b*-PtBA as shown in Scheme 1.5) in a solvent system where the first block was marginally soluble, the second block was

insoluble, and the final block was soluble. The helix morphology is extensively studied, including, the evaluation of the dynamics of the structural change, and the dimensions of these MAs. We also propose that helices are the most thermodynamically stable structure for this ABC triblock copolymer in this solvent system.

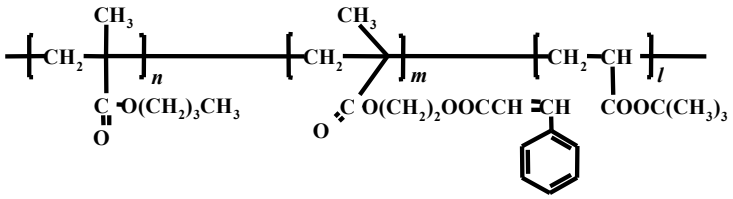

Scheme 1.5. Structure of PBMA-*b*-PCEMA-*b*-PtBA the ABC triblock copolymer used in Chapter 2 to make helices.

The objective of the second section of the project was to study the structures formed by a linear ABC triblock copolymer, including both Hamburger-type and segmented cylinder aggregates. This morphology was formed using poly(*tert*-butyl acrylate)-*block*-poly(2-cinnamoyloxyethyl methacrylate)-*block*-poly(succinated glyceryl monomethacrylate) (PtBA-*b*-PCEMA-*b*-PSGMA, as shown in Scheme 1.6) in a solvent system where the first block was soluble, the second block was insoluble, and the final block was complexed with (-)-sparteine (a hindered chiral diamine) to form an insoluble phase. An extensive study of this morphology was done, including the mechanism and kinetics of formation, as well as the dimensions of the MAs. We include possible reasons for the formation of this ABC triblock copolymer morphology, including the fact that it is a kinetically trapped, as opposed to a thermodynamically stable, morphology. We also chemically modified this structure first to make a permanent structure, and

then later to form Janus-type particles. This is a simple and novel way to produce Janus-type particles, which can be used as molecular building blocks and for further assembly.

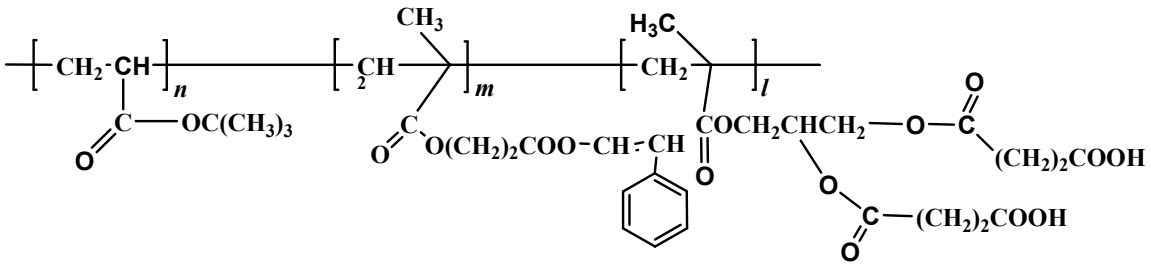

Scheme 1.6. Structure of PtBA-*b*-PCEMA-*b*-PSGMA the ABC triblock copolymer used in Chapter 3 to make Hamburger-type and striped cylinder aggregates.

1.5 References

1. Cameron, N.; Corbierre M.; Eisenberg, A. *Can. J. Chem.* **1999,** 77, 1311-1326.

2. Ding, J.; Liu G.; Yang, M. *Polymer,* **1997,** 38, 5497-5502.

3. Lee, J.; Hirao, S.; Nakahama, S. *Macromolecules,* **1989,** 22, 2602-2606.

4. Adams, M.; Lavansanifar, A.; Kwon, G. *J. Pharm. Sci.* **2003,** 92, 1343-1355.

5. Kataoka, A.; Harada, A.; Nagasaki, Y. *Adv. Drug Deliver. Rev.* **2001,** 47, 113-131.

6. Zhang, L.; Eisenberg, A. *J. Am. Chem. Soc.* **1996,** 118, 3168-3181.

7. Lysenko, E.; Bronich, T.; Slonkina, E.; Eisenberg, A.; Kabanov, V.; Kabanov, A. *Macromolecules,* **2002,** 35, 6351-6361.

8. Zhang, L.; Eisenberg, A. *Polymers for Advanced Technologies,* **1998,** 9, 677-699.

9. Hillmyer, M.; Lodge, T. *J. Pol. Sci. Part A: Pol. Chem.* **2001,** 40, 1-8

10. Weaver, J.; Bannister, I.; Robinson K.; Bories-Azeau, X.; Armes, S.; Smallridge, M.; McKenna, P. *Macromolecules,* **2004,** 37, 2395-2403.

11. Li, Y.; Gong, Y.-K.; Nakashima, K. *Langmuir,* **2002,** *18,* 6727-6729.

12. Kataoka, K.; Togawa, H.; Harada, A.; Yasugi, K.; Matsumoto, T.; Katayose, S. *Macromolecules,* **1996,** *29,* 8556-8557.

13. Kataoka, K.; Harada, A.; Wakebayashi, D.; Nagasaki, Y. *Macromolecules,* **1999,** *32,* 6892-6894.

14. Harada, A.; Kataoka K. *Macromolecules,* **1995,** 28, 5294-5299.

15. Gohy, J.-F.; Varshney, S.; Jérôme, R. *Macromolecules,* **2001,** *34,* 3361-3366.

16. Zintchenko, A.; Dautzenberg, H.; Tauer, K.; Khrenov V. *Langmuir,* **2002,** *18,* 1386-1393.

17. Bronich, T.; Kabanov, A.; Kabanov, V.; Yu, K.; Eisenberg, A. *Macromolecules,* **1997,** 30, 3519-3525.

18. Guo, A.; Liu, G.; Tao, J. *Macromolecules,* **1996,** 29, 2487-2493.

19. Liu, G.; Qiao, L.; Guo, A. *Macromolecules,* **1996,** 29, 5508-5510.

20. Liu, G.; Stewart, S. *Poly. Mat. Sci. Eng.* **1999,** 81, 10-11.

21. Sankaran, V.; Cummins, C.; Schrock, R.; Cohen, R.; Silbey, R. *J. Am. Chem. Soc.* **1990,** 112, 6858-6859.

22. Liu, G.; Yan, X.; Li, Z.; Zhou, J.; Duncan, S. *J. Am Chem. Soc.* **2003,** 125, 14039-14045.

23. Hu, J.; Liu, G.; Nijkang, G. *J. Am. Chem. Soc.* **2008,** 130, 3236-3237.

24. Walther, A.; Dreschsler, M.; Rosenfeldt, S.; Harnau, L.; Ballauff, M.; Abetz, V.; Műller, A. *J. Am. Chem. Soc.* **2009,** 131, 4720-4728.

25. Liu, G.; Ding, J. *Adv. Mater.* **1998,** 10, 69-71.

26. Zheng, R.; Liu, G.; Yan, X. *J. Am. Chem. Soc.* **2005,** 127, 15358-15359.

27. Unpublished scheme prepared by Dr. Guojun Liu.

28. Boker, A.; Herweg, T.; Reihs, K. *Macromolecules,* **2002,** 35, 4929-4937.

29. Ishizu, K.; Ikemoto, T.; Ichimura, A. *Polymer,* **1999,** 40, 3147-3151.

30. Yan, X.; Liu, G.; Li, H. *Langmuir,* **2004,** 20, 4677-4683.

31. Russell, T. *Curr. Opin. Col. Inter. Sci.* **1996,** 1, 107-115.

32. Luo, L.; Eisenberg, A. *Angew. Chem. Int. Ed.* **2002,** 41, 1001-1004.

33. Njikang, G.; Han, D. H.; Wang, J.; Liu, G. J. *Macromolecules,* **2008,** 41, 9727-9735.

34. Njikang, G.; Kwan, I.; Wu, G.; Liu, G. *Polymer,* **2009,** 50, 5262-5267.

35. Platonova, O.; Bronstein, L.; Solodovnikov, S.; Yanovskaya, I.; Obolonkova, E.; Valetsky, P.; Wenz, E.; Antonietti, M. *Colloid & Polym. Sci.* **1997,** 275, 426-431.

36. Liu, G.; Yan, X.; Lu, Z.; Curda, S.; Lal, J. *Chem. Mater.* **2005,** 17, 4985-4991.

37. Bockstaller, M.; Kolb, R.; Thomas, E. *Adv. Mater.* **2001,** 13, 1783-1786.

38. Zhou, Z.; Liu, G.; Han, D. *ACS Nano,* **2009,** 3, 165-172.

39. Underhill, R.; Liu, G. *Chem. Mater.* **2000,** 12, 2082-2091.

40. Yan, X.; Liu, G.; Liu, F.; Tang, B.; Peng, H.; Pakhomov, A.; Wong, C. *Angew. Chem. Int. Ed.* **2001,** 40, 3593-3596.

41. Park, M.; Harrison, C.; Chaikin, P.; Register, R.; Adamson, D. *Science,* **1997,** 276, 1401-1404.

42. Kowalewski, T.; Tsarevsky, N.; Matyjaszewski, K. *J. Am. Chem. Soc.* **2002,** 124, 10632-10633.

43. Yan, X.; Liu, G.; Li, Z. *J. Am. Chem. Soc.* **2004,** 126, 10059-10066.

Chapter 2 – Helical Morphology made by an ABC Triblock Copolymer in a Mixed Solvent System.

2.1 Preface

The material in this chapter has been published as, **Self-Assembled ABC Triblock Copolymer Double and Triple Helices**, in *Angewandte Chemie, International Edition*, 2009, 48, 6144-6147.

2.2 Introduction

Many block copolymers self-assemble into various structures in block selective solvents. These structures can include spheres,[1] vesicles,[2-5] nanotubes,[6-8] and cylinders. They are the result of the insoluble blocks of the copolymer aggregating to form micelle-like aggregates (MAs) stabilized by the soluble blocks, etc. The composition of the block copolymer, the interfacial tension between the solvent and the insoluble block and other factors determine the morphology of these systems.

The cylinder structures can be linear,[9,10] branched,[11] looped,[3,12,13] and segmented.[14,15] Occasionally, cylinders may exhibit secondary structures, such as cylinder helices, or segmented cylinders. Diblock copolymers containing a chiral block can produce cylinders that twist into single-handed helices, due to the orientation in the cylinder cores.[16,17] Achiral ABC triblock copolymers have recently been shown to self-assemble in block-selective solvents into cylinder

helices[18] or twisted cylinders with helical sections[19] due to the interplay of unique surface forces.

While there have been no reports of cylinder helix formation from achiral diblock copolymers in block selective solvents, and such reports have been rare for achiral triblock copolymers, the helical morphology has been observed in block copolymer solids. For example, Krappe *et al.*[20] discovered the formation of helical B cylinders on the surface of straight C cylinders in an ABC triblock copolymer solid. Recent work by Jinnai *et al.* has found that the assembly of an ABC triblock copolymer forms a solid double helical morphology.[21] Helical cylinders have also been observed for the A block of an AB diblock copolymer that had undergone self-assembly in the confinement of the tubular pores of an anodized alumina membrane.[22]

In this chapter we report the formation of a cylinder helix by direct self-assembly of an achiral ABC triblock copolymer in block-selective solvents. There have been two examples of achiral self-assembly by ABC triblock copolymers to form helices in solvent systems. Pochan, Wooley and coworkers[18] reported an assembly of an achiral triblock copolymer, aided by the addition of a complexing agent (multiamines), while Liu and coworkers[19] have produced twisted cylinders by an indirect method. Pochan, Wooley and coworkers[18] found that the complexing agent interacted with one of the blocks and twisted the cylinders, presumably due to the uniaxial compression of the cylinders along the cylinder

axis. Liu and coworkers[19] produced twisted cylinders with helical sections from an ABC triblock copolymer, by an indirect method, in a selective solvent for the terminal A and C blocks. This twisting was thought to occur for two reasons. First, the A and C blocks were highly incompatible and segregated out on the surface of the B cylinders. Second, the A chains were much longer than the C chains and the repulsion between the surface A chains was thus stronger than that between the C chains and this lateral force imbalance was thought to drive the twisting of these cylinders. We have found a system that directly produces a regular block copolymer double helix with no other aggregating agents other then block-selective solvents.

The helices in this study were prepared from the triblock copolymer poly(*n*-butyl methacrylate)-*block*-poly(2-cinnamoyloxyethyl methacrylate)-*block*-poly(*tert*-butyl acrylate) (PBMA-*b*-PCEMA-*b*-PtBA shown in Scheme 2.1), where the number of BMA units (*n*) was 350, the number of CEMA units (*m*) was 160, and the number of tBA units (*l*) was 160. This determination was made by a combination of NMR and light scattering GPC.

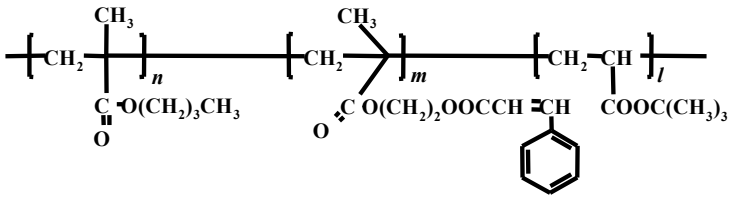

Scheme 2.1. Structure of PBMA-*b*-PCEMA-*b*-PtBA, polymer used for helix formation.

Cylinder helices with highly-regular pitches were prepared in mixtures of dichloromethane (DCM) and methanol (MeOH), where DCM solubilizes every block of the copolymer and MeOH is selective to dissolve PtBA. The solubility of PBMA was found to be marginal when the helices were formed. Initially, the PCEMA block segregated from the solvent phase and formed the cores of the spherical micelle-like aggregates (SMAs) and the PBMA and PtBA chains formed the mixed corona. However, the SMAs fused with time into short cylinders. In these solvent mixtures, the PCEMA blocks segregated from the solvent phase and formed the cores of the SMAs and the PBMA and PtBA chains formed the mixed corona. Since the PBMA chains were only marginally soluble, with presumably a compact conformation, insufficient steric stabilization was provided by PBMA and PtBA, and the SMAs fused with time into short cylinders. These cylinders and SMAs then fused further into short helices and eventually long helices. The helices probably formed in order to decrease unfavorable contact between PBMA and the solvent.

2.2.1 Objectives

This chapter will study a triblock copolymer helix formed from PBMA-*b*-PCEMA-*b*-PtBA. This morphology formed by this copolymer will be extensively studied, including the mechanism and kinetics of formation, the particle dimensions, the solvation condition of the blocks and the hydrodynamic diameter, and will be discussed. We will also propose a thermodynamic structure for the ABC triblock copolymer helices.

2.2.2 Experimental Design Considerations

The study of a series of PBMA-*b*-PCEMA-*b*-PtBA polymers was done in various solvents. This choice of this polymer was made for several reasons. First the PCEMA block can be stained by OsO_4 and made visible for TEM, while the other blocks will be unstained. PCEMA can also be photocrosslinked to lock in self-assembled structures and make permanent nanostructures. The PtBA block of the polymer can be hydrolyzed to PAA. Once hydrolyzed the PAA can be stained with $UO_2(AcO)_2$ while the other two blocks are unstained. PAA also makes the sample water dispersible.

The choice of solvent system was also made for several reasons. Dichloromethane, tetrahydrofuran and chloroform are good solvents for all of the blocks of the copolymer. Methanol is a known poor solvent for PCEMA and was found to be poor for PBMA. Solvent composition is very important as the helical morphology forms for only a very small window of solvent range (~81-85% methanol).

2.3 Experimental

2.3.1 Materials

Chloroform (ACS reagent), methanol (99.8+%), and dichloromethane (99.5+%) were purchased from Fisher Scientific, and used as received. Inhibitor-free tetrahydrofuran (THF) was purchased from Fisher Scientific, and was passed through an Innovative Technology purification system equipped with two alumina

columns before use. Osmium tetraoxide (OsO_4) and uranyl acetate [$UO_2(AcO)_2$] were purchased from Electron Microscopy Sciences and were used as received. Pyridine (Aldrich 99+%) was refluxed with calcium hydride (Aldrich, reagent grade, 95 %) overnight and distilled prior to use. Cinnamoyl chloride (98%, predominantly *trans*), trifluoroacetic acid (99+%) and triethylsilane (99 %) were purchased from Aldrich and were used as received. Methanol-d_4 (D, 99.8%), methylene chloride-d_2 (D, 99.9%) and pyridine-d_5 (D, 99.5%) were purchased from Cambridge Isotope Laboratories Inc. and used as received.

2.3.2 Polymers

To establish the solvation states of the different blocks of the triblock copolymer PBMA-*b*-PCEMA-*b*-PtBA under helix formation conditions, three homopolymers PBMA, PCEMA, and PtBA as well as a diblock copolymer PCEMA-*b*-PtBA were used. These polymers, including the triblock copolymer, were all derived from precursors prepared by anionic polymerization. The anionic polymerization conditions used have been previously described by our group,[24,25] the conditions used are included in Appendix A.

All polymers were characterized by an Agilent size-exclusion chromatograph (SEC) equipped with a Wyatt Dawn Helios-II light scattering detector (LS), and an Optilab rEX refractive index detector. The light operating wavelength of both detectors was 658 nm. The SEC columns used were Waters μStyragel HR 5, HT 4 and HT 500 Å and the eluant used was THF. The specific refractive index

increments dn_r/dc were determined using the Wyatt Optilab rEX refractive index detector. The repeat unit number ratios between the different blocks of the triblock copolymer and diblock copolymer were determined from ^{1}H NMR by comparing the integrals of the proton peaks from the different blocks in pyridine-d_5. Table 2.1 summarizes the molecular properties of the polymer used.

Evidently, all polymers used in this study had low polydispersity. The number of repeat units for the BMA, CEMA, and tBA triblock copolymer were 350, 160, and 160 respectively. In the diblock copolymer there were 80 and 250 units of CEMA and tBA, respectively. The repeat unit numbers for the PtBA, PBMA and PCEMA homopolymers were 100, 460 and 200, respectively. All molecular block lengths are accurate to $\pm$10 units.

Table 2.1. Characteristics of the polymers used in this study.

Sample	dn_r/dc (mL/g)	SEC M_w/M_n	SEC-LS $10^{-4} \times M_n$ (g/mol)	NMR $n/m/l$	*N*	*M*	*l*
Triblock	0.118	1.06	11	2.2/1.0/1.0	350	160	160
Diblock	0.111	1.05	5.2	0/1.0/3.3		80	250
PtBA	0.053	1.05	1.4	0 / 0 / 1			100
PBMA	0.067	1.08	6.5	1 / 0 / 0	460		
PCEMA	0.156	1.01	5.1	0 / 1 / 0		200	

2.3.3 Polymer Solubility Tests

Visual inspection revealed that $PtBA_{100}$ was soluble in DCM/MeOH, $CHCl_3$/MeOH and THF/MeOH with the f_{MeOH} (methanol fraction) value ranging between 0 and 100%. To determine the critical methanol fraction f^*_{MeOH}, above which $PBMA_{460}$ and $PCEMA_{200}$ became insoluble, the following protocol was utilized. All

solubility measurements were done at room temperature which was approximately 20 ^{o}C.

$PBMA_{460}$ or $PCEMA_{200}$ was first dissolved in DCM at 5 mg/mL. Methanol was then added to these polymer solutions. After a rough estimate was obtained for f^{*}_{MeOH} from a visual turbidity test, several samples with a f_{MeOH} interval of 2.5% were prepared near the estimated f^{*}_{MeOH} value. The samples were observed immediately and one day after MeOH addition for turbidity. The required f_{MeOH} to induce cloudiness immediately after MeOH addition was 47.5% for a solution of $PCEMA_{200}$ in DCM and 87.5% for a solution of $PBMA_{460}$ in DCM. Only 46.0% of MeOH was required for turning a DCM solution of $PCEMA_{200}$ cloudy one day after MeOH addition. Meanwhile for $PBMA_{460}$, the f^{*}_{MeOH} value was 85%.

A similar protocol was followed for f_{MeOH} in the $CHCl_3$/MeOH and THF/MeOH systems. The f^{*}_{MeOH} values after one day for the THF/MeOH mixtures were 80.0% for PBMA and 49.0% PCEMA. In $CHCl_3$/MeOH these values were 85.0% for PBMA and 49.0% for PCEMA.

2.3.4 Helix Preparation

Helix preparation in DCM/MeOH involved first dissolving the triblock copolymer in DCM at 5 mg/mL. To this solution in a vial under vigorous stirring, MeOH was added quickly (~1 min) to reach a f_{MeOH} value of 82 %. The vial was sealed and

placed in a closed dessicator containing a reservoir of DCM/MeOH mixture with a f_{MeOH} value of 82 %, in order to minimize evaporation-induced solvent composition change inside the vial. The solution was stirred for at least 3 weeks before observation by TEM. Helices in DCM/MeOH at other f_{MeOH} values and in THF/MeOH or $CHCl_3$/MeOH were prepared similarly.

In order to follow the helix formation process, samples were taken at pre-designated times, and were aspirated on carbon-coated copper grids for TEM analysis. Cross-linking of the PCEMA domains of the MAs was achieved by irradiation for three hours in a UV cell under magnetic stirring using a focused UV beam from a 500-W mercury lamp. The light was filtered with a 270 nm cut-off filter to remove higher energy UV light.

In order to hydrolyze the PtBA chains of the cross-linked MAs and facilitate the TEM observation of the resultant poly(acrylic acid) (PAA) chains, the samples were first dried by rotary evaporation. The solids were then dispersed in DCM before triethylsilane, at three molar equivalents relative to the tBA groups, and trifluoroacetic acid, at 1/3 the volume of DCM, were added. This mixture was stirred overnight before removal of volatile components by rotary evaporation. To ensure complete removal of residual acid, methanol was added, followed by additional rotary evaporation of the volatile components. This procedure was repeated thrice. The sample was then redispersed in 10 mL of pyridine, and the pH of the resulting solution was ~7.

2.3.5 NMR Studies

The triblock or diblock copolymer were stirred in DCM-d_2 (~8 mg/mL) for one h in order to ensure molecular dissolution. This solution was then filtered into a clean vial through a 0.45 μm PTFE syringe filter. Filtered *d*-MeOH was then added until the desired solvent composition was reached (70-92 % (v/v) d-methanol). The samples were stirred for one hour before the samples were sealed in an NMR tube, and ^{1}H NMR was run on a 500 MHz Bruker AM-500 spectrometer. Signal intensities were obtained by performing line fitting using WinNuts.[26]

2.3.6 Transmission Electron Microscopy

MAs were aspirated onto carbon-coated copper grids. After drying at room temperature for one h, the specimens were stained by OsO_4 for two h or with $UO_2(AcO)_2$ staining techniques before Transmission Electron Microscopy (TEM) observation. Staining by $UO_2(AcO)_2$ was done by equilibrating a grid with drops of a $UO_2(AcO)_2$ solution in MeOH/DCM at v/v = 80/20 for 25 min. After removing the droplets, excess staining reagent was removed by rinsing the grids with methanol droplets ten times. All TEM observations were made on a Hitachi 7000 instrument operated at 75 kV.

2.3.7 Transmission Electron Tomography

After helix sample aspiration and staining by OsO_4, some 10-nm Au colloidal solution (GCN005, BBInternational Ltd., UK) was sprayed on a TEM grid. TEM tomography analysis was done using a JEM-2200FS (JEOL Co. Ltd., Japan)

instrument operated at 200 kV. Only the transmitted and elastically scattered electrons with energy loss between 0 and ±15 eV were used for imaging. The images or projections were collected at sample stage tilting angles ranging from -70^{o} to +75^{o} in 1^{o} intervals. The series of images were aligned by the fiducial marker method[27] using the Au particles. The 3-D images were reconstructed based on the filtered back projection method.[28] The mean alignment error, averaged over all of the fiducial markers, was 0.76 nm, which was less than the pixel resolution, regardless of the tilt angles.

2.3.8 Atomic Force Microscopy

Specimens were prepared by aspiration of solution samples onto cleaned silicon wafers or freshly cleaved mica surfaces. All samples were analyzed by tapping-mode atomic force microscopy (AFM) using a Veeco multimode instrument equipped with a Nanoscope IIIa controller. The tips used were AppNano ACT Tapping mode AFM probes with tip radii of 5-6 nm, tip aspect ratios of 3:1 to 5:1, force constants of 25-75 N/m and resonance frequencies of 200-400 kHz.

2.3.9 Dynamic Light Scattering Measurements

Dynamic light scattering (DLS) measurements were carried out at room temperature on a Brookhaven BI-200 SM instrument equipped with a BI-9000AT digital correlator and a He-Ne laser (632.8 nm). Measurements were done at 90°. Samples were clarified by filtration through 0.1 μm PTFE filters. The data

was treated by the Cumulant method[29] to yield particle hydrodynamic diameter d_h and polydispersity K_2^2/K_4, the square root of which gives the percent standard deviation. The refractive index n_r of a DCM/MeOH mixture was estimated using the following equation[30]

$$n_r = n_{r1} f_{MeOH} + n_{r2}\left(1 - f_{MeOH}\right) \qquad (1)$$

where n_{r1} and n_{r2} are the refractive indices of MeOH and DCM, respectively. The viscosity, η, of a solvent mixture was calculated using:[31]

$$\ln\eta = \phi_1 \ln\eta_1 + \phi_2 \ln\eta_2 \qquad (2)$$

with η_1 and η_2 representing the viscosities of solvents 1 and 2, respectively, and ϕ_1 and ϕ_2 being the molar fractions for solvents 1 and 2.

2.4 Results and Discussion

Cylindrical helices were prepared from the triblock copolymer PBMA-*b*-PCEMA-*b*-PtBA by stirring the polymer in DCM/MeOH with f_{MeOH} between 82% and 85% for three weeks or longer. Immediately after MeOH addition, only spherical and cylindrical MAs were observed. To elucidate the structure and the mechanism of formation of the helices, the helix formation process was followed in a DCM/MeOH mixture having a f_{MeOH} value of 82%.

2.4.1 Spherical and Short Cylindrical Micelle-like Aggregates.

The initial spherical and cylindrical MAs were first characterized. Figure 2.1a shows a TEM image of MAs aspirated on a carbon-coated copper grid for ten

min after their preparation in DCM/MeOH with $f_{MeOH} = 82\%$. The specimen was stained by OsO_4 which selectively stains the PCEMA block. To observe the PtBA chains in the MAs, we irradiated a freshly prepared MA solution with UV light to cross-link the PCEMA block, and then treated the resultant cross-linked MAs with trifluroacetic acid in order to hydrolyze the PtBA block to PAA. This was then followed by redispersion of the MAs in pyridine. Figure 2.1b shows such a sample with PAA stained by $UO_2(AcO)_2$.

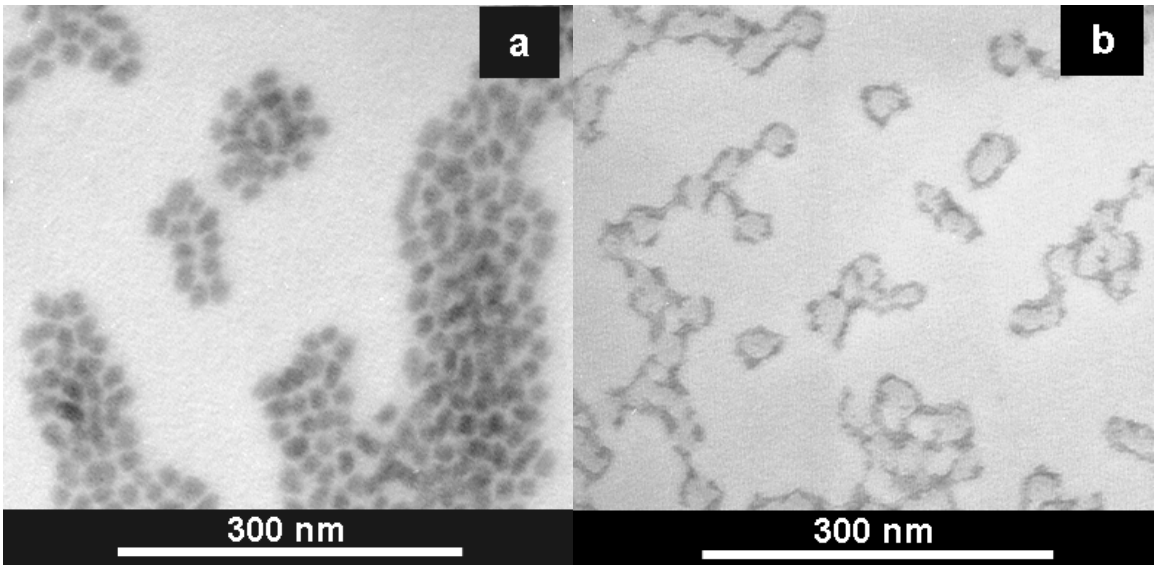

Figure 2.1. TEM images of MAs aspirated from DCM/MeOH with $f_{MeOH} = 82\%$. The specimen for image **(a)** was stained by OsO_4. The sample for image **(b)** was first irradiated with UV light to cross-link PCEMA and then treated with trifluroacetic acid to hydrolyze PtBA. The resultant PAA chains were stained by $UO_2(AcO)_2$.

Dark circles and some elongated objects are seen in Figure 2.1a. Many of the dark circles seem to be separated from one another by a light gray boundary. The average diameter of the dark circles is 18±2 nm. In Figure 2.1b light circles and elongated light objects are seen. They are all surrounded by dark rims. Around the individual or isolated (not clustered) light circles, the dark rims were

fairly uniform along the whole periphery, except for occasional dark bumps or broken sections. The average diameter of the light circles shown in Figure 2.1b is 20±2 nm, which correlates within measurement error to the size of the dark circles in Figure 2.1a.

The circles are projections of the PCEMA cores of spherical MAs. The cores appeared dark in Figure 2.1a from OsO_4 staining, and light in Figure 2.1b due to the lack of staining by $UO_2(AcO)_2$. The rather uniform dark rims in Figure 2.1b suggests that PAA or its precursory PtBA chains occurred throughout the whole shell. The slightly elongated objects would have been projections of the PCEMA cores formed by the fusion of the spherical MAs.

Two sets of experiments were performed to probe the location of PBMA chains. In one set, we determined that a f_{MeOH} value of 87.5 vol% was required to induce, within minutes, the phase separation of a homopolymer of PBMA with 460 repeat units from DCM/MeOH solution. Given enough time, such as one day, the homopolymer at ~1 mg/mL phase separated from DCM/MeOH at a lower f_{MeOH} value of 85%. Since the PBMA block in the triblock was 350 units long, shorter than 460 units, a critical f_{MeOH} above 85% should be required to induce its insolubility. Thus, the PBMA block was marginally soluble and would not have segregated out from the solvent phase at $f_{MeOH} = 82\%$. The PBMA block should have existed as a part of the corona.

In the second set of experiments we used ^{1}H NMR to learn about the structure of the aggregates. Solution NMR allows us to probe the structure of the polymer by observing the differences in the peak intensities. The peak intensity will change when you change the solvation conditions of the individual blocks of the copolymer.

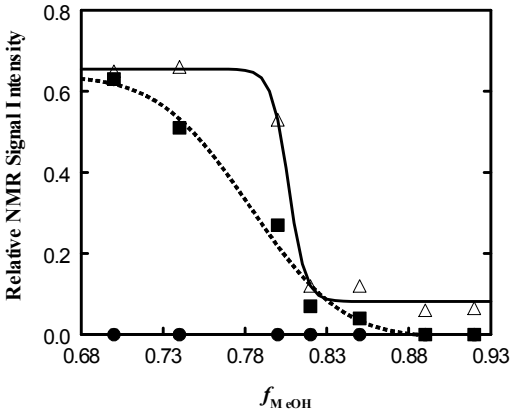

Figure 2.2. Plot of variation in I_{RBMA}/I^0_{RBMA} (■), I_{RCEMA}/I^0_{RCEMA} (•), and I_{RtBA}/I^0_{RtBA} (Δ) as functions of f_{MeOD}.

We dissolved the triblock copolymer at 5.0 mg/mL in DCM-d_2 and determined the intensity of some characteristic PBMA peaks between 3.8 and 4.0 ppm relative to that at 5.3 ppm for $CHDCl_2$, an impurity in the solvent DCM-d_2. This relative peak intensity was given the symbol I^0_{RBMA}. Similarly, we determined the relative intensity I^0_{RCEMA} for PCEMA peaks between 4.0 and 4.4 ppm and I^0_{RtBA} for the PtBA singlet peak between 1.35 and 1.5 ppm. This sample was then diluted with different amounts of MeOH-d_4 and the resultant samples were analyzed within one to three hours for the relative intensities I_{RBMA}, I_{RCEMA}, and I_{RtBA}. Figure 2.2 plots I_{RBMA}/I^0_{RBMA}, I_{RCEMA}/I^0_{RCEMA}, and I_{RtBA}/I^0_{RtBA} as functions of f_{MeOD}.

The data of Figure 2.2 shows that the PBMA signals decreased gradually when f_{MeOD} was increased from 70% to 85% and became invisible for $f_{MeOD} \geq$ 89%. The PtBA signals experienced an abrupt decrease between f_{MeOD} = 80% and f_{MeOD} = 82% and then stabilized above f_{MeOD} = 82%. The PCEMA signals were not seen in DCM-d_2/ MeOH-d_4 with f_{MeOD} between 70% and 93%.

The disappearance of, or a decrease in the intensity of a NMR signal of a proton can be caused by a slower tumbling of the proton. This slower tumbling motion can be caused by the compaction of a polymer coil or the total collapsing of a block from the solvent phase. The gradual slowing down of the tumbling motion first leads to peak broadening, and eventually makes the peaks undetectable.[32] The absence of PCEMA peaks when f_{MeOD} values were between 70% and 93% was in agreement with our observation that a PCEMA homopolymer with 200 CEMA units started to precipitate out of solution from DCM/MeOH at $f_{MeOH} =$ 47.5%, a value well below $f_{MeOD} =$ 70%. These results confirm the TEM observations, which indicated that at $f_{MeOH} =$ 82% the PCEMA formed the core of the spherical and cylindrical MA structures.

The decrease of the PBMA signals with increasing f_{MeOD} values between 70% and 89% suggests that the gradual compaction of the PBMA chains as the solvent quality deteriorated for PBMA. The disappearance of the PBMA signals

somewhere between f_{MeOD} = 85% and 89% was in agreement with our polymer solubility test results, which indicated that the PBMA homopolymer started to phase separate immediately from DCM/MeOH at f_{MeOH} = 87.5% and slowly at f_{MeOH} = 85%. The low residual PBMA signals at f_{MeOH} = 82% suggest that PBMA had a somewhat compact conformation at this solvent composition but did not completely collapse from the solvent phase. The marginal solubility of PBMA also suggests the presence of PBMA in the corona of the MAs.

The distribution of two soluble blocks in the coronas of MAs can be intriguing. As first hypothesized by Hoppenbrowers *et al.*,[33] the solubilized A and C chains on the surface of the insoluble B core of a triblock copolymer can be either uniformly distributed throughout the corona, or segregated. Depending on the incompatibility, the segregation may yield MAs with patched surfaces[34,35] or Janus MAs[19] (with half of the surface covered by A and half by C). The following observations suggest that the PtBA and PBMA chains were randomly mixed with one another in the corona. First, the two polymers are very similar structurally. Their compatibility in the solvated state is supported by the very close solubility parameters calculated for them based on group contributions,[36] which were 15.5 and 16.1 $MPa^{1/2}$, for PtBA and PBMA respectively. Second, our NMR analysis of a PCEMA-*b*-PtBA diblock copolymer in DCM-d_2/MeOH-d_4 with f_{MeOD} = 85% yielded $I_{RtBA}/I^0_{RtBA} \approx$ 100%. If the PtBA and PBMA blocks were segregated on the surface of the MAs, one would expect to see a significantly larger

I_{RtBA}/I^0_{RtBA} for the PtBA block with the triblock copolymer. In reality, the PtBA signals decreased with the PBMA signals. Third, the TEM image in Figure 2.1b suggests that the PtBA chains are distributed evenly on the surface of the MAs.

Scheme 2.2 illustrates our current understanding of the chain distribution in the triblock copolymer spherical MAs at $f_{MeOH} \approx 82\%$. The PCEMA collapsed from the solvent phase to form the core. The PBMA chains assume more compact conformations than those of PtBA due to the deterioration of the solvation conditions. The PtBA and PBMA chains are randomly distributed among one another, while the PtBA chains serve to stabilize the MAs.

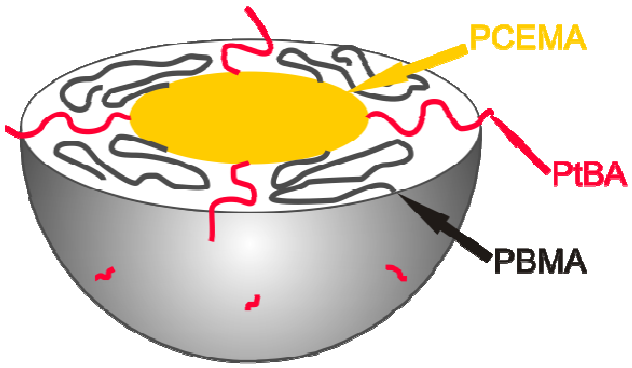

Scheme 2.2. Schematic representation of the chain packing within the spherical MAs.

Besides the TEM and ^{1}H NMR analyses, we also performed a DLS study of the MAs two hours after their preparation at $f_{MeOH} =$ 82%. The average hydrodynamic diameter (d_h) and DLS polydispersity (K_2^2/K_4) were 68 ± 1 nm and 0.06 (24.5% deviation), respectively. That the value of d_h was greater than that of d_{TEM} is expected, because DLS probed the size of the solvated MAs

including the coronal PBMA and PtBA chains. When comparing these measured values, one should also realize that the sample contained not only spherical MAs but also some short cylinders and fused spherical MAs (which we did not measure for d_{TEM}), which would produce a d_h value larger than that for the spherical MAs.

We finish this section by noting that the TEM PCEMA core radius of ~10 nm is small. At 160 units, the PCEMA block has a fully-stretched chain length of 40 nm. Assuming a characteristic ratio C_∞ of 6.0, a typical value for atactic poly(methyl methacrylate),[37] the root-mean-square end-to-end distance of this chain in the unperturbed state was estimated to be 6.7 nm. The core chains of diblock copolymer spherical micelles should normally be stretched more than those in the unperturbed state.[10,38,39] We cannot conclude this with certainty here, because we do not know how much smaller the actual radius of the spherical MAs was than the TEM radius of ~10 nm, and we expected the observed MAs were flattened somewhat when aspirated from solvent onto a TEM grid.[8] This smaller triblock copolymer MA size is common and has been seen before by others[40,41] and by us.[33] This reduced MA size, and thus aggregation number, might have resulted from the fact that the B core chain of an ABC triblock copolymer is more likely to stretch across the whole core with the terminal A and C blocks emanating from the opposite sides of the core.

2.4.2 Multiple Helices.

Stirring a triblock copolymer dispersion in DCM/MeOH with f_{MeOH} values between 82 and 85 % for a long time converted the spherical and cylindrical MAs seen initially, into cylinder helices. Our results indicated that a polymer concentration of ~1.0 mg/mL was optimal for the production of individual helices. Higher polymer concentrations led to entangled helices, or helix lumps. We also noticed that longer equilibration times, up to the longest tested equilibration time of three months, helped produce the most individual helices. Figure 2.3a and b show TEM images of a helical sample that was obtained from equilibrating a triblock copolymer with DCM/MeOH at f_{MeOH} = 82% for three months, then aspirated on a carbon-coated copper grid, and then stained with OsO_4.

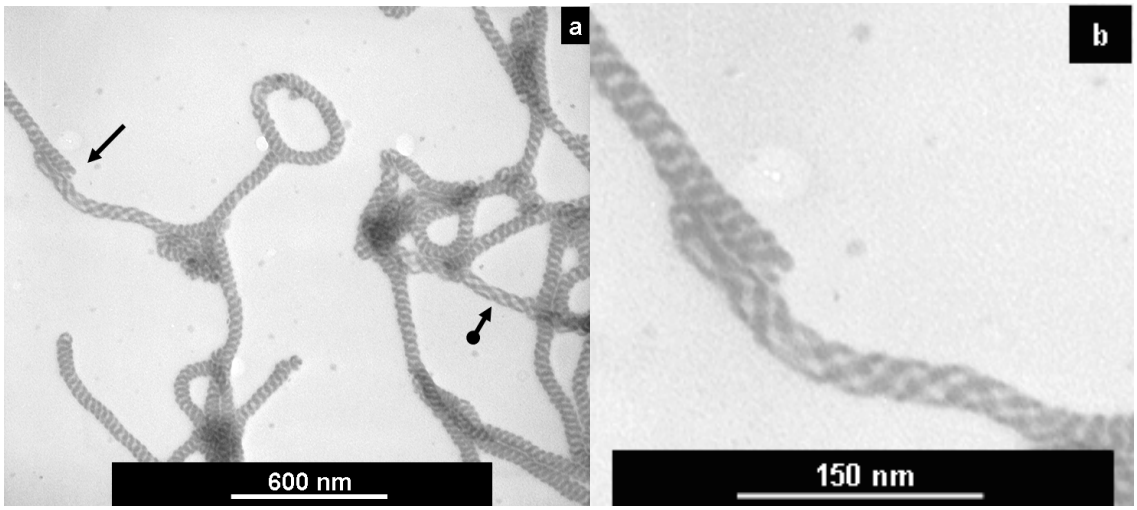

Figure 2.3. TEM images (a) at low and (b) at high magnification of the helices aspirated from DCM/MeOH at $f_{MeOH} = 82\%$, three months after the triblock solution preparation stained with OsO_4.

Since OsO_4 stained only the PCEMA domains, the TEM images (Figure 2.3a and b) suggest that the PCEMA domains formed helices. Most of the helices seemed

to be double helices, while occasionally triple helices were observed, with two examples marked by arrows in Figure 2.3a.

A normal TEM image gives the projection of a 3-D structure at one observation angle and this information can be misleading. To confirm the conclusion of our results of Figure 2.3, we performed TEM tomography analysis of a helix sample. Such an analysis involved taking projections of the helices on the sample stage rotating angles from -70 to 75^{o} at 1^{o} intervals, and then computer assisted 3-D reconstruction of the images from the many projections. Figure 2.4a shows the 3-D images of a left-handed double helix confirming unambiguously the results of Figure 2.3. Figure 2.4 b shows a section of a right-handed triple helix.

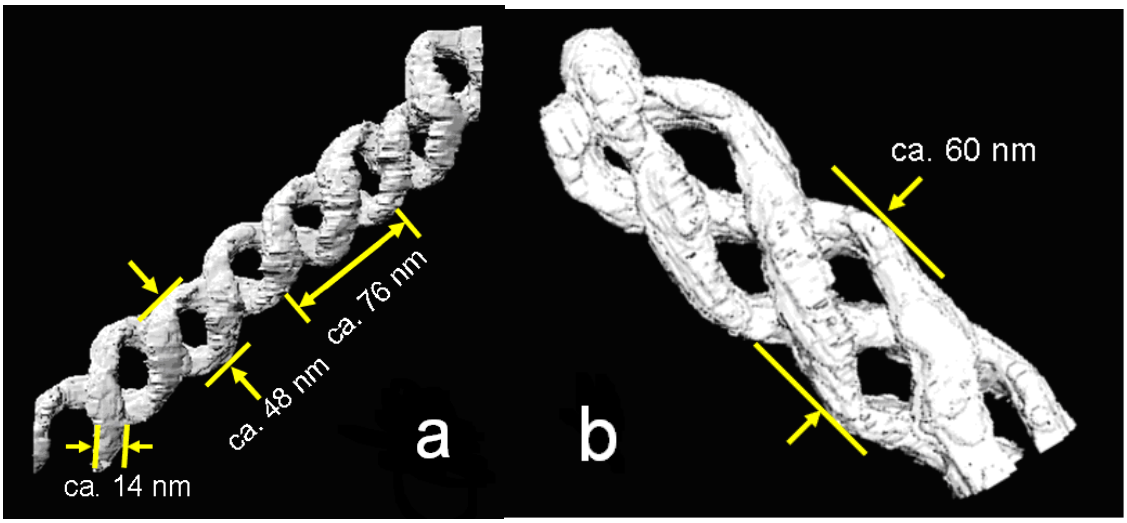

Figure 2.4. Computer reconstructed images of double (a) double and triple (b) helices, aspirated from DCM/MeOH at $f_{MeOH} =$ 82% three months after the triblock sample preparation. The reconstruction was done by computer after TEM tomography imaging.

Although the structures are slightly flattened due to aspiration and the images are slightly pixilated due to computer reconstruction, both double and triple helices are clearly depicted here.

Since the majority of the helices were double helices, our discussion hereafter will focus on the double helical structure, the major product. A quantitative analysis of the 3-D images of several double helices indicated that the PCEMA cylinders had an elliptical cross-section with a width of 14 nm, and a height of 10 nm. The helices flatten substantially after aspiration from solution as they had an average height of 19 nm and a width of 48 nm. The average pitch length was 76 nm.

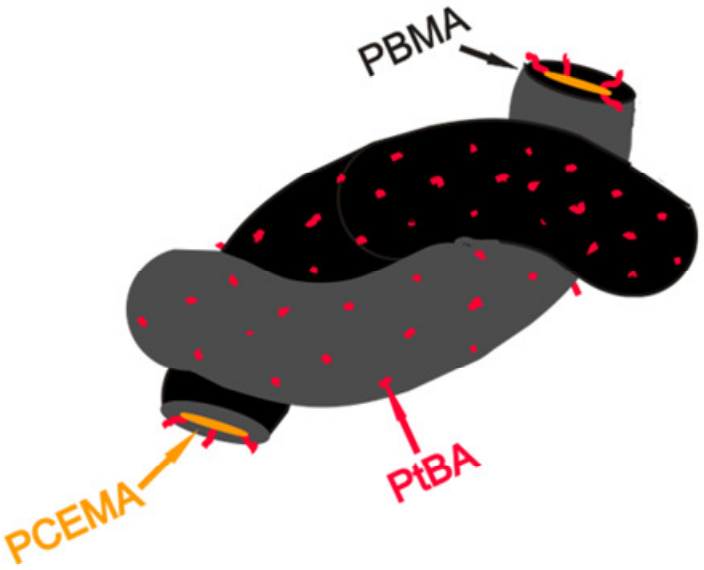

Scheme 2.3. Schematic representation of chain packing in the double helix. The PBMA layers were given slightly different colors (black vs. gray) in the two associating cylinders in the helix to facilitate the visual differentiation of the two.

Based on our observations made on the chain distribution in the spherical MAs, we believe that the PBMA and PtBA chains should be again more or less evenly distributed in the corona. Scheme 2.3 shows the double helix structure according to our understanding. Thus, the apparently "void" space deduced from TEM between the two PCEMA cylinders is due to the solvent-swollen PBMA and PtBA chains in the native solvated state of the double helices.

The absence of actual void space was confirmed by AFM analysis. Figure 2.5a and Figure 2.5b show a 3-D topography and a 2-D phase image of a helix sample, respectively. The average height and width of these helices were 37 ± 4 and 97 ± 13 nm, respectively. While some roughness was indeed detected on the surface of these helices (such as in the marked regions), no void spaces were detected between the ridges, below which PCEMA cylinders most likely lay.

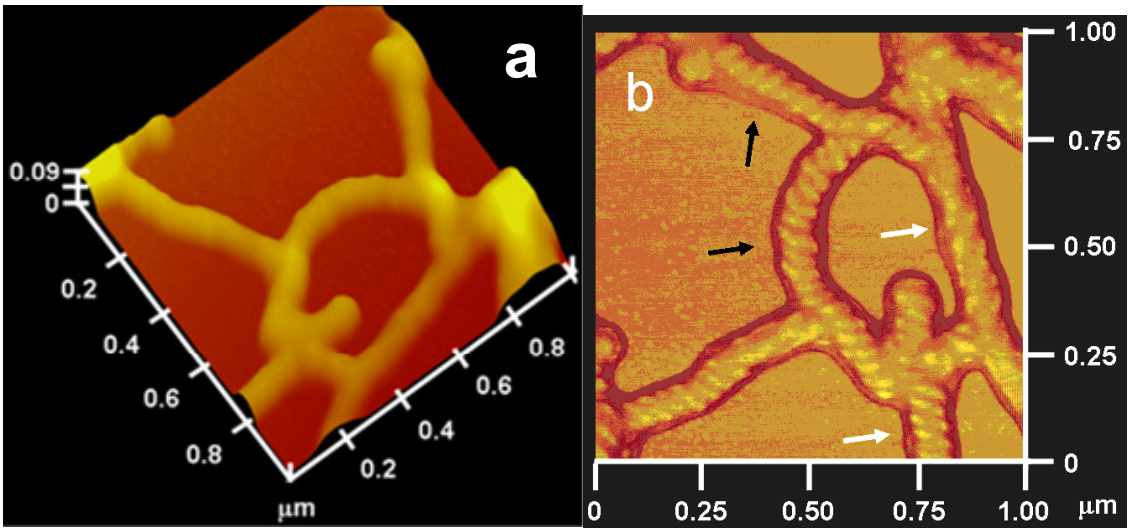

Figure 2.5. AFM topography (a) and phase (b) images of a helix sample where the black arrows show left-handed and the white arrows show right-handed helices.

The helical structure of the PCEMA domains is evident in the phase image of Figure 2.5b. The slanting directions of the PCEMA domains seem to suggest that the helices marked by white arrows are left-handed and those by black arrows are right-handed. The lack of single handedness was expected because the polymer contained no chirality to induce single handedness.

2.4.3 Transition from Small MAs to Multiple Helices.

The transition of the MAs structure from small spheres to multiple helices was observed using dynamic light scattering (DLS). Figure 2.6 shows how the hydrodynamic light scattering diameters d_h varied with time for aggregates of the triblock copolymer prepared in DCM/MeOH at $f_{MeOH} = 82\%$. Larger structures were formed over time as the aggregates increased in size after longer time.

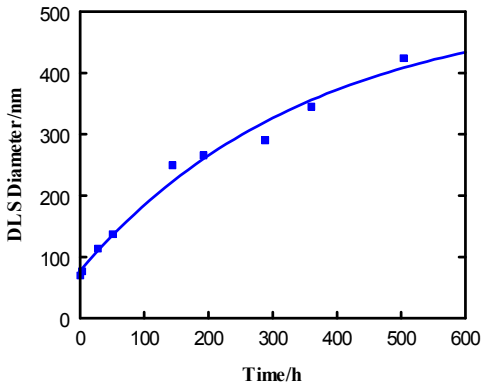

Figure 2.6. Plot of d_h variation as a function of time for a MA sample prepared in DCM/MeOH at $f_{MeOH} =$ 82%.

We followed the structural evolution in detail by taking samples for TEM analysis at different sample aging times. Figure 2.7 shows TEM images of these samples aspirated on carbon-coated copper grids and stained by OsO_4.

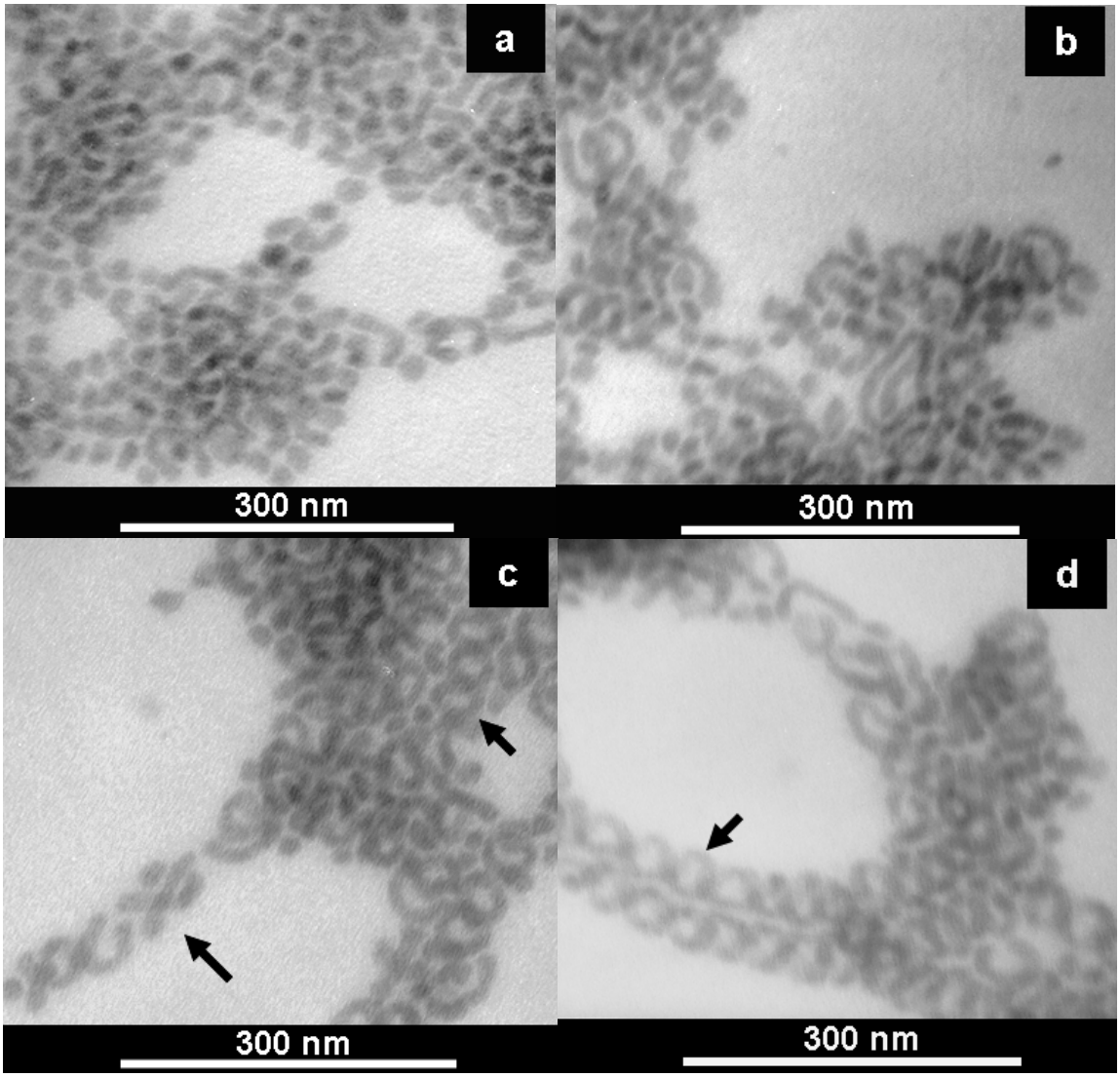

Figure 2.7. TEM images of MAs aspirated from DCM/MeOH at $f_{MeOH} = 82\%$ after one day (**a**), eight days (**b**), 16 days (**c**). The short arrow indicates a helical section, while the long arrow designates a crossing section. At 24 days (**d**), the arrow indicates an isolated helix, after the triblock sample preparation.

Immediately after MeOH addition to give a f_{MeOH} value of 82%, mostly spherical MAs were observed (Figure 2.1a). After one day, more cylindrical MAs are seen (Figure 2.7a). After eight days, the cylinders appeared to become elongated, while the population of curved cylinders increased (Figure 2.7b). After 16 days, most of the cylinders were curved, while some had aggregated to crosses, which

are precursors to helices (Figure 2.7c). Short helical sections were also seen, and are marked by arrows in the Figure 2.7c. At 24 days, isolated long helices were observed, along with cylinders, which were in the process of converting to helices (Figure 2.7d).

2.4.4 Driving Force for Double and Triple Helix Formation.

The fact that the spherical MAs fused initially into cylinders, and then these cylinders intertwined into double and triple helices, suggesting that the helices should be thermodynamically favorable compared to the spherical and cylindrical MAs. As mentioned before, the PCEMA block would have collapsed and phase-separated from the solvent phase at $f_{MeOH} \approx 46\%$, where the PBMA and PtBA blocks were both well solvated. The spherical MAs were probably the thermodynamically favored product at this point because the highly swollen PtBA and PBMA chains were best accommodated in the corona of a spherical micelle, which has the largest interfacial curvature among the typically observed morphologies, including cylinders and vesicles. As the methanol fraction was increased to $f_{MeOH} \approx 82\%$, the PBMA coronal chains compacted substantially, trapping some of the soluble PtBA chains among them. According to the geometric packing parameter theory, the size of the coronal block or the head block had decreased significantly relative to the size of the tail or core block. The most preferred MA geometry should be cylinders. This explains why we observed the initial spherical to cylindrical MA transformation.

The cylinders reassembled into helices as a result of the lower Gibb's free energy of the helices, relative to straight cylinders. As we mentioned previously, PBMA was marginally soluble in DCM/MeOH at $f_{MeOH} \approx 82\%$. In order to minimize the contact between the PBMA block and the solvent, the cylinders could have coagulated and precipitated out of solution. This did not occur for two reasons. First, the soluble PtBA chains prevented precipitation, by stabilizing the structure. Second, the solvent was marginal for PBMA, but not yet poor. A compromise was for the cylinders to twist into double or triple helices, and thus minimize PBMA-solvent contact, while still allowing the PtBA chains to remain in solution.

How double helix formation helped reduce PBMA and solvent contact is best shown in Figure 2.8, which shows how a green and a red pipe cleaner are twisted into a double helix. The metal wire core in this example would represent the PCEMA core of the cylindrical MAs. The green and red bristles can be viewed as the coronal PBMA and PtBA chains. The PtBA chains are equivalent to the PBMA chains here, unless we dye some of the green and red bristles to a different color. Obviously, there is more contact between the bristles and the air (PBMA and solvent in the case of triblock cylinders) on the left side per unit pipe cleaner length than on the right side where the pipe cleaners are twisted. In the pipe cleaner case, the core wires retained their cylindrical cross-section. Meanwhile the PCEMA cores deformed to acquire an elliptical cross-section, mainly to ensure the formation of a compact double helix, and to minimization the contact between the PBMA block and the solvent.

Figure 2.8. Photograph of two pipe cleaners twisting into a double helix.

2.4.5 Multiple Helices in Other Solvent Systems.

Aside from DCM/MeOH, helices were found to form also in THF/MeOH and chloroform ($CHCl_3$)/MeOH mixtures. Figure 2.9 shows TEM images of helices aspirated from THF/MeOH with $f_{MeOH} =$ 77% and $CHCl_3$/MeOH with $f_{MeOH} =$ 83%. Again, the helices were formed only after weeks of equilibrating of the triblock MAs systems.

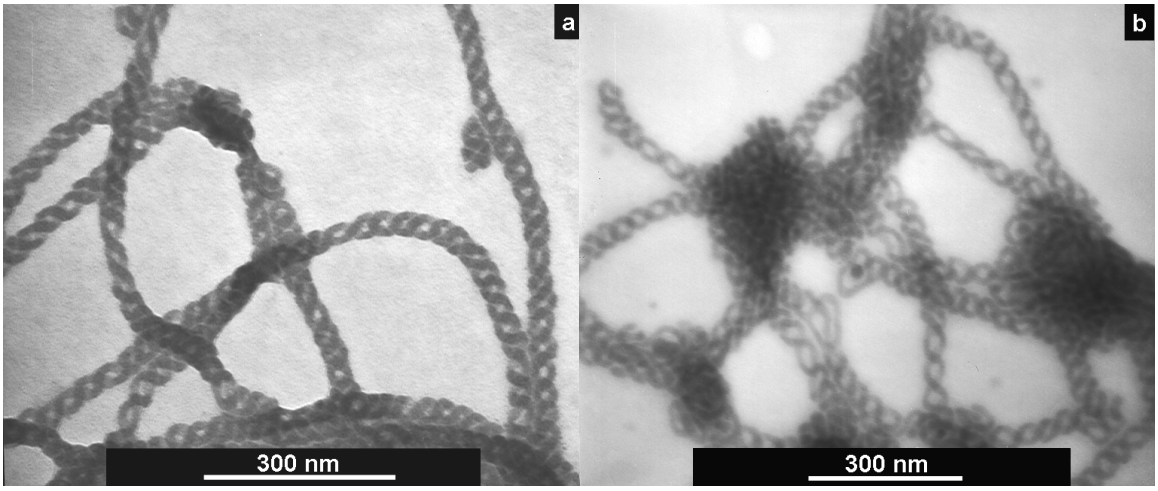

Figure 2.9. TEM images of helices aspirated from THF/MeOH with $f_{MeOH} =$ 77% (a) and $CHCl_3$/MeOH with $f_{MeOH} =$ 83%. The MA solutions were aged for three weeks before their aspiration. The aspirated samples were stained by OsO_4 for two hours.

To help understand helix formation in these cases, we again determined the critical f_{MeOH} for inducing visual cloudiness to the $PBMA_{460}$ and $PCEMA_{200}$

solutions one day after MeOH addition. These were 80.0% and 49.0% for THF/MeOH mixtures, and 85.0% and 49.0% for the $CHCl_3$/MeOH mixtures. While PtBA was soluble in all of these mixtures, the PBMA block of the triblock copolymer was again in a marginally solvated state or compact state in these THF/MeOH and $CHCl_3$/MeOH mixtures. These results suggest the solvated state of the blocks of the polymer (marginal for PBMA, poor for PCEMA, and good for PtBA) rather than the exact solvent properties were the reason for the formation of helices in this polymer system.

2.5 Conclusions

A PBMA-*b*-PCEMA-*b*-PtBA sample has been synthesized and characterized. MAs were prepared in DCM and MeOH mixtures, where DCM was a common solvent for all of the three blocks of the copolymer, and MeOH solubilized only the PtBA block. Immediately after methanol addition to f_{MeOH} between 82% and 85% to a DCM solution of the triblock copolymer, the copolymer formed SMAs. Our TEM analysis indicated that the PCEMA block formed the core of the SMAs. ^{1}H NMR analysis indicated that the PCEMA block was fully collapsed from the solvent phase, and that the PBMA coils had substantially shrunk, but were not fully collapsed at f_{MeOH} = 82%. The ^{1}H NMR results also suggest that the PBMA and PtBA chains were mixed in the corona in both the initially formed spheres and the helices. With time, the SMAs fused first into short cylinders. The cylinders and SMAs then fused further into short helices and eventually long helices. The structure of the helices was established by routine TEM, AFM, DLS,

^{1}H NMR, and by TEM tomography. The helices were formed mainly to decrease the unfavorable contact between PBMA and the solvent, and were stabilized by the PtBA chains. While the helices had been reproduced in other binary solvent mixtures including THF/MeOH and $CHCl_3$/MeOH, it will be interesting to examine if this morphology can be reproduced using other analogous triblock copolymers.

2.6 References

1. Lazzari, M.; Liu, G.; Lecommandoux, S. *Block Copolymers in Nanoscience*. Wiley-VCH: Weinheim, Germany, 2006.

2. Zhang, L.; Eisenberg, A. *Science,* **1995,** *268*, 1728-1731.

3. Ding, J.; Liu, G.; Yang, M. *Polymer,* **1997,** *38*, 5497-5501.

4. Ding, J.; Liu, G. *Macromolecules,* **1997,** *30*, 655-657.

5. Discher, D.; Eisenberg, A. *Science,* **2002,** *297*, 967-973.

6. Liu, G. *Adv. Polym. Sci.* **2008,** *220*, 29-64.

7. Raez, J.; Manners, I.; Winnik, M. *J. Am. Chem. Soc.* **2002,** *124*, 10381-10395.

8. Njikang, G.; Han, D. H.; Wang, J.; Liu, G. J. *Macromolecules,* **2008,** 41, 9727-9735.

9. Price, C. *Pure Appl. Chem.* **1983,** *55*, 1563-1572.

10. Tao, J.; Stewart, S.; Liu, G.; Yang, M. *Macromolecules,* **1997,** *30*, 2738-2745.

11. Jain, S.; Bates, F. *Science,* **2003,** *300*, 460-464.

12. Chen, Z.; Cui, H.; Hales, K.; Li, Z.; Qi, K.; Pochan, D.; Wooley, K. *J. Am. Chem. Soc.* **2005,** *127*, 8592-8593.

13. Zhu, J.; Liao, Y.; Jiang, W. *Langmuir,* **2004,** *20*, 3809-3812.

14. Cui, H.; Chen, Z.; Zhong, S.; Wooley, K.; Pochan, D. *Science,* **2007,** *317*, 647-650.

15. Li, Z.; Kesselman, E.; Talmon, Y.; Hillmyer, M.; Lodge, T. *Science,* **2004,** *306*, 98-101.

16. Cornelissen, J.; Fischer, M.; Sommerdijk, N.; Nolte, R. *Science,* **1998,** *280*, 1427-1430.

17. Geng, Y.; Discher, D.; Justynska, J.; Schlaad, H. *Angew. Chem. Int. Ed.* **2006,** *45*, 7578-7581.

18. Zhong, S.; Cui, H.; Chen, Z.; Wooley, K.; Pochan, D. *Soft Matter,* **2008,** *4*, 90-93.

19. Hu, J.; Njikang, G.; Liu, G. *Macromolecules,* **2008,** *41*, 7993-7999.

20. Krappe, U.; Stadler, R.; Voigtmartin, I. *Macromolecules,* **1995,** *28*, 4558-4561.

21. Jinnai, H.; Kaneko, T.; Matsunaga, K.; Abetz, C.; Abetz, V. *Soft Matter,* **2009,** 5, 2042-2046.

22. Xiang, H.; Shin, K.; Kim, T.; Moon, S.; McCarthy, T.; Russell, T. *Macromolecules,* **2005,** *38*, 1055-1056.

23. Li, J.; Ness, J.; Cheung, W. *J. Appl. Polym. Sci.* **1996,** *59*, 1733-1740.

24. Liu, F.; Liu, G. *Macromolecules,* **2001,** *34*, 1302-1307.

25. Yan, X.; Liu, G.; Li, H. *Langmuir,* **2004,** *20*, 4677-83.

26. WinNuts 1D Version – 19990713.

27. Lawrence, M. *Macromolecules,* **1997,** *30*, 2110-2119.

28. Crowther, R.; DeRosier, D.; Klug, A. *Proc. R. Soc. London* **1970,** *A317*, 319-340.

29. Berne, B.; Pecora, R. *Dynamic Light Scattering with Applications to Chemistry, Biology, and Physics*. Dover Publications, Inc.: Mineola, New York, 1976.

30. Huglin, M. *Light Scattering from Polymer Solutions*. Academic Press: London, 1972; p 34.

31. Jouyban, A.; Khoubnasabjafari, M.; Vaez-Gharamaleki, Z.; Fekari, Z.; Acree, W. *Chem. Pharm. Bull.* **2005,** *53*, 519-523.

32. Akitt, J.; Mann, B. *NMR and Chemistry: an Introduction to Modern NMR Spectroscopy*. 4th ed.; S. Thornes: Cheltenham, UK, 2000.

33. Hoppenbrouwers, E.; Li, Z.; Liu, G. *Macromolecules,* **2003,** *36*, 876-881.

34. Zheng, R.; Liu, G.; Yan, X. *J. Am. Chem. Soc.* **2005,** *127*, 15358-15359.

35. Gohy, J.; Khousakoun, E.; Willet, N.; Varshney, S.; Jerome, R. *Macromol. Rapid Commun.* **2004,** *25*, 1536-1539.

36. van Krevelen, D. *Properties of Polymers - Their Correlation with Chemical Structure; Their Numerical Estimation and Prediction from Additive Group Contributions*. 3rd ed.; Elsevier Science: Amsterdam, 1997.

37. Brandrup, J.; Immergut, E. *Polymer Handbook*. 3rd ed.; John Wiley & Sons: New York, 1989; p VII 3 -47.

38. Jain, S.; Bates, F. *Macromolecules,* **2004,** *37*, 1511-1523.

39. Forster, S.; Zisenis, M.; Wenz, E.; Antonietti, M. *J. Chem. Phys.* **1996,** *104*, 9956-9970.

40. Hadjichristidis, N.; Iatrou, H.; Pitsikalis, M.; Pispas, S.; Avgeropoulos, A. *Progr. Polym. Sci.* **2005,** *30*, 725-782.

41. Tsitsilianis, C.; Sfika, V. *Macromol. Rapid Commun.* **2001,** *22*, 647-651.

Chapter 3 – Hamburger and Striped Cylinders from Assembly of an ABC Triblock Copolymer

3.1 Preface

The material in this chapter has been accepted by *Soft Matter* for publication as, **ABC Triblock Copolymer Hamburger-like Micelles, Segmented Cylinders, and Janus Particles**.

3.2 Introduction

Block copolymers aggregate by self-assembly in block-selective solvents, to form various micelles and micelle-like aggregates (MAs). It is also possible to use other agents to cause block copolymers to aggregate and induce block collapse by complexation.[1] This block-complex formation can be used to induce the formation of various types of MAs. The type of MA formed is dependent upon the composition of the copolymer, the interfacial tension between the solvent, and the block copolymer-complex, and also the amount and type of complexing agent used. Block copolymer assembly can lead to various structures, including spheres,[2] vesicles,[3-5] nanotubes,[7-9] and various types of cylinders.[10-16] These structures have possible applications in nanofabrication, lithography, drug delivery, and functional materials.

Various agents that form complexes with diblock copolymers have been used, in order to direct the assembly of these copolymers. The amount of complexing agent used (or the ratio of the complexing agent to the complexed block), and the

type of agent used, can affect the properties of the aggregates that are formed.[1,17-19] There have also been studies of the effect of the change of pH and the addition of salts on the behavior of these systems.[20] With the use of ABC triblock copolymers, it is possible to use block-selective solvents, along with complexing agents to further control the aggregate formation. Our group has recently been investigating novel structures obtained from ABC linear triblock copolymers.[21-22]

In this chapter, the formation of hamburger and striped cylinder MAs by assembly directed by (-)-sparteine, a chiral diamine, in a block-selective solvent system is reported. There have been several instances where similar structures have been reported in the literature. Work by Lodge *et al*. with ABC *mikto*-arm triblock copolymers has produced interesting nanostructures.[23-24] From this work they discovered that striped cylinders, disks with multiple lobes and compartment micelles could be formed. Recent work by Pochan *et al.* with ABC linear triblock copolymers with organic diamines[25-28] has also lead to the formation of interesting nanostructures. They have found that striped cylinders,[25] disks,[26] stacks of disks[27] and other lamellar-type structures could be prepared.[28] Ma *et al.* used theoretical calculations to explain the formation of striped cylinders and hamburger-type MAs in ABC star triblock copolymer systems.[29] They used self-consistent field theory to model the polymer in dilute solution.

This chapter reports the use of amine complexation in a block-selective solvent system of an ABC linear triblock copolymer. In our system, the block copolymer forms hamburger-type MAs as well as striped cylinders. Also in this chapter, the transformation of hamburger-type MAs into flattened Janus-type particles is discussed. Janus-type particles are interesting structures due to their segregated functionality. Janus particles are particles that have one type of functionality on one side, and a second type on the other side. Different groups have made various types of Janus particles including spheres, cylinders, sheets and disks. Block copolymers have been used by several groups to make different types of Janus particles. Notably, polystyrene-*block*-polybutadiene-*block*-poly(methyl methacrylate) block copolymers have been used by several groups to make Janus structures, and they include Janus spheres,[30] cylinders,[31] and disks.[30]

The nanostructures in this study were prepared from poly(*tert*-butyl acrylate)-*block*-poly(2-cinnamoyloxyethyl methacrylate)-*block*-poly(succinated glyceryl monomethacrylate) (PtBA-*b*-PCEMA-*b*-PSGMA, as shown in Scheme 3.1), where the number of tBA units (*n*) was 110, the number of CEMA units (*m*) was 190, and the number of SGMA units (*l*) was 120. This determination was made by a combination of NMR and light scattering GPC.

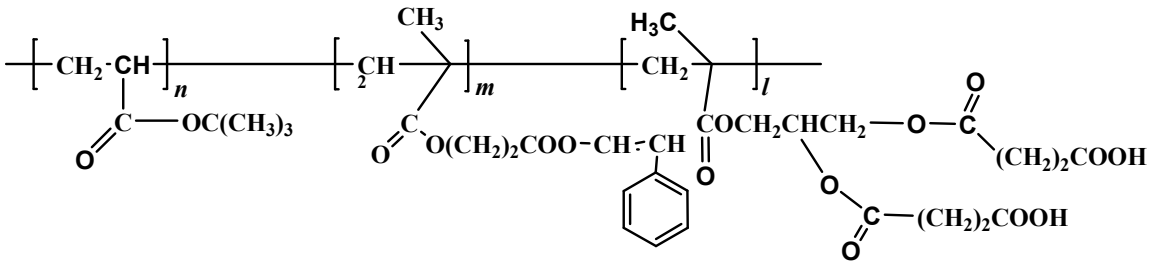

Scheme 3.1. Structure of PtBA-*b*-PCEMA-*b*-PSGMA polymer used for the study discussed in this chapter.

The MAs were prepared by dissolution of the triblock copolymer into a mutual solvent, THF, and complexation with (-)-sparteine at a molar ratio, *r*, of 0.20.

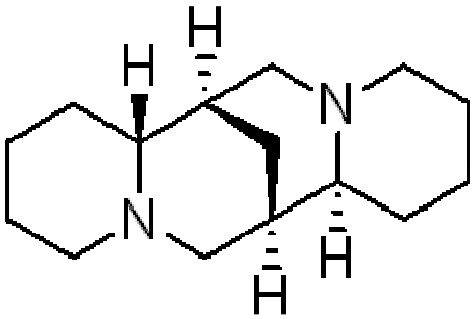

Scheme 3.2. Structure of (-)-sparteine.

Then 1- or 2-propanol was added to the polymer dispersions to give solvent mixtures of THF and 1- or 2-propanol (THF / (1 or 2-Pro) with different 1- or 2-propanol fractions, f_{Pro}, before heating. Here 1- and 2-propanol are selectively poor towards the PCEMA block (as shown by solubility studies). The particles made from 1-propanol provided more hamburger-type MAs, while those made from 2-propanol formed more striped cylinders. The PtBA block of the copolymer was grafted out of the PCEMA phase and served to stabilize these structures. The MAs prepared in this chapter were also crosslinked by exposure to UV light in order to prepare permanent hamburger structures. This provides stability to

the structures which allowed the subsequent removal of the sparteine by dialysis. This yielded the fragmented particles, which were the Janus-type particles that had PtBA chains on the convex surface and PSGMA chains on the flat surface.

3.2.1 Objectives

This chapter will study the hamburger and striped cylinder morphologies, and Janus particles made from, PtBA-*b*-PCEMA-*b*-PSGMA, an ABC triblock copolymer, in mixtures of THF, (-)-sparteine and 1- or 2-propanol. The process of formation, dimensions of the structures and the solubilities of the blocks of the polymers were studied. A number of techniques were used to study these morphologies. TEM was used to study the size of the structures and the morphology formed, and with the help of selective staining to pinpoint the location of the blocks of the copolymer. AFM was used to help study the size and height of the structures. Solubility testing was used to help understand the solvated states of the individual blocks of the copolymer in the mixture. ^{1}H NMR was used to help analyze the solvated states of the copolymer blocks *in situ*. The formation of these interesting kinetically trapped structures is explained.

3.2.2 Experimental Design Considerations

A study of PtBA-*b*-PCEMA-*b*-PSGMA was done in various solvents. This choice of this polymer was made for several reasons. First the PCEMA block can be stained by OsO_4 and made visible for TEM, while the other blocks will be unstained. PCEMA can also be photocrosslinked to lock in self-assembled

structures and make permanent nanostructures. PSGMA can be stained by $UO_2(AcO)_2$ while the other two blocks would be unstained. The PtBA block of the polymer can be hydrolyzed to PAA. Once hydrolyzed the PAA can be stained with $UO_2(AcO)_2$ with the PSGMA block. PAA will also make the structure water dispersible.

The choice of solvent system was also made for several reasons. Tetrahydrofuran is a good solvent for all of the blocks of the copolymer. Both 1- or 2-Propanol are good solvents for PtBA and PSGMA. 1- or 2-Propanol are known poor solvents for PCEMA and was found to be poor for the PSGMA (-)-sparteine complex. The amount of (-)-sparteine used in this study has been chosen to give well phase separated aggregates.

3.3 Experimental

3.3.1 Materials

Isopropanol (99.5+%), and methanol (99.8+%) were purchased from Fisher Scientific, and used as received. Inhibitor-free tetrahydrofuran (THF) was purchased from Fisher Scientific, and was passed through an Innovative Technology purification system, equipped with two alumina columns before use. Osmium tetraoxide (OsO_4) and uranyl acetate [$UO_2(AcO)_2$] were purchased from Electron Microscopy Sciences, and used as received. RuO_4 was prepared by the addition of 1 mL of sodium hypochlorite (Aldrich 10-13 %) in water to 20 mg of ruthenium tricholoride trihydrate (Aldrich) prior to use.[32] Pyridine (Aldrich 99+%)

was refluxed with calcium hydride (Aldrich, reagent grade, 95 %) overnight, and distilled prior to use. Cinnamoyl chloride (98%, predominantly *trans*), 1-propanol (99.5+%) and succinic anhydride (99+%) were purchased from Aldrich, and used as received. Isopropanol-d_8 (D, 99%), tetrahydrofuran-d_8 (D, 99.5%) and pyridine-d_5 (D, 99.5%) were purchased from Cambridge Isotope Laboratories, and used as received.

3.3.2 Polymers

PtBA-*b*-PCEMA-*b*-PSGMA was derived from PtBA-*b*-PCEMA-*b*-PGMA, where PGMA denotes poly(glyceryl monomethacrylate). The preparation of PtBA-*b*-PCEMA-*b*-PGMA has been reported before,[33-34] the procedure for the synthesis is included in Appendix A. PtBA-*b*-PCEMA-*b*-PSGMA was then produced by the reaction of the hydroxyl groups of the PGMA with succinic anhydride to yield PSGMA groups by methods described previously.[33] In order to ensure an essentially quantitative reaction, the molar ratio used between succinic anhydride and the hydroxyl groups of PGMA was 5.0.

PtBA-*b*-PCEMA-*b*-PSGMA was characterized in the PtBA-*b*-PCEMA-*b*-PSMA form in order to ensure that there was no association between different polymer chains due to H-bond formation. The structure of poly(solketyl methacrylate) (PSMA) is given below:

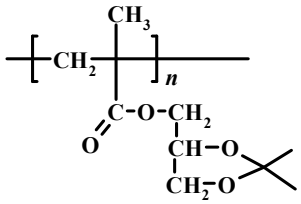

PSMA

Scheme 3.3. Structure of PSMA.

This polymer was analyzed by ^{1}H NMR in pyridine-d_5 to determine the repeat unit number ratios *l/m/n*. The specific refractive index increment dn_r/dc and light scattering molecular weight of the copolymer were determined in THF. The polydispersity index M_w/M_n of the sample was measured by SEC in THF, based on polystyrene standards. By combining the information obtained from ^{1}H NMR, light scattering and SEC, the weight average repeat unit numbers l_w, m_w, and n_w for the triblock copolymer were calculated to be 110, 190 and 120 for the PtBA, PCEMA and PSMA blocks, respectively (Table 3.1). The polydispersity index of the polymer was low, as the precursor to this polymer was prepared by anionic polymerization. All molecular block lengths are accurate to $\pm$10 units.

Table 3.1. Characteristics of polymers used in this study

Sample	dn_r/dc (mL/g)	SEC M_w/M_n	SEC-LS $10^{-4} \times M_n$ (g/mol)	NMR $n/m/l$	*n*	*m*	*l*
Triblock	0.181	1.06	8.7	0.93/1.7/1.0	110	190	120
PtBA	0.053	1.05	1.4	1 / 0 / 0	100		
PCEMA	0.156	1.01	5.1	0 / 1 / 0		200	
PSMA	0.067	1.04	1.4	0 / 0 / 1			70

Three homopolymers PtBA, PCEMA, and PSGMA were synthesized and used as models to check the solubility of the three blocks of the triblock under different

solvation conditions. Their characteristics are also listed in Table 3.1. The polydispersity indices of these samples were also low.

3.3.3 Polymer Solubility Tests

Visual inspection revealed that $PtBA_{100}$ and $PSGMA_{70}$ were soluble in THF/1- or 2-propanol at any mixing ratios. To determine the critical propanol volume fraction (f^*_{POH}), above which $PCEMA_{200}$ became insoluble, $PCEMA_{200}$ was first dissolved in THF at 5 mg/mL. 1- or 2-Propanol was added to the polymer solution until turbidity just developed. For 1-propanol, f^*_{POH} was found to be 54% while it was found to be 50% for 2-propanol. In THF at 5 mg/mL, (-)-sparteine at 11 mol% relative to the SGMA groups was sufficient to cause a $PSGMA_{70}$ solution to turn cloudy. All solubility measurements were done at room temperature which was approximately 20 ^oC.

3.3.4 Micelle-like Aggregate (MA) Preparation

Unless mentioned otherwise, the following protocol was used to prepare MAs. Initially 2-3 mg of the polymer was dissolved in 0.15 mL of THF. To this was then added a (-)-sparteine solution dissolved in 1- or 2-propanol at 8.4 M to a final sparteine content of 20 mol% relative to the SGMA groups. The rest of 1 or 2-propanol was added over 5 min until f_{POH} reached 95%. The final P1 concentration was always ~1 mg/mL. This solution was then sealed in a vial and stirred at 70 ^oC in an oil bath for a pre-designated time before spraying onto nitrocellulose-coated copper grids for TEM observation.

3.3.5 ^{1}H NMR Study

The triblock copolymer was first dissolved in THF-d_8 for 30 min. Next, a small amount of (-)-sparteine (50 mol% to PSGMA groups) was added to the solution. Isopropanol-d_8 was then slowly added to the mixture until the desired concentration was reached (polymer concentration of ~2.0 mg / mL). The solution was sealed in a vial, and then stirred at 70 ^{o}C in an oil bath for one day before observation. The samples were then transferred into an NMR tube, and analyzed on a 500 MHz Bruker AM-500 spectrometer. These samples were also aspirated onto nitrocellulose-coated copper grids for TEM analysis. Signal intensities were obtained by performing line fitting using WinNuts.[35]

3.3.6 Janus Particle Preparation from Hamburger-like MAs

Hamburger-like MAs in THF/1-propanol at $f_{POH} = 95\%$ containing 20 mol% (-)-sparteine were crosslinked for 30 min using light produced by a 500-W Hg lamp and had passed through a 270-nm cutoff filter. This caused 35% of PCEMA double bonds to undergo dimerization as determined by UV spectroscopy of the peak height at 270nm. The sample was then transferred into a dialysis bag (12-14000 MW cut-off, Spectra Pore) and dialyzed against acidic methanol (1mL conc. HCl diluted with 150mL MeOH) for 24 h with the solution outside the dialysis tube changed 3 times. The resulting MA solution was acidic,

and the MAs did not disperse well. A portion of this suspension, 0.5 mL, was concentrated to < 0.10 mL before the addition of 2 mL of DMF. The mixture was sonicated in Branson 1200 sonicator for 5 min before it was dialyzed against DMF for 24 h with DMF, which was changed 3 times. After dialysis, the sample was sonicated for 30 min and sprayed onto carbon-coated copper grids for observation by TEM.

3.3.7 Transmission Electron Microscopy (TEM)

MAs were aspirated onto nitrocellulose or carbon coated copper grids and dried at room temperature for 1 hour. The specimens were then stained by OsO_4 vapor for 2 h, RuO_4 vapor for 45 min, or $UO_2(AcO)_2$ solution before TEM observation. Staining solutions of $UO_2(AcO)_2$ were prepared in the solvent (or mixture) from which the sample was sprayed. Staining was performed by equilibrating a sprayed sample on a TEM grid with a drop of the $UO_2(AcO)_2$ solution for 20 mins. After removing the droplet, the excess $UO_2(AcO)_2$ was removed by rinsing the grid with droplets of solvent ten times. All transmission electron microscopy (TEM) observations were made on a Hitachi 7000 instrument operated at 75 kV.

3.3.8 Atomic Force Microscopy (AFM)

Specimens were prepared by aspiration of solution samples onto cleaned silicon wafers, or freshly cleaved mica surfaces. All samples were analyzed by tapping-mode atomic force microscopy (AFM), using a Veeco multimode

instrument equipped with a Nanoscope IIIa controller. The tips used were AppNano ACT Tapping mode AFM probes with tip radii of 5-6 nm, tip aspect ratios of 3:1 to 5:1, force constants of 25-75 N/m, and resonance frequencies of 200-400 kHz.

3.4 Results and Discussion

3.4.1 Triblock Copolymer Characterization

The PtBA-*b*-PCEMA-*b*-PSGMA sample was characterized in the PtBA-*b*-PCEMA-*b*-PSMA form to ensure that there was no association between different polymer chains due to H-bonding. The repeat unit number ratios (*l/m/n*), were calculated from the intensities of the ^{1}H NMR peaks of the blocks of the copolymer. The specific refractive index increment dn_r/dc and light scattering molecular weight of the copolymer were determined in THF. The polydispersity index M_w/M_n of the sample was measured by SEC in THF based on polystyrene standards. By combining the information obtained from ^{1}H NMR, light scattering and SEC the weight average repeat unit numbers l_w, m_w, and n_w for the triblock copolymer were calculated to be 110, 190 and 120 for the PtBA, PCEMA and PSMA blocks, respectively (Table 3.1).

3.4.2 Triblock Copolymer Stability

The MAs prepared in this chapter were made from PtBA-*b*-PCEMA-*b*-PSGMA in a mixture of THF, (-)-sparteine and 1- or 2-propanol after heating at 70 ^{o}C. We confirmed the stability of PtBA (a polymer that has a labile ester group) at these

conditions. The polymer was studied using ^{1}H NMR in deuterated THF which showed cleavage of the *tert*-butyl under acidic conditions (Figure 3.1).[36]

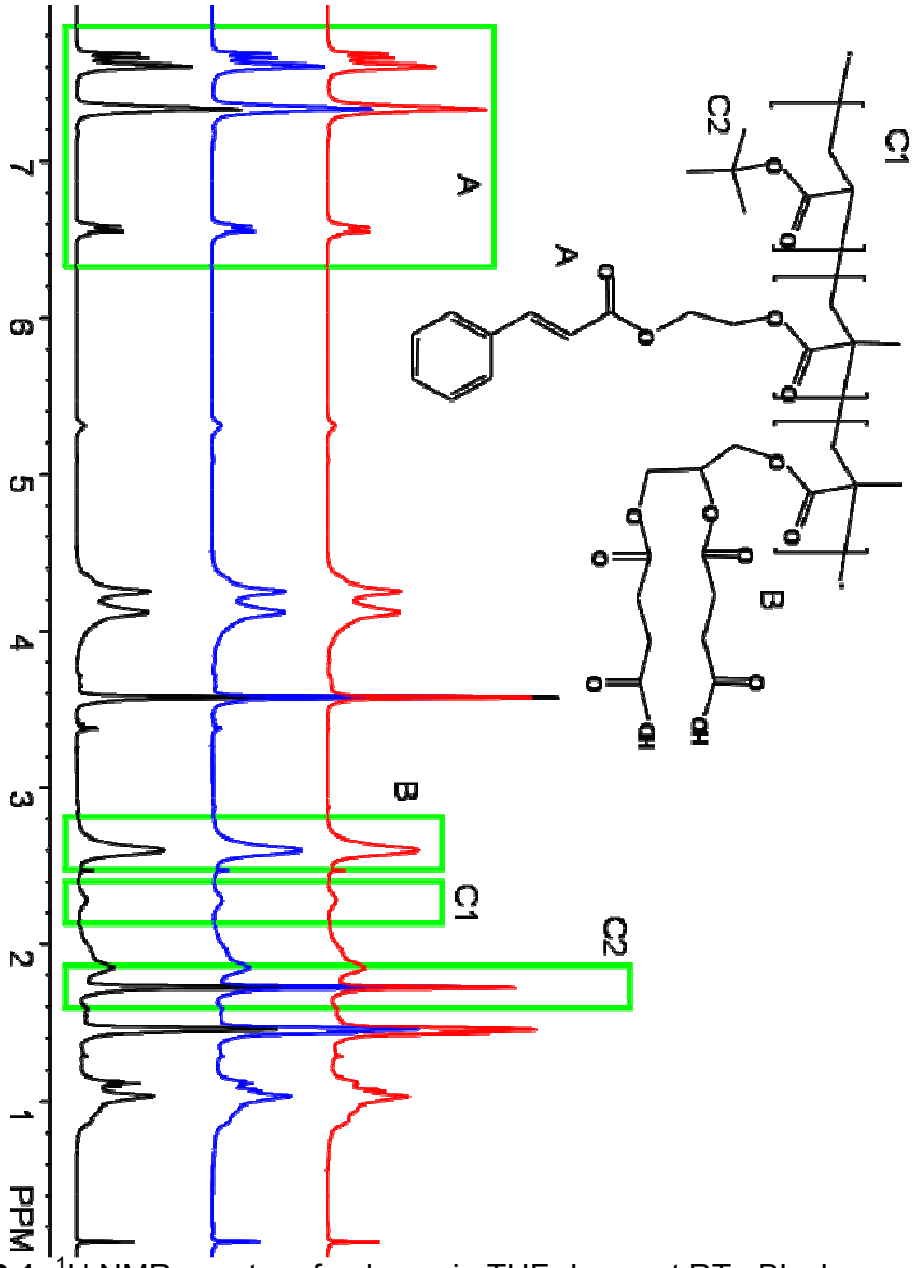

Figure 3.1. ^{1}H NMR spectra of polymer in THF-d_8 run at RT: Black sprectrum – ^{1}H NMR initially after heating for one hour at 70 ^{o}C, Blue sprectrum – ^{1}H NMR run after heating at 70 ^{o}C for one day, Red sprectrum – ^{1}H NMR run after heating at 70 ^{o}C for two days.

After heating for 2 days at 70 ^{o}C, there was a 75% decrease in the intensity of the PtBA proton peak at 1.7 ppm (Figure 3.2). This suggests the loss of 75% of

the *tert*-butyl groups and confirmed the instability of the tBA groups under the studied conditions (Figure 3.2).[36] However, if the polymer was heated in the presence of (-)-sparteine (with a 0.50 molar ratio (*r*) of (-)-sparteine to SGMA) no *tert*-butyl group cleavage was detected in either THF-d_8 or THF-d_8/2-propanol-d_8 (volume fraction of 95%). This was probably due to the reduced acidity of the mixture after (-)-sparteine addition. Also, the addition of (-)-sparteine causes the aggregation of the PSGMA block and the segregation of the PtBA block from the PSGMA block. To retain electric neutrality, the dissociated protons of PSGMA should remain close to the carboxylate anions. So the acidity experienced by the PtBA block will be minimized when the PtBA and PSGMA blocks are segregated. Thus the stability of the PtBA block ensured that the MAs observed in this study were those of PtBA-*b*-PCEMA-*b*-PSGMA rather than those of the hydrolysis products.

This ^{1}H NMR analysis indicates that upon formation of the hamburger MAs, there is no breakdown of the *t*-butyl groups of the PtBA block due to the complexation of the PSGMA block. The difference in ratio of $I_{tBA-t-butyl} \big/ I_{tBA-backbone}$ between the samples without isopropanol-d_8 (40-45) and the sample with isopropanol-d_8 (25) is due to the difficulty of getting a good peak fit for the PtBA backbone peak of the isopropanol-d_8 sample (due to over estimation).

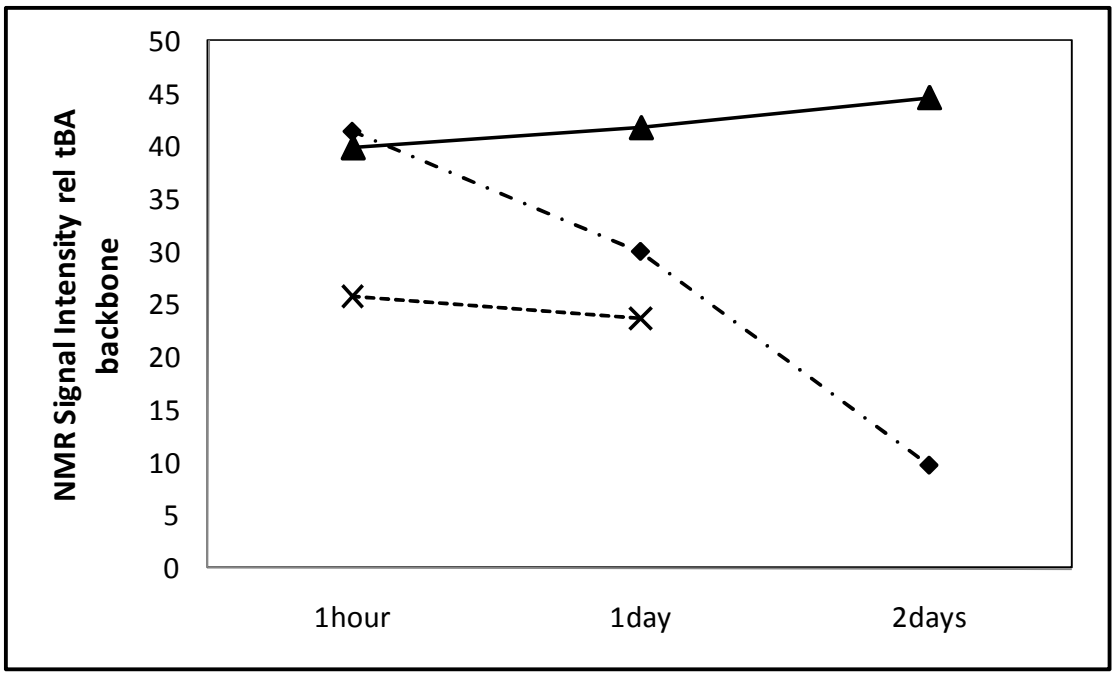

Figure 3.2. Plots of variation in $I_{tBA-t-butyl}/I_{tBA-backbone}$ (♦) in THF-d_8, $I_{tBA-t-butyl}/I_{tBA-backbone}$ (▲) in THF-d_8/(-)-sparteine with r = 0.50, and $I_{tBA-t-butyl}/I_{tBA-backbone}$ (X) in THF-d_8/(-)-sparteine/isopropanol-d_8 with r = 0.50 and $f_{\mathrm{Pro}} =$ 0.95, after heating at 70 ^{o}C with ^{1}H NMR run at 70 ^{o}C.

3.4.3 Micelle-like Aggregates (MAs) in 1- and 2-Propanol

The MAs were prepared by heating the triblock copolymer at 70 ^{o}C for at least one day. This elevated temperature was used, because the copolymer did not disperse well at room temperature after either 1- or 2-propanol was added. In 1- or 2-propanol, only the PCEMA block of PtBA-*b*-PCEMA-*b*-PSGMA was not soluble, and the polymer formed a mixture of spherical and cylindrical MAs as confirmed by TEM (Figures 3.3 and 3.4). There were minimal spherical MAs formed by the polymer in 1-propanol and with more in the 2-propanol case. In the case of samples prepared from THF/1- or 2-propanol only spherical MAs were observed. In 1- or 2-propanol with (-)-sparteine with r = 0.20, bilayers and

vesicular aggregates were formed. After spraying from THF/(-)sparteine with *r* = 0.20, ill-defined spherical particles with PSGMA cores were observed. The addition of (-)-sparteine into a spherical, PtBA-*b*-PCEMA-*b*-PSGMA, MA solution in THF/1- or 2-propanol at $f_{\mathrm{Pro}} =$ 95% led to the formation of what appeared to be bilayers and vesicles. Figures 3.3 and 3.4 show typical TEM images of the MAs mentioned above. The visible parts of the structures in Figures 3.3 and 3.4 are the PCEMA cores of PtBA-*b*-PCEMA-*b*-PSGMA because only the PCEMA block was stained by OsO_4. The object in the center of Figure 3.3b appears to be a broken vesicle, while the two round items at the bottom left and right may be bilayers (due to their uniform gray colour).

The addition of 1- or 2-propanol ($f_{\mathrm{Pro}} =$ 95%) to a polymer in THF with (-)-sparteine with *r* = 0.20 led to the formation of a mixture of hamburgers and segmented cylinders (more hamburgers in 1-propanol, and more segmented cylinders in 2-propanol).

Table 3.2 includes the average particle size of these samples. As mentioned previously the morphology changed upon the addition of both THF and the chiral amine, (-)-sparteine. In both 1- and 2-propanol, the polymer forms a mostly cylindrical morphology (Figures 3.3a and 3.4a). When the solvent composition includes 5% THF the morphology is exclusively spheres (Figures 3.3c and 3.4c). This type of morphological transition has been seen before by Zhang *et al*.[37]

This is due to the change in the interfacial tension between the solvent, the soluble PtBA and PSGMA, and the insoluble PCEMA blocks.

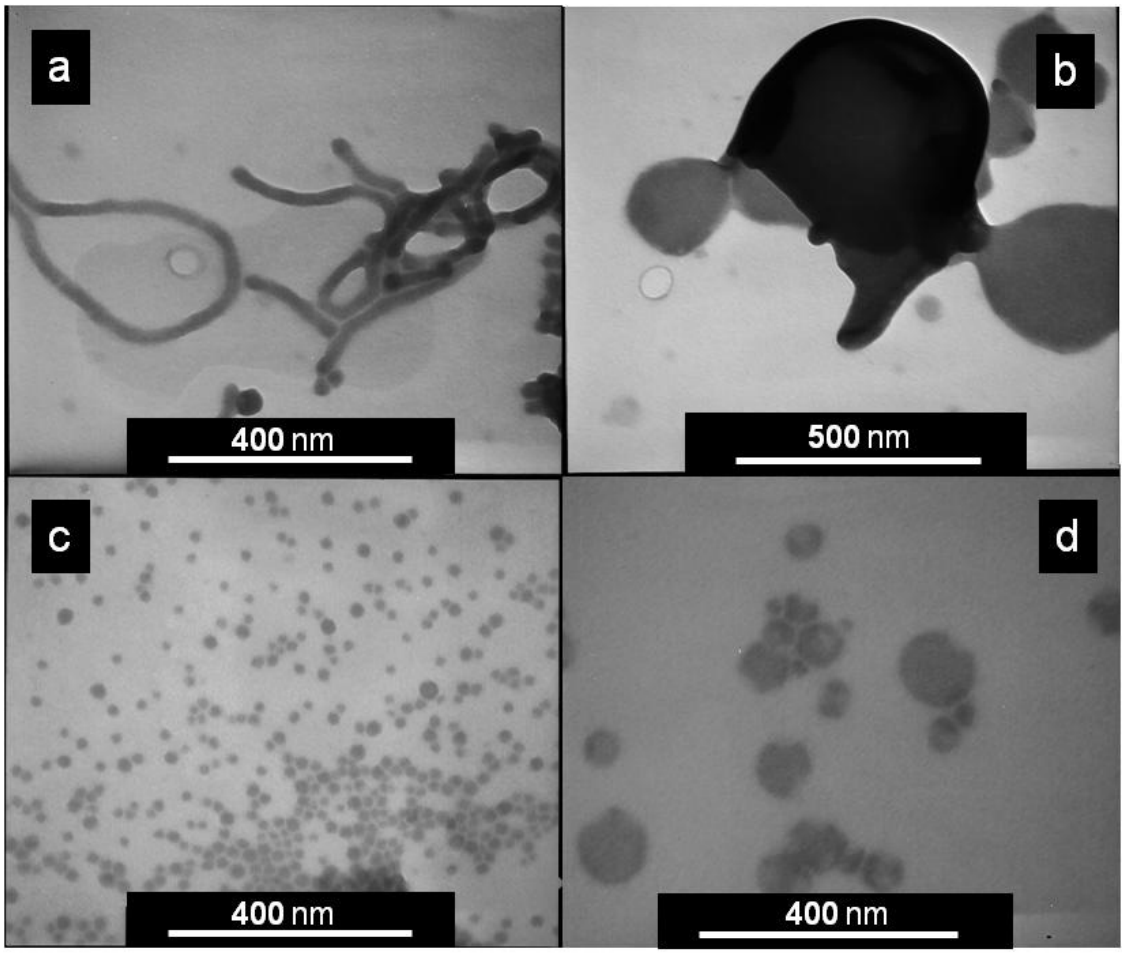

Figure 3.3. TEM images of MAs aspirated from: 1-propanol (**a**), 1-propanol/(-)-sparteine with r = 0.20 (**b**), THF/1-propanol with $f_{\mathrm{Pro}} =$ 95% (**c**), and THF/1-propanol/(-)-sparteine with $f_{\mathrm{Pro}} =$ 95% and r = 0.20 (**d**). The staining agent used was OsO_4.

The addition of (-)-sparteine to a solution of the polymer in THF, and addition of 1- or 2-propanol, induces the formation of the hamburger and striped cylinder type MAs (Figures 3.5a and 3.5b). Here the reagent listing order is the same as the sequence of THF, (-)-sparteine, and propanol addition into the polymer sample. The formation of these aggregates starting in THF allows the collapse

of the PSGMA block by complexation with (-)-sparteine before PCEMA block collapse. THF also serves to plasticize the core blocks in the aggregates, and allow for the formation of better-defined MAs. The effect of varying these parameters (propanol content, (-)-sparteine content and reagent addition order) was studied and is reported later in this chapter. Similar hamburger and striped cylinder morphologies have been reported before by Li *et al.*[23] in an ABC *mikto*-arm system, and has been shown to be possible by theoretical calculations by Ma *et al.*[29] for ABC star triblock copolymers.

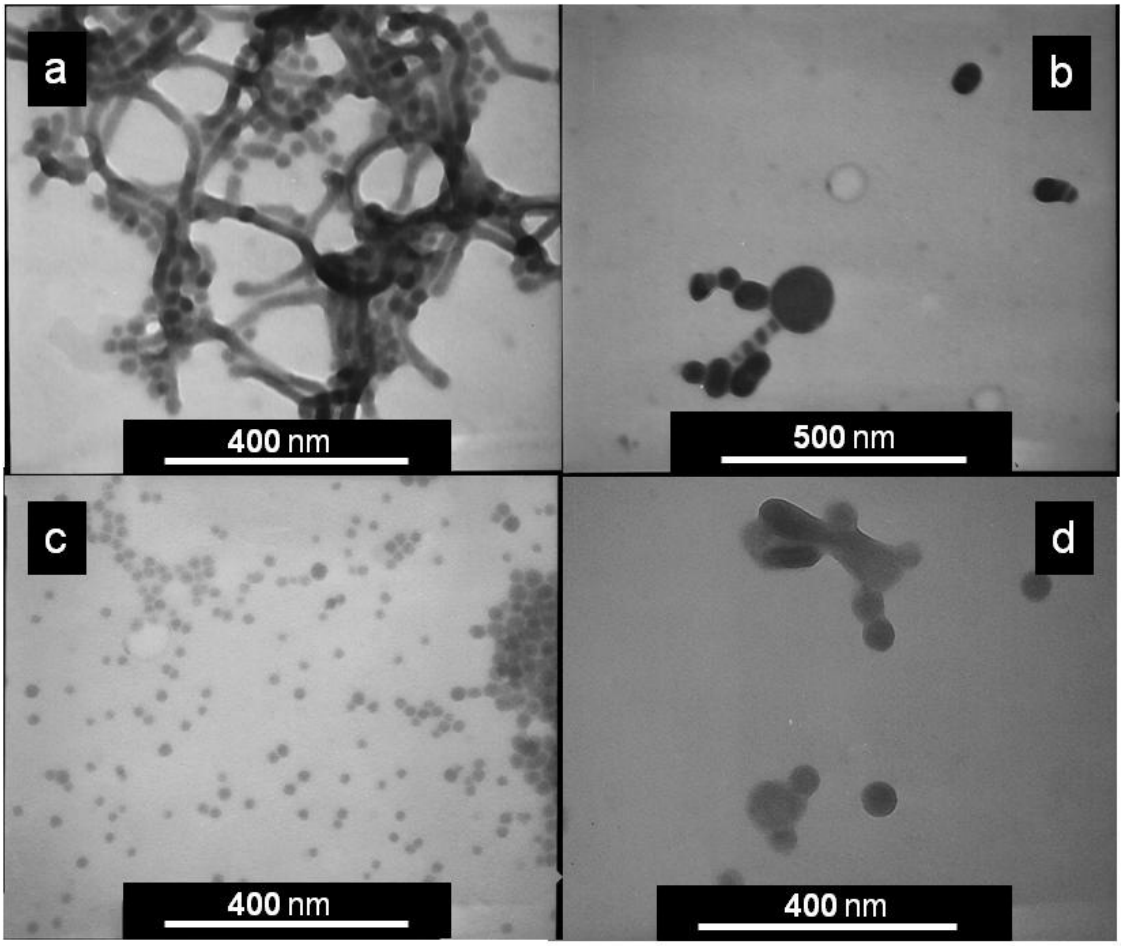

Figure 3.4. TEM images of MAs aspirated from: 2-propanol (**a**), 2-propanol/(-)-sparteine with *r* = 0.20 (**b**), THF/2-propanol with $f_{\mathrm{Pr}o} =$ 95% (**c**) and THF/2-propanol/(-)-sparteine with $f_{\mathrm{Pr}o} =$ 95% and *r* = 0.20 (**d**). The staining agent used was OsO_4.

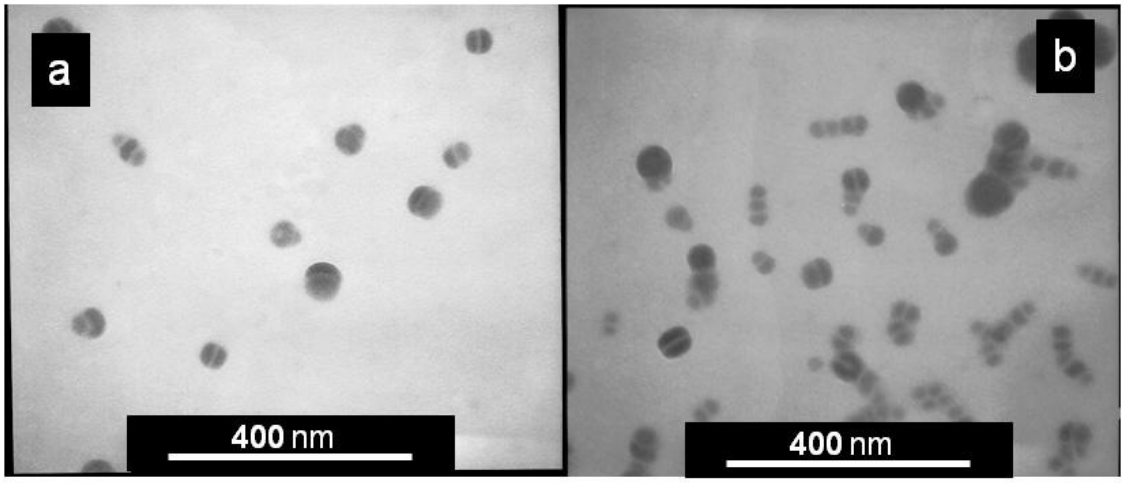

Figure 3.5. TEM images of MAs aspirated from: THF/(-)-sparteine/1-propanol with r = 0.20 and $f_{\mathrm{Pro}} = 95\%$ (**a**) and THF/(-)-sparteine/2-propanol with r = 0.20 and $f_{\mathrm{Pro}} = 95\%$ (**b**). The staining agent used was OsO_4.

A surprising feature of Figure 3.5a was that most of the hamburgers seemed to lie sidewise on the TEM grid so that the "filling" was visible. This behavior may originate from the fact that most of the hamburgers were longer along their axial direction. Due to their length, the hamburgers may have preferred to lie on their side, providing more contact between the hamburgers and their substrate. Despite this, we note the existence of a few solid dark circles which may represent hamburgers that were standing upright. These particles may have landed in a position intermediate between lying and standing upright.

The PCEMA domain size in the 1- and 2-propanol systems are similar within error (27 vs. 25 nm), this is the diameter of the cylinders seen in these samples. The asterisk beside these entries in Table 3.2 indicates that the PCEMA domain size of these entries is the diameter of the cylinders in these samples as opposed

to all other samples where the diameters are those of spherical particles. The addition of a small amount of (-)-sparteine to either system causes a large amount of aggregation to occur, and a large increase in the size of the average PCEMA domain size (from 27 to 100 nm, and 25 to 58 nm). Meanwhile the addition of a small amount of THF to the 1- and 2-propanol systems leads to particles of a different morphology (spherical vs. cylindrical), and a slightly smaller average PCEMA domain size (from 27 to 20 nm, and 25 to 20 nm). These samples prepared in the different propanol systems also have the same PCEMA domain size (20 vs. 20 nm). The total (whole particle) PCEMA domain size of the aggregates from THF/(-)-sparteine and 1- or 2-propanol with r = 0.20 and $f_{\mathrm{Pr}o} =$ 95%, are similar within error (55 vs. 52 nm).

Table 3.2. Characteristics of MAs prepared in this study.

Solvent	Sample	Average PCEMA domain size (nm)
1-Propanol	Figure 3.3a	27* +/- 3
2-Propanol	Figure 3.4a	25* +/- 2
1-Propanol/(-)-sparteine with r = 0.20	Figure 3.3b	100+
2-Propanol/(-)-sparteine with r = 0.20	Figure 3.4b	58 +/- 22
THF/1-Propanol with $f_{\mathrm{Pr}o} =$ 95%	Figure 3.3c	20 +/- 3
THF/2-Propanol with $f_{\mathrm{Pr}o} =$ 95%	Figure 3.4c	20 +/- 3
THF/1-propanol/(-)-sparteine with $f_{\mathrm{Pr}o} =$ 95% and r = 0.20	Figure 3.3d	Irregular
THF/(-)-sparteine/2-propanol with $f_{\mathrm{Pr}o} =$ 95% and r = 0.20	Figure 3.4d	Irregular
THF/(-)-sparteine/1-propanol with r = 0.20 and $f_{\mathrm{Pr}o} =$ 95%	Figure 3.5a	55 +/- 9
THF/(-)-sparteine/2-propanol with r = 0.20 and $f_{\mathrm{Pr}o} =$ 95%	Figure 3.5b	52 +/- 13

3.4.4 Solvent Composition

The solvent composition used to make the MAs was varied to see what impact it had on the morphology of the aggregates produced.

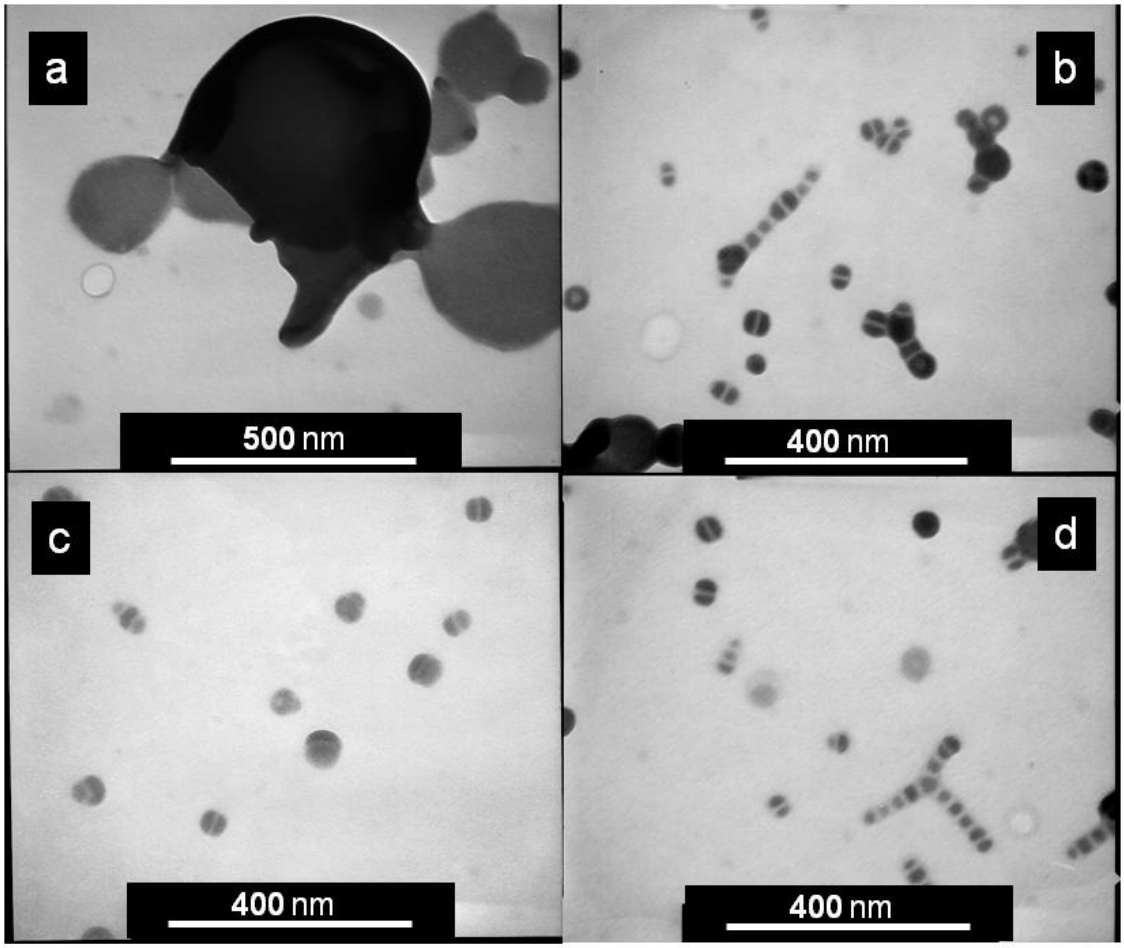

Figure 3.6. TEM images of MAs aspirated from: 1-propanol/(-)-sparteine with r = 0.20 (**a)**, THF/(-)-sparteine/1-propanol with r = 0.20 and $f_{\mathrm{Pro}} =$ 98% (**b)**, THF/(-)-sparteine/1-propanol with r = 0.20 and $f_{\mathrm{Pro}} =$ 95% **(c)** and THF/(-)-sparteine/1-propanol with r = 0.20 and $f_{\mathrm{Pro}} =$ 90% **(d)**. The staining agent used was OsO_4.

The aggregate structure in 1-propanol with no THF contained large disk-like MAs of hundreds of nanometers in size (Figure 3.6a). When the solvent composition began to incorporate THF, the structures changed to hamburger type aggregates

and short chains (Figure 3.6b). Upon increasing the THF content, this produced little change in the aggregate structure (Figure 3.6c, d). A similar effect was seen in the 2-propanol/THF system (Figure 3.7a-d).

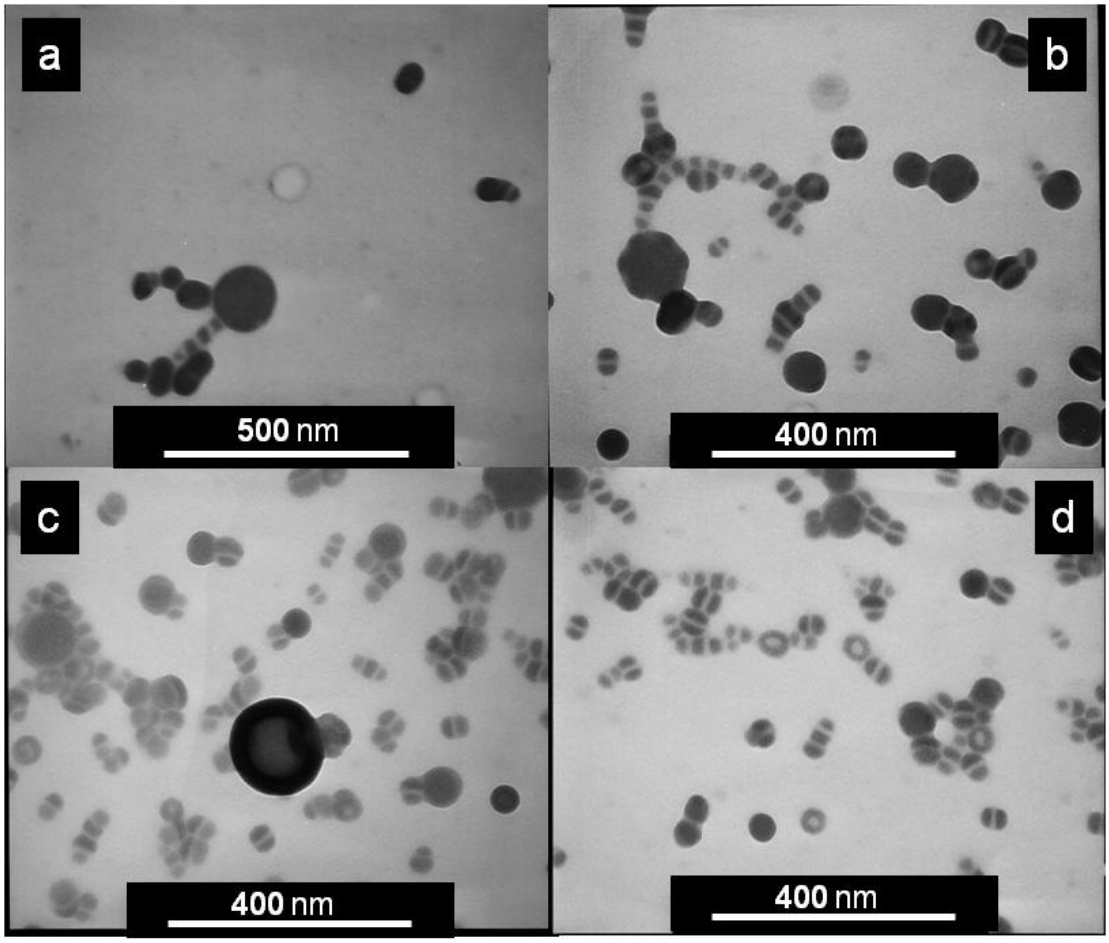

Figure 3.7. TEM images of MAs aspirated from: 2-propanol/(-)-sparteine with r = 0.20 (**a)**, THF/(-)-sparteine/2-propanol with r = 0.20 and $f_{\mathrm{Pr}o}$ = 98% (**b)**, THF/(-)-sparteine/2-propanol with r = 0.20 and $f_{\mathrm{Pr}o}$ = 95% **(c)** and THF/(-)-sparteine/2-propanol with r = 0.20 and $f_{\mathrm{Pr}o}$ = 90% **(d)**. The staining agent used was OsO_4.

The lack of change of MA morphology with change in solvent composition may be due to the presence of a small amount of THF. The addition of a small amount (2 vol%) of THF appeared to be necessary to plasticize the PCEMA domains of the MAs, and provide some chain mobility. Further increases of the

THF content did not appear to significantly change the observed aggregate structure, and it can be inferred that chain mobility and other properties did not significantly change.

3.4.5 (-)-Sparteine Content

The amount of (-)-sparteine was varied to determine its impact on the formation of the MAs. The polymer forms spherical MAs (20 +/- 3 nm) in 1-propanol/THF with $f_{\mathrm{Pr}o} =$ 95% (Figure 3.8a). Hamburgers and striped cylinders were produced by the addition of (-)-sparteine before the subsequent addition of 1-propanol. With the incorporation of a small amount (r = 0.10) of (-)-sparteine into the structure, the formation of hamburger type MAs were observed (Figure 3.8b).

Addition of (-)-sparteine causes complexation of the PSGMA block with (-)-sparteine (discussed in Section 3.4.8) and aggregation of the PSGMA block. An increase of the amount of (-)-sparteine leads to slightly larger aggregates (40 +/- 8 nm vs. 55 +/- 9 nm, as shown in Figures 3.8b vs. 3.8c). Increasing further the (-)-sparteine content, the percentage of the striped cylinder morphology increased (Figure 3.8d), and the formation of some disk-like MAs. This change of morphology may be due to the increase in the amount of (-)-sparteine, which allows for more interaction between the collapsed PSGMA and (-)-sparteine.

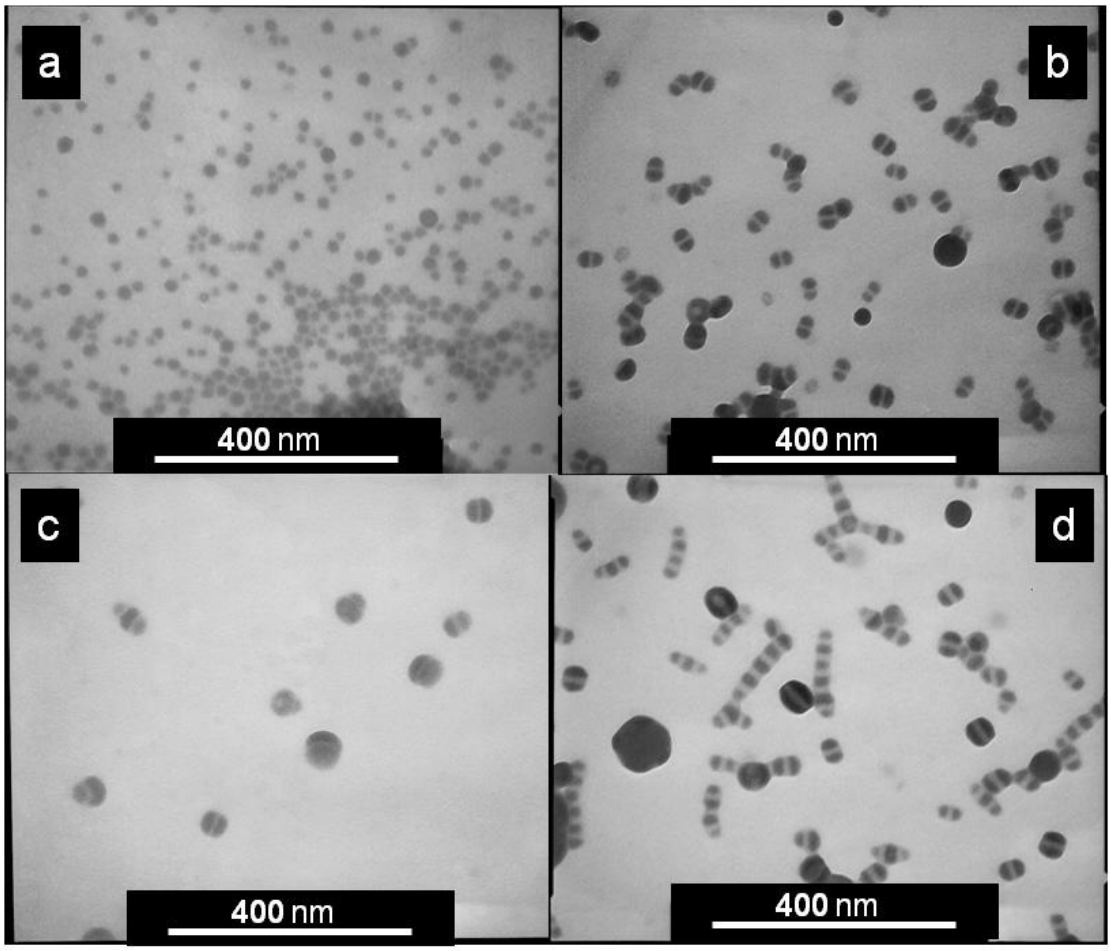

Figure 3.8. TEM images of MAs aspirated from: THF/1-propanol with $f_{\mathrm{Pr}o} =$ 95% (**a)**, THF/(-)-sparteine/1-propanol with *r* = 0.10 and $f_{\mathrm{Pr}o} =$ 95% (**b)**, THF/(-)-sparteine/1-propanol with *r* = 0.20 and $f_{\mathrm{Pr}o} =$ 95% **(c)** and THF/(-)-sparteine/1-propanol with *r* = 0.65 and $f_{\mathrm{Pr}o} =$ 95% **(d)**. The staining agent used was OsO_4.

Similar to the 1-propanol case, the polymer in THF/2-propanol solvent mixture with $f_{\mathrm{Pr}o} =$ 95% forms spherical MAs of 20 +/- 3 nm (Figure 3.4c). The addition of *r* = 0.10 (-)-sparteine before the 2-propanol addition, caused the formation of MAs that were predominantly of the striped cylinder morphology (Figure 3.9a). This contrasts with the predominant formation of hamburger type MAs seen in the 1-propanol case. Increase in the amount of (-)-sparteine, to *r* = 0.20, lead to

the formation of more hamburger type MAs (Figure 3.9b). Finally, the further increase of the amount of (-)-sparteine leads to the formation of disk-like MAs (Figures 3.9c and d).

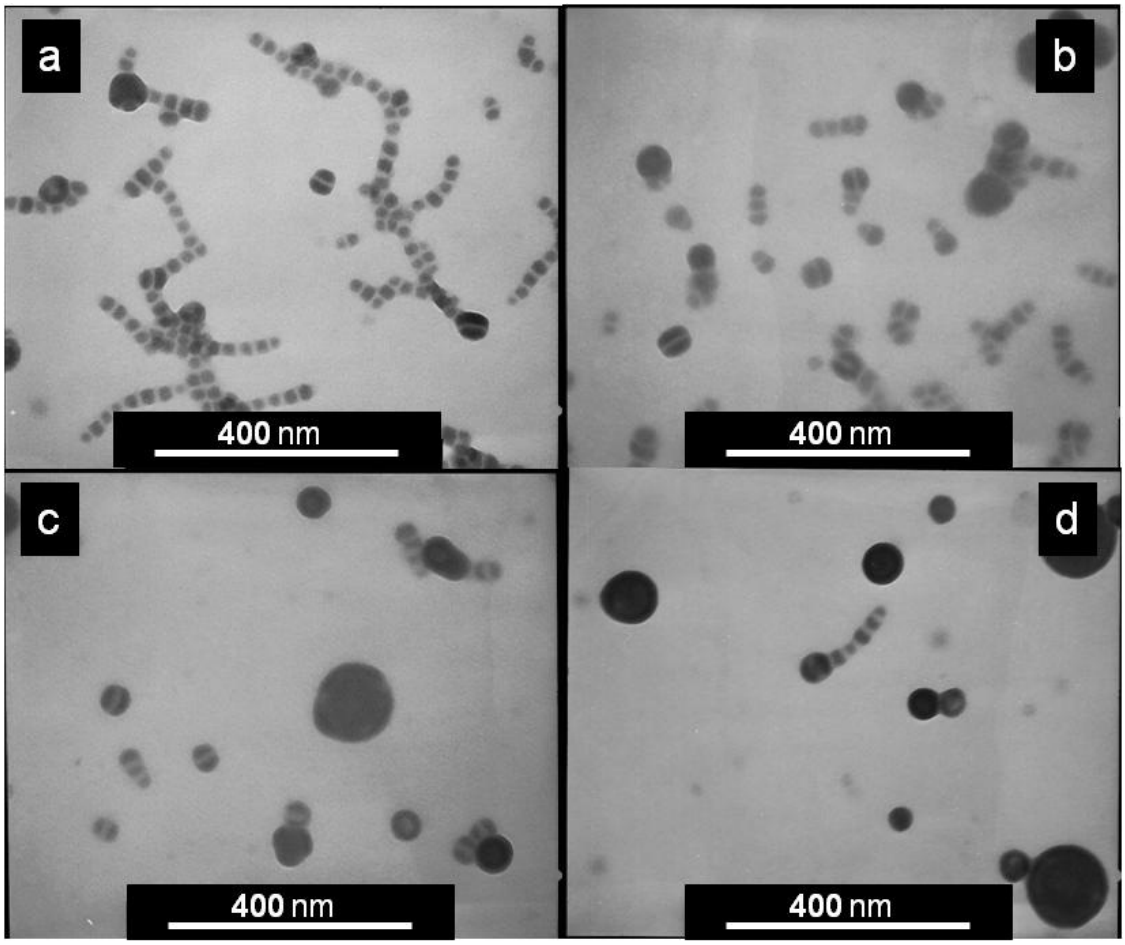

Figure 3.9. TEM images of MAs aspirated from: THF/(-)-sparteine/2-propanol with *r* = 0.10 and $f_{\mathrm{Pro}} =$ 95% (**a**), THF/(-)-sparteine/2-propanol with *r* = 0.20 and $f_{\mathrm{Pro}} =$ 95% (**b**), THF/(-)-sparteine/2-propanol with *r* = 0.50 and $f_{\mathrm{Pro}} =$ 95% **(c)** and THF/(-)-sparteine/2-propanol with *r* = 0.65 and $f_{\mathrm{Pro}} =$ 95% **(d)**. The staining agent used was OsO_4.

There were minor differences between the systems prepared in 1- and 2-propanol cases that cannot be readily explained. In both cases, a small amount of (-)-sparteine was needed to form the morphologies of interest, but in the presence of 1-propanol, at low *r*, a majority of hamburger MAs were formed,

while in 2-propanol, a majority of striped cylinders were formed. An increase of *r*, the amount (-)-sparteine, in the 1-propanol system yields striped cylinders, while in the 2-propanol case, it yields hamburger MAs. In both cases (*r* = 0.20, 0.50) there appeared to be a mixture of striped cylinders and hamburger-type MAs formed. Finally, further increases of the (-)-sparteine content eventually lead to the formation of what appeared to be disk-like MAs for both propanol cases (*r* = 0.65). These aggregates are uniformly shaded, opposed to vesicular aggregates, which would have a dark ring around a slightly lighter core. The difference between the 1- and 2-propanol cases is the relative amount of hamburger vs. striped cylinder aggregates.

3.4.7 Effect of Order of Reagent Addition on Polymer Aggregation

As seen earlier the addition of the reagents in a different order caused drastically different morphologies to form. In all cases, the polymer was first dissolved in THF. In the first case, 1-propanol was added to $f_{\mathrm{Pr}o} = 95\%$, then (-)-sparteine was added to *r* = 0.20. The polymer formed spherical MAs in 1-propanol/THF with $f_{\mathrm{Pr}o} = 95\%$ (Figure 3.10a) with the PCEMA block as the core of spherical aggregates. After addition of (-)-sparteine, hamburger MAs were not formed (as in Figure 3.10c). Instead the polymer formed only disk-like aggregates and spherical MAs (Figure 3.10b). Thus, a change in the order of reagent addition changed the final MA structure. If the hamburger-type morphology is a true thermodynamic morphology, the same morphology should result, regardless of

reagent addition sequence. Due to this reason, the hamburger-type MAs may be a kinetically-trapped morphology.

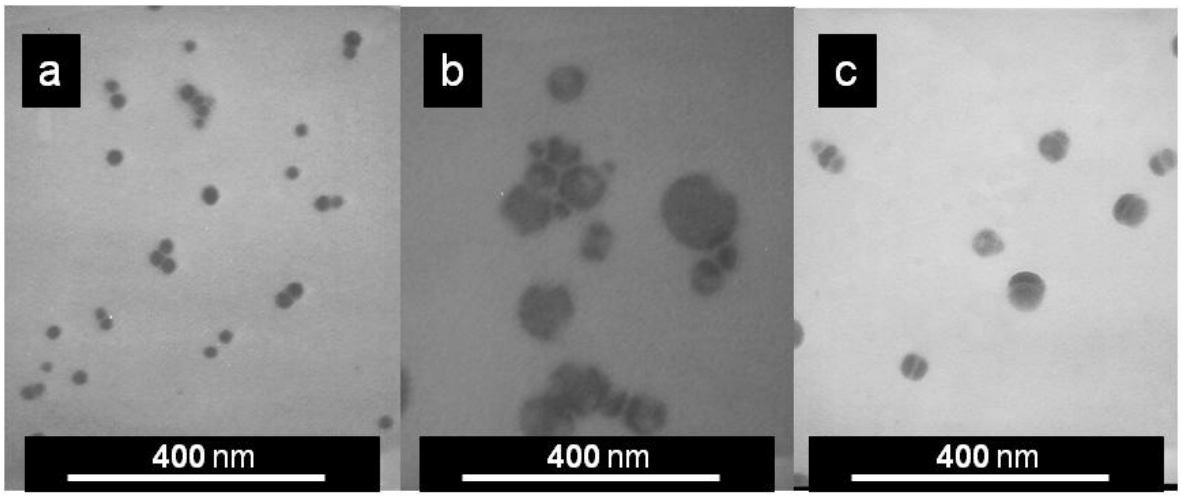

Figure 3.10. TEM images of MAs aspirated from THF/1-propanol with $f_{\mathrm{Pr}o} =$ 95% at 70 °C (**a)**, the same system after addition (-)-sparteine (*r* = 0.20) and heated at 70 °C (**b**) and THF/(-)-sparteine/1-propanol with *r* = 0.20 and $f_{\mathrm{Pr}o} =$ 95%. The staining agent used was OsO_4.

Similarly, the polymer formed spherical MAs in THF/2-propanol (Figure 3.11a) and the change in the addition order of the reagents caused formation of disk-like MAs (Figure 3.11b), and other amorphous aggregates unlike when the (-)-sparteine was added before 2-propanol (Figure 3.11c).

Bilayers and vesicles were prepared in THF/propanol/(-)-sparteine mixtures, but predominantly hamburgers and segmented cylinders were prepared in THF/(-)-sparteine/propanol when the propanol and (-)-sparteine addition sequence was reversed. Thus, different types of MAs were prepared simultaneously from a given protocol, and the types of MAs prepared changed depending on the detailed protocol under a given set of final conditions. These

are symptomatic of a nonergodic system,[38-39] which is unable to reach its lowest free energy state due to the slow kinetics of chain exchange. Nonergodicity should not be surprising for block copolymer MAs in general,[9,23] and for block copolymer MAs containing carboxyl and amino complexed domains in particular.[15]

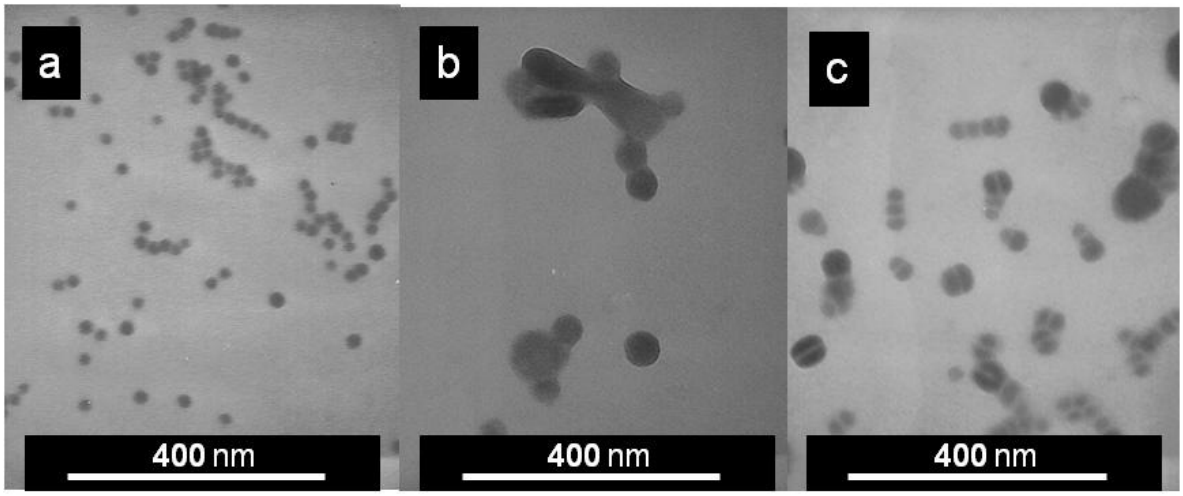

Figure 3.11. TEM images of MAs aspirated from THF/2-propanol with $f_{\mathrm{Pr}o} =$ 95% at 70 °C (**a)**, the same system after addition (-)-sparteine (*r* = 0.20) and heated at 70 °C (**b**) and THF/(-)-sparteine/2-propanol with *r* = 0.20 and $f_{\mathrm{Pr}o} =$ 95%. The staining agent used was OsO_4.

3.4.8 Aggregate Structure

Four sets of experiments were used to probe the location of the polymer blocks within the hamburger and striped cylinder structures. In the first set, homopolymer solubility was used to model individual block solubility, and to deduce their separate locations. It was determined that 54 vol% of 1-propanol and 50 vol% of 2-propanol were required to induce the phase separation of the $PCEMA_{200}$ homopolymer. Then it was found that both $PSGMA_{70}$ and $PtBA_{100}$ homopolymers were soluble in both 1- and 2-propanol. However, upon the

addition of a small amount of (-)-sparteine (11 mol%), the $PSGMA_{70}$ homopolymer was found to phase separate from THF with neither 1- or 2-propanol present. Thus in this system, only PtBA was solubilized, and should form the corona, while PCEMA and PSGMA were insoluble and should form the new phases.

In the second set of experiments, we used ^1H NMR to learn about aggregate structure. Solution ^1H NMR allows us to probe the structure of the triblock copolymer, by observing the differences in peak intensities The peak intensities will change when you change the solvation conditions of the individual blocks of the copolymer.

The ^1H NMR plots in Figure 3.12 shows the ^1H NMR spectra of the polymer in various solvated conditions after heating for 2 days at 70 ^oC. The addition of (-)-sparteine appears to cause the collapse of the PSGMA block, while all the other peaks remain unchanged (blue spectrum). The subsequent addition of the isopropanol-d_8 appears to cause the collapse of all the characteristic polymer peaks (indicative of aggregate formation), although there appears to be a significant amount of remaining PtBA, and a small amount of the PCEMA peaks (red spectrum).

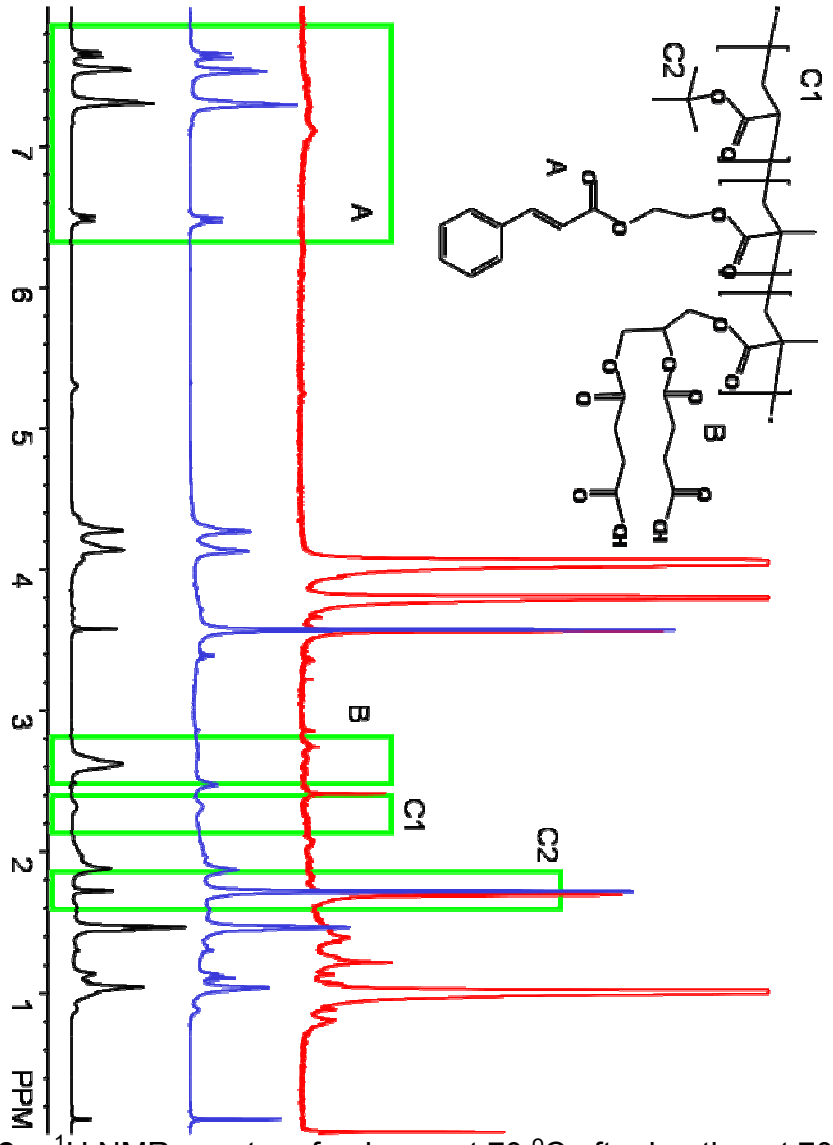

Figure 3.12. ^{1}H NMR spectra of polymer at 70 ^{o}C after heating at 70 ^{o}C for 2 days: Black spectrum – ^{1}H NMR in THF-d_8, Blue spectrum – ^{1}H NMR in THF-d_8/(-)-sparteine with r = 0.50, Red spectrum – in THF-d_8/(-)-sparteine/isopropanol-d_8 with r = 0.50 and $f_{\mathrm{Pr}o-D} = 95\%$.

To quantify the changes seen in Figure 3.12, we determined the intensity of some characteristic PCEMA peaks between 7.22 and 7.40 ppm in a solution of the copolymer in THF-d_8 relative to an impurity in the solvent THF-d_8 at 3.58 ppm. This relative peak intensity was given the symbol I^0_{RCEMA}. Similarly, we determined the relative intensity I^0_{RSGMA} for PSGMA peak between 2.51 and 2.78

ppm, and I^0_{RtBA} for a PtBA peak between 2.22 and 2.43 ppm. The relative intensities I_{RSGMA}, I_{RCEMA}, and I_{RtBA} were also calculated for each sample. Figure 3.13 plots I_{RSGMA}/I^0_{RSGMA}, I_{RCEMA}/I^0_{RCEMA}, and I_{RtBA}/I^0_{RtBA} as functions of the solvation conditions of these samples, which were analyzed after two days of heating at 70 °C, with the ^{1}H NMR spectra also recorded at 70 °C.

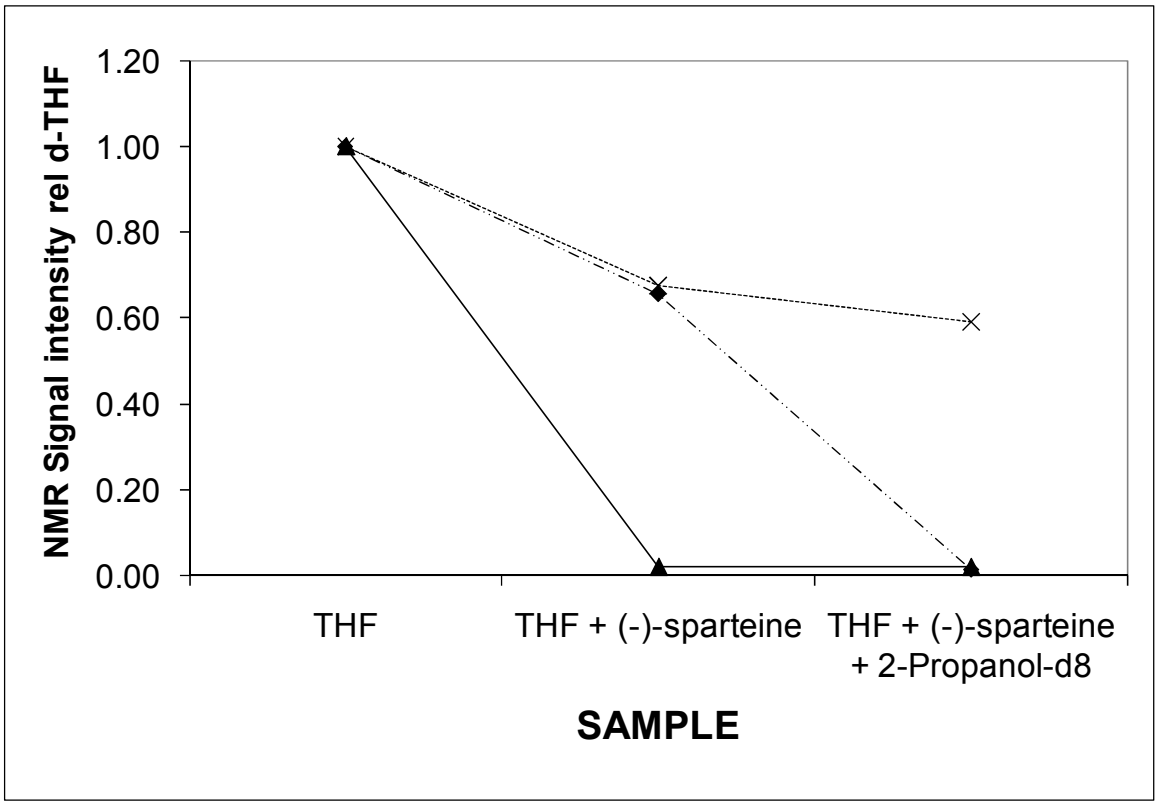

Figure 3.13. Plots of variation in I_{RSGMA}/I^0_{RSGMA} (▲), I_{RCEMA}/I^0_{RCEMA} (♦), and I_{RtBA}/I^0_{RtBA} (X) for PtBA-*b*-PCEMA-*b*-PSGMA as functions of solvation condition, at 70 °C.

The ^{1}H NMR results in Figure 3.13 show three things. First, as expected after addition of (-)-sparteine, *r* = 0.50, there is complete collapse of the PSGMA block of the copolymer. There is no change after subsequent 2-propanol addition ($f_{\mathrm{Pro-}D}$ = 95%). This is presumably due to the complexation of the carboxylate

groups with (-)-sparteine, with no increase after 2-propanol addition (due to stable complex formation). Second, there is partial PCEMA block collapse after the addition of (-)-sparteine and complete collapse after 2-propanol addition. The initial collapse of the PCEMA peak is due to the slowing of the tumbling, caused by the collapse of the PSGMA groups. The subsequent, almost complete, collapse of the PCEMA peak is due to the insolubility of the PCEMA block after the addition of isopropanol-d_8. Third, there is partial collapse of the PtBA block after the addition of (-)-sparteine, and another slight collapse after the 2-propanol addition. Both of these partial collapses are due to the collapse of the other blocks (first the PSGMA block, and then the PCEMA block). The fact that the PtBA signal remains is evidence that the PtBA domain is located on the exterior of the formed structures and also that it remains solvated. ^{1}H NMR data in the hambuger and striped cylinder systems shows that both the PSGMA and PCEMA blocks are collapsed, while the PtBA block remains partially solvated.

In the third set of experiments, selective staining was used to stain the polymer blocks and study the MA structures. First the MAs of the polymer formed in THF with (-)-sparteine were studied. Figure 3.14 shows the polymer solution after addition of (-)-sparteine, r = 0.20. Some of the particles appear to have a light core and a dark shell. Our belief is that the PSGMA block formed the core and the PCEMA block formed the shell because OsO_4 stained the shell selectively.

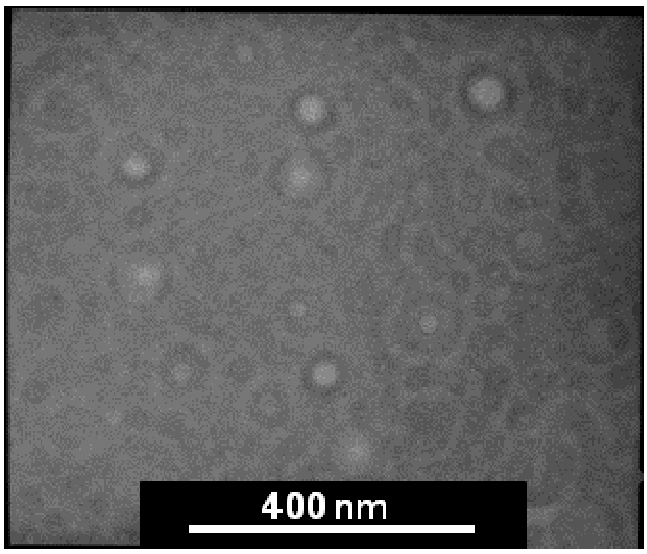

Figure 3.14. TEM image of MAs formed from a polymer solution in THF after the addition of (-)-sparteine *r* = 0.20, stirred for 30 min. Sample was stained with OsO_4.

Next the triblock copolymer aggregates were observed in the THF/1-propanol system with $f_{\mathrm{Pro}} =$ 95%. In this system, we observed the formation of well phase separated spherical domains (Figure 3.15a) of PCEMA that were stained by OsO_4 of 20 +/- 3 nm in size. We also found localized dark patches (carboxylic acid groups from PSGMA) on the surface of what appear to be spherical aggregates (Figure 3.15b) when stained by $UO_2(AcO)_2$. The interior of the dark rim of these spherical aggregates is 23 +/- 3 nm in size, which is comparable to the size of the PCEMA domains shown stained by OsO_4. From the above observations of the spherical MAs in the THF/1-Propanol system, the PCEMA block is located at the core, while the PSGMA block is positioned on the surface. The PtBA block is also presumably found on the surface of these aggregates.

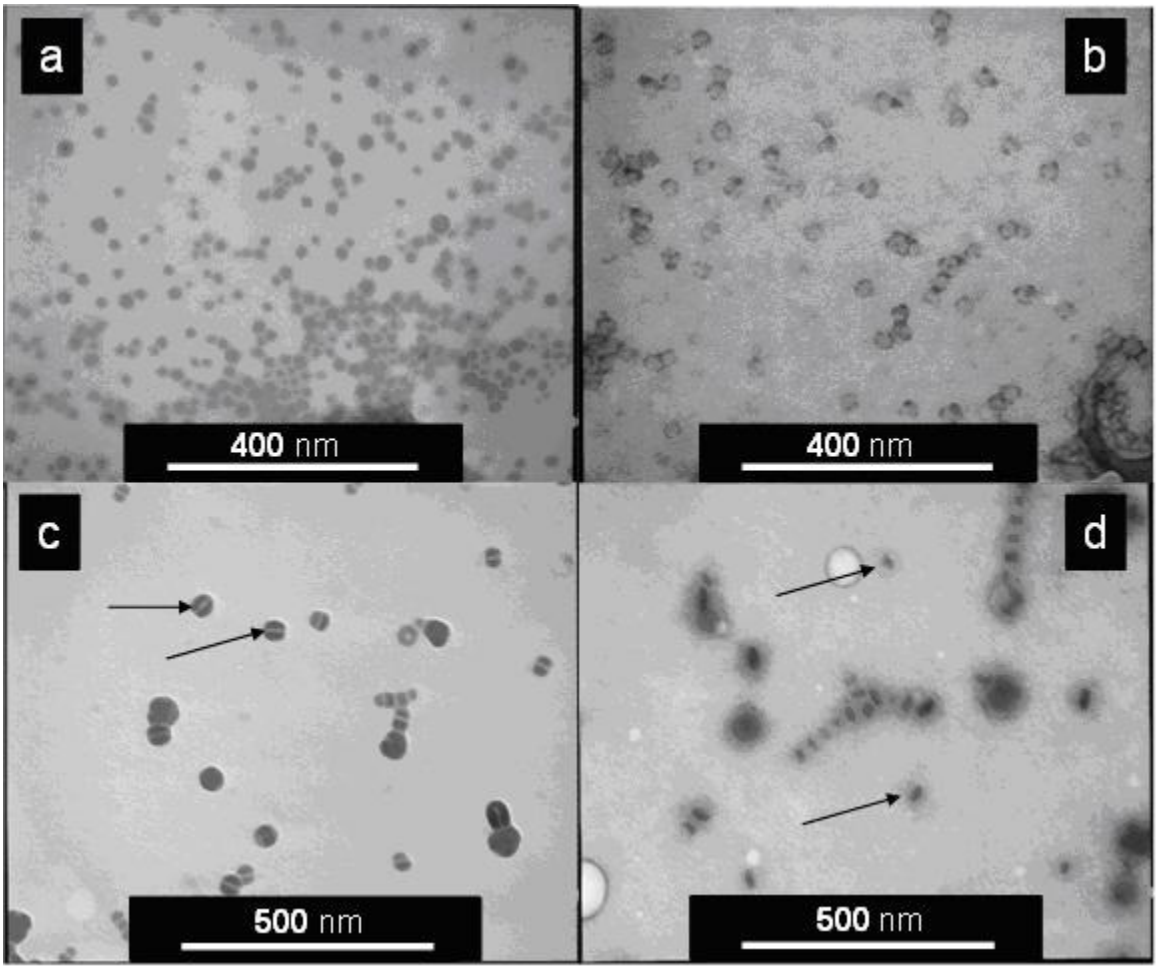

Figure 3.15. TEM images of MAs aspirated from THF/1-propanol with $f_{\mathrm{Pro}} = 95\%$: stained by OsO_4 (**a**), stained by $UO_2(AcO)_2$ (**b**). MAs prepared from THF/(-)-sparteine/1-propanol with $r = 0.20$ and $f_{\mathrm{Pro}} = 95\%$: stained by OsO_4 (**c**), and stained by $UO_2(AcO)_2$ (**d**).

MAs formed in THF/(-)-sparteine/1-propanol with $r = 0.20$ and $f_{\mathrm{Pro}} = 95\%$ were observed to form the hamburger-type aggregates (Figure 3.15c, d). In Figure 3.15c we observe dark areas, which are PCEMA domains stained by OsO_4, and appear to be separated from each other by significantly lighter areas (which correspond to PSGMA domains). The inverse is observed in Figure 3.15d, where the PSGMA domains stained by $UO_2(AcO)_2$ appear dark while the intervening PCEMA domains appear lighter. The arrows in Figures 3.15c and d

highlight this contrast. In Figure 3.15c some of the particles have two dark domains sandwiching one light domain, while in Figure 3.15d, there appear to be individual dark domains, surrounded by two domains of lighter material (highlighted by arrows in Figure 3.15d). This means that the PSGMA (carboxylic acid rich $UO_2(AcO)_2$ stained) domains are localized at the center of the hamburger MAs (corresponding to the filling), while the PCEMA domains are localized at the outer part of the hamburger MAs (representing the bun). TEM does not show where the PtBA is located (because it is unstained), but it likely coats the outside of the structure, and keep the aggregates dispersed in the solvent (see Scheme 3.4). This makes sense since they are covalently linked to the PCEMA groups and as such must stretch out of the PCEMA domains.

Quantitative analysis of Figure 3.15c yielded a total particle size of 55 +/- 9 nm and an individual PCEMA bun thickness of 15 +/- 2 nm (center to edge) and a width of 30 +/- 4 nm (edge to edge). The thickness of the PSGMA filling was 8 +/- 2 nm. From Figure 3.15d we get a thickness of 10 +/- 2 nm for the PSGMA segments (see Scheme 3.5 for help understanding the details).

We also observed the polymer aggregates in the THF/2-propanol system with $f_{\mathrm{Pr}o} = 95\%$. Similar to the previous system (Figure 3.15a), we observed the formation of cleanly phase-separated spherical MAs (Figure 3.16a) of PCEMA of 20 +/- 3 nm. These compared well with the interior of the aggregates (Figure 3.13b) when stained by $UO_2(AcO)_2$ that were 24 +/- 3 nm. The MAs formed from

THF/(-)-sparteine/2-propanol with *r* = 0.20 and $f_{\mathrm{Pro}} = 95\%$, were striped cylinder type MAs (Figure 3.16c, d). Figure 3.16c shows that the PCEMA phases (stained by OsO_4) of the MAs appear to be adjacent to the light areas, which correspond to the PSGMA domains. Similarly, Figure 3.16d shows the PSGMA phases (stained by $UO_2(AcO)_2$) of the MAs which appear to be close to the light areas, which correspond to the PCEMA domains. This can be seen when looking at the ends of the MAs. For the PCEMA block staining (Figure 3.16c), the MAs end in a dark domain (PCEMA stained by OsO_4). When PSGMA was stained (Figure 3.16d), the structures end in lighter domains (corresponding to the unstained PCEMA domains). The end capping of the cylinders with PCEMA domains is logical because the PtBA chains can coat the end caps (if they are PCEMA but not if they are PSGMA).

Quantitative analysis of Figure 3.16c yields a diameter of 24 +/- 2 nm and a length of 19 +/- 2 nm for the PCEMA domains. The length of the complexed PSGMA domains was 7 +/- 2 nm which was in agreement with 8 +/- 3 nm determined from Figure 3.16c and d, respectively. This is best understood by looking at Scheme 3.4.

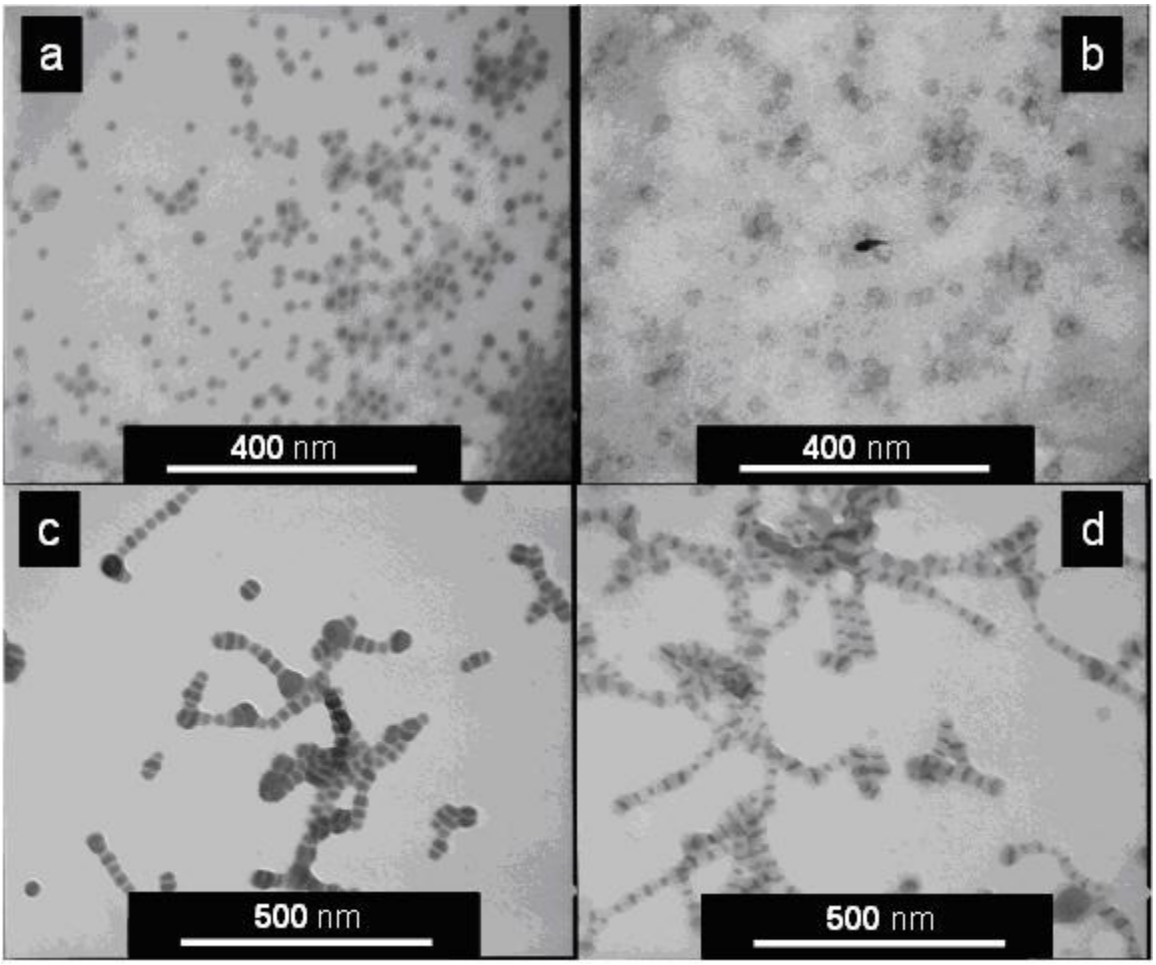

Figure 3.16. TEM images of MAs aspirated from THF/2-propanol with $f_{\mathrm{Pro}} = 95\%$: stained by OsO_4 (**a**), stained by $UO_2(AcO)_2$ (**b**). MAs prepared from THF/(-)-sparteine/2-propanol with $r = 0.20$ and $f_{\mathrm{Pro}} = 95\%$: stained by OsO_4 (**c**), and stained by $UO_2(AcO)_2$ (**d**).

In the final set of experiments, AFM was used to study the MAs. The AFM topography images yields information about the complete structure, as opposed to previous techniques, which gave insight about individual blocks.

AFM (Figures 3.17a, b) probed the whole structure of the MAs of the PtBA-*b*-PCEMA-*b*-PSGMA produced in THF/(-)-sparteine/1- or 2-propanol systems. AFM also shows that there is a slight hourglass (grooves) structure to

the aggregates. The grooves in the structure were seen in both the 1- and 2-propanol systems, with both the hamburger and striped cylinder structures. These grooves occurred because the PtBA was not grafted to the surfaces of the PSGMA segments of the structures.

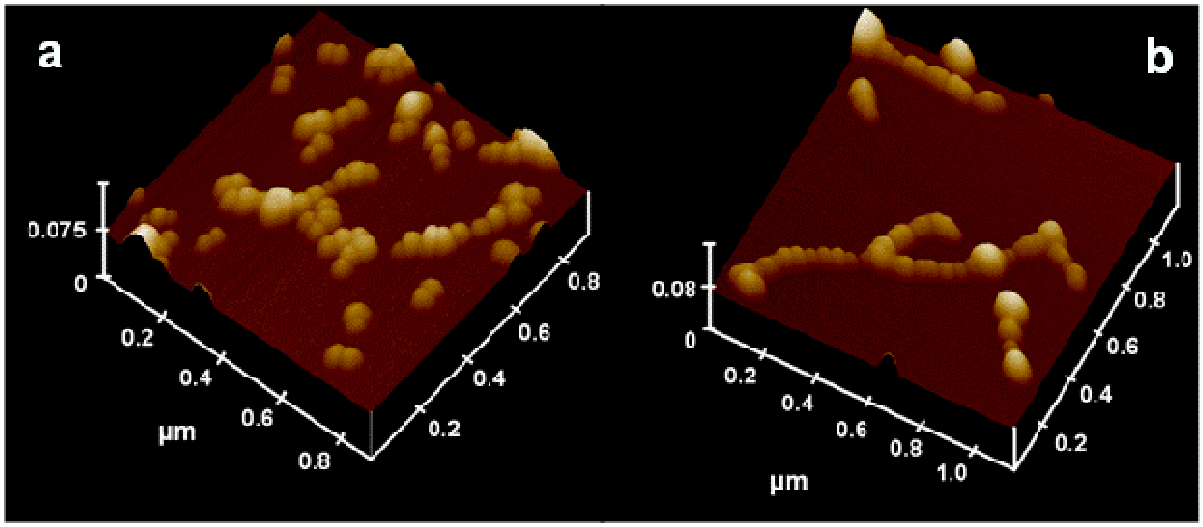

Figure 3.17. AFM height images of MAs aspirated on freshly cleaved mica surfaces: from THF/(-)-sparteine/1-propanol with r = 0.20 and f_{Pro} = 95% (**a**), THF/(-)-sparteine/2-propanol with r = 0.20 and f_{Pro} = 95% (**b**).

The hamburgers seem to become flattened significantly by spraying while the segmented cylinders do not. Prying open the cylindrical stubs of the segmented cylinder would require the motion of multiple parts of the cylinder, while prying open a hamburger requires the motion of a single PSGMA domain. The two buns are held together by PSGMA chains, which are soluble in the solvent mixture in which the sample is dispersed. Since there is only 20 mol% of the (-)-sparteine used in the system, some of which may have partitioned into the solvent phase, the hamburgers are loosely held together by an insoluble fraction of the PSGMA chains. Those chains not bound to the (-)-sparteine should be

highly compatible with the solvent phase (since they are soluble in it). Thus, the complexed PSGMA domains should be highly swollen and the phases should be loosely bound together.

A quantitative analysis of the striped cylinders in Figure 3.17b yielded PtBA/PCEMA height 31 +/- 8 nm (Figure 3.17b). This compared favorably with the TEM diameter of 24 +/- 2 nm for the PCEMA stubs. This confirmed that we have in fact prepared segmented cylinders as the vertical AFM diameter was comparable to the horizontal TEM diameter.

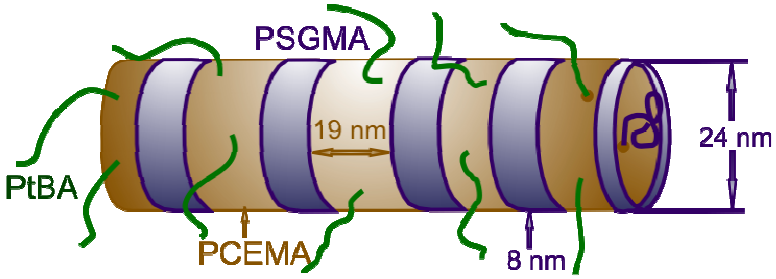

Scheme 3.4. Schematic representation of chain packing in striped cylinder MAs.

The quantitative analysis of the hamburger particles in Figure 3.17a gave a height of the bun of 18 +/- 7 nm. This was much smaller than the TEM diameter of 55 +/- 9 nm for the whole hamburger particle, or even 30 +/- 4 nm for the PCEMA domain in half of the particle. As will be shown later, the two halves of the hamburger particles were treated and separated to yield Janus particles and the TEM analysis of the Janus particles indicated a hemispherical shape. This suggests that the buns were flattened or lay slanted on the silicon wafers, after spraying for AFM from solution.

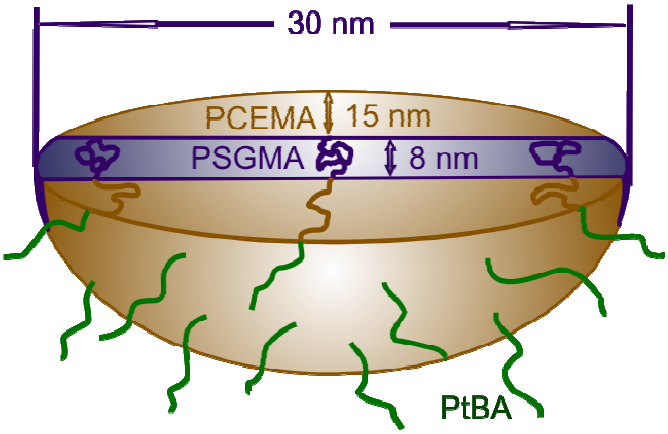

Scheme 3.5. Schematic representation of chain packing in the hamburger-type MAs.

Schemes 3.4 and 3.5 illustrate our current understanding of structure of the hamburger particles. The PSGMA has complexed with the chiral amine, (-)-sparteine, and collapsed to form the core of our structure. The PCEMA block segregates out, to form the shell around these cores. Meanwhile, the PtBA chains remain solubilized and serve to stabilize the structures.

The ratio of the root-mean-square end-to-end distance of the PCEMA chains in a theta solvent, *p*-xylene, calculated for random flight chains, and the characteristic ratio C_∞ was 12.8.[40] Using this the unperturbed root-mean-square end-to-end distance R_n of 10.9 nm was calculated for the PCEMA block with 195 repeat units. Thus the PCEMA chains should be stretched somewhat at the center of the buns, and more coiled near the edge of the buns as illustrated in Scheme 3.5 (as 15 nm is larger than 10.9 nm while near the edge the PCEMA phase thickness is considerably less).

The C_∞ value for PSGMA is unknown. Based on the bulkiness of the pendant group of SGMA, the C_∞ value should be fairly large.[41] Assuming it was close to the 12.8 value for PCEMA (which also has a fairly bulky pendant group), we calculated a R_n value of 8.4 for the PSGMA block of 120 units. This value compares well with the thickness determined experimentally for the PSGMA filling of the hamburgers or the length of the PSGMA segments in the striped cylinders. Therefore, the PSGMA chains should not be stretched significantly in these structures as illustrated in Schemes 3.4 and 3.5.

3.4.6 Aggregate Formation Process

The formation of hamburgers and segmented cylinders was observed by analyzing the TEM samples sprayed at different times after 1- or 2-propanol addition to the polymer solution containing (-)-sparteine. Figure 3.18 compares TEM images of samples sprayed from THF/(-)-sparteine/1-propanol with *r* = 0.20 and $f_{\mathrm{Pr}o} = 95\%$. Initially, after aggregate formation (Figure 3.18a) the MAs did not appear to be well defined. After they were annealed for a short time at 70 ^{o}C, the block segregation in the MAs appeared to become more distinct (Figures 3.18b-d). The elevated temperature provided mobility, which was a key component for the phase separation of the MAs. The hamburger-type and striped cylinder morphologies did not appear to change but the phase segregation merely became more distinct after the initial observation time period.

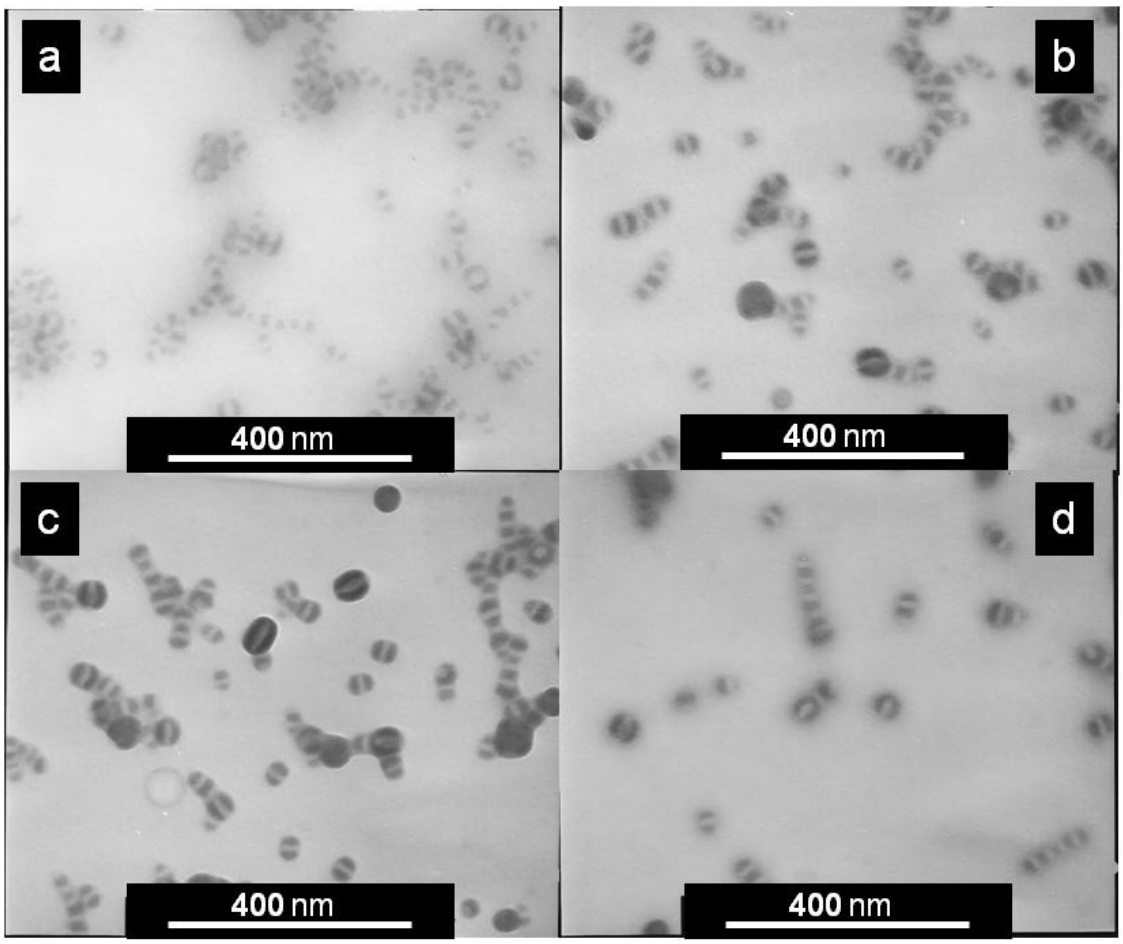

Figure 3.18. TEM images of MAs aspirated from THF/(-)-sparteine/1-propanol with r = 0.20 and $f_{\mathrm{Pro}} =$ 95%: initially after formation (**a)**, heated for one hour at 70 ^{o}C (**b)**, heated for eight hours at 70 ^{o}C **(c)** and finally heated for 18 hours at 70 ^{o}C **(d)**. Samples stained by OsO_4.

In a similar manner to the 1-propanol case, the 2-propanol MAs also did not appear well defined initially after aggregate formation (Figure 3.19a), and proceeded to become more distinct as time progressed (Figures 3.19b-d). This improvement in clarity is due to the improved phase separation that occurred after annealing at 70 ^{o}C for several hours.

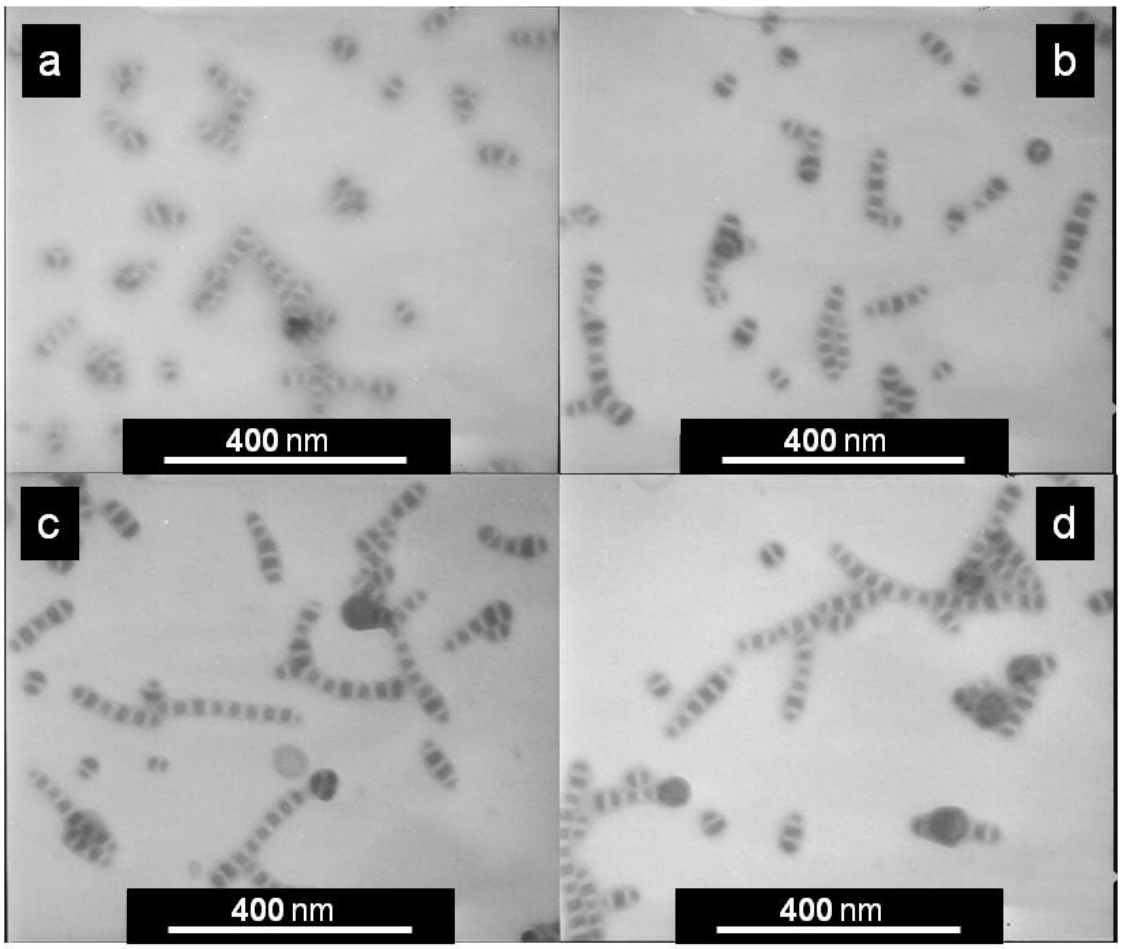

Figure 3.19. TEM images of MAs aspirated from THF/(-)-sparteine/2-propanol with r = 0.20 and $f_{\mathrm{Pro}} = 95\%$: initially after formation (**a)**, heated for one hour at 70 ^{o}C (**b)**, heated for eight hours at 70 ^{o}C **(c)** and finally heated at 18 hours 70 ^{o}C **(d)**. All samples were stained by OsO_4.

As mentioned previously, spherical MAs with PSGMA cores were formed first in THF/(-)-sparteine before the addition of propanol. The addition of 1- or 2-propanol caused the PCEMA block to become insoluble. Normally this would cause the formation of core-shell-corona MAs from a linear ABC triblock copolymer system with insoluble B and C blocks. The interesting hamburger and segmented cylinder MAs were formed because the PSGMA block was insoluble in the solvent system only when complexed with (-)-sparteine. Despite the

collapse of this block, the complexed PSGMA still contains a significant amount of solvent, and the interfacial tension between the complexed PSGMA block and solvent phase should therefore be low, perhaps due to incomplete complexation of the PSGMA block. The favorable interaction between the PSGMA phase and the solvent phase was the reason that the MAs formed hamburger-like structures rather than the traditional spherical MAs with a PSGMA core, PCEMA shell and PtBA corona.

The segment cylinders were formed by the fusion of multiple hamburgers. The fusion of these hamburgers is possible because the PtBA block was relatively short and unable to fully shield the PCEMA buns of the hamburgers from each other. When two hamburgers approached each other, a fluctuation in the concentration of PtBA chains may lead to the exposure of PCEMA bun surfaces which would lead to the fusion of the two hamburgers. The repeat of this process would lead to the "polymerization" of the hamburgers into segmented cylinders.[23]

3.4.10 Hamburger MAs as Precursors for Janus Particles

If the chains were packed as what were depicted in Scheme 3.5, the hamburger-like aggregates may be broken apart to yield Janus particles. The buns of the hamburger particles should be Janus particles, with the flat side bearing grafted PSGMA chains and the convex side bearing the grafted PtBA chains. To demonstrate this, one set of these hamburger-type aggregates (THF/(-)-sparteine/1-propanol with r = 0.20 and $f_{\mathrm{Pr}o} =$ 95%) was treated to

photocrosslink the PCEMA structure. In order to remove (-)-sparteine, we dialyzed the crosslinked hamburgers against acidic methanol solution and DMF. The hamburgers were eventually separated with the aid of ultrasonication. Figure 3.20 shows TEM and AFM images of the separated buns.

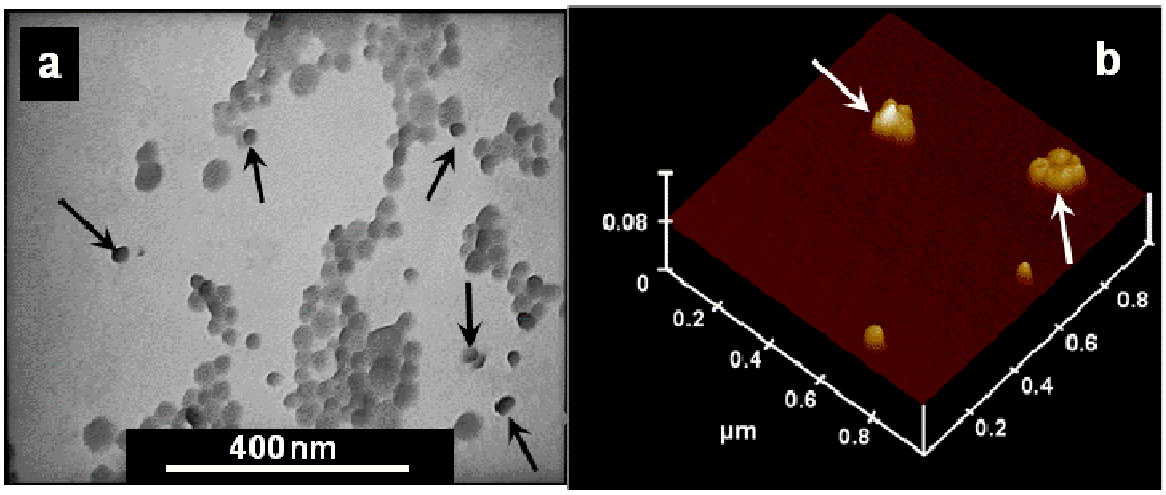

Figure 3.20. Janus particles made from hamburger MAs: TEM image of Janus particles stained by RuO_4 for 30 min **(a)**, and AFM height image of the Janus Particles sprayed on freshly cleaved mica **(b)**.

Janus particles were produced by the cleavage of the hamburger-type particles (Figure 3.20a, b). In Figure 3.20a, the dark PCEMA domains appear circular (~30nm), which is similar to the diameter of the individual PCEMA domains from Figure 3.5a. These suggest that the circular objects were probably the hemispherical Janus particles lying flat in the plane of the image. Occasionally we see a few particles (as indicated by arrows) lying sideways (Figure 3.20a) showing their hemispherical shape. Similarly, in the AFM image, a few hemispherical particles (as indicated by the arrows in Figure 3.20b) can be seen.

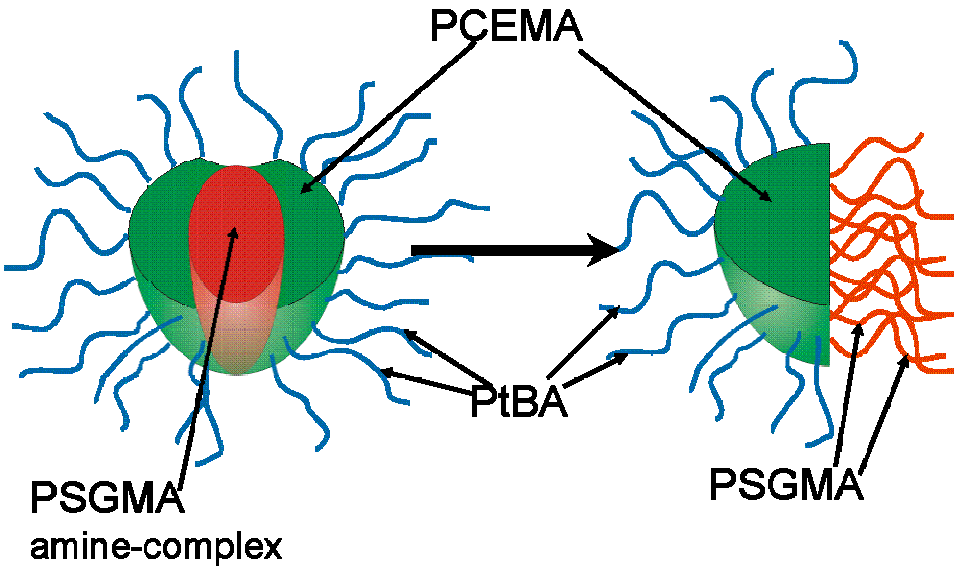

Scheme 3.6. Schematic representation of the transformation of hamburger-type MAs (left) into Janus-type hemi-spherical particles (right).

These structures are interesting, because this method for the use of hamburger-type MAs as precursors for Janus particles is new, and relatively straightforward. This method can potentially be used to make more complicated structures in the future. The carboxylic acid groups of these flattened Janus particles can be used to attach to a variety of substituents such as functionalized surfaces or vesicles.

3.5 Conclusions

The triblock copolymer PtBA-*b*-PCEMA-*b*-PSGMA has been synthesized and characterized. All blocks of the copolymer were found to be soluble in THF. The diamine (-)-sparteine was complexed with the carboxyl groups of the PSGMA block and this complexation caused the PSGMA block to become insoluble. The addition of 95% vol% of 1- or 2-propanol causes the PCEMA block to become

insoluble as well. The polymer formed hamburger-type MAs and striped cylinders if it was first complexed with (-)-sparteine in THF and then made to aggregate by the addition of either 1- or 2-propanol. In the hamburgers, the complexed PSGMA block formed the 'filling', while the PCEMA block formed the 'buns' and the hamburgers were dispersed in the solvent mixture by the soluble PtBA block which was grafted onto the surface of the 'buns'. The main body of the cylinders was made from stacking alternating PCEMA and complexed PSGMA segments with the PtBA chains grafted onto the PCEMA segments. TEM, AFM and solubility tests were used to support these structural assignments. More interestingly, we were able to separate the hamburgers into two halves after crosslinking the PCEMA domain and removing (-)-sparteine from the system by dialysis. These halves of the hamburgers were Janus particles with PSGMA chains on one face, and PtBA chains on the other face of the buns. These Janus particles should have application as dispersant agents for Pickering emulsions.[42-43]

3.6 References

1. Bronich, T.; Kabanov, A.; Kabanov, V.; Yu, K.; Eisenberg, A. *Macromolecules.* **1997,** *30*, 3519-3525.

2. Lazzari, M.; Liu, G.; Lecommandoux, S. *Block Copolymers in Nanoscience*. Wiley-VCH: Weinheim, Germany, 2006.

3. Zhang, L.; Eisenberg, A. *Science* **1995,** *268*, 1728-1731.

4. Ding, J.; Liu, G.; Yang, M. *Polymer* **1997,** *38*, 5497-5501.

5. Ding, J.; Liu, G. *Macromolecules* **1997,** *30*, 655-657.

6. Discher, D.; Eisenberg, A. *Science* **2002,** *297*, 967-973.

7. Liu, G. *Adv. Polym. Sci.* **2008,** *220*, 29-64.

8. Raez, J.; Manners, I.; Winnik, M. *J. Am. Chem. Soc.* **2002,** *124*, 10381-10395.

9. Njikang, G.; Han, D. H.; Wang, J.; Liu, G. J. *Macromolecules* **2008,** *41*, 9727-9735.

10. Price, C. *Pure Appl. Chem.* **1983,** *55*, 1563-1572.

11. Tao, J.; Stewart, S.; Liu, G.; Yang, M. *Macromolecules* **1997,** *30*, 2738-2745.

12. Jain, S.; Bates, F. *Science* **2003,** *300*, 460-464.

13. Chen, Z.; Cui, H.; Hales, K.; Li, Z.; Qi, K.; Pochan, D.; Wooley, K. *J. Am. Chem. Soc.* **2005,** *127*, 8592-8593.

14. Zhu, J.; Liao, Y.; Jiang, W. *Langmuir* **2004,** *20*, 3809-3812.

15. Cui, H.; Chen, Z.; Zhong, S.; Wooley, K.; Pochan, D. *Science* **2007,** *317*, 647-650.

16. Li, Z.; Kesselman, E.; Talmon, Y.; Hillmyer, M.; Lodge, T. *Science* **2004,** *306*, 98-101.

17. Kabanov, A.; Bronich, T.; Kabanov, V.; Yu, K.; Eisenberg A. *J. Am. Chem. Soc.* **1998,** *120,* 9941-9942.

18. Bronich, T.; Popov, A.; Eisenberg, A.; Kabanov, V.; Kabanov, A. *Langmuir* **2000,** *16,* 481-489.

19. Harada, A.; Kataoka, K. *Macromol. Symp.* **2001,** *172*, 1–9.

20. Solomatin, S.; Bronich, T.; Bargar, T.; Eisenberg, A.; Kabanov, V. Kabanov, A. *Langmuir* **2003,** *19,* 8069-8076.

21. Zheng, R.; Liu, G.; Yan, X. *J. Am. Chem. Soc.* **2005,** *127*, 15358-15359.

22. Hu, J.; Njikang, G.; Liu, G. *Macromolecules* **2008,** *41*, 7993-7999.

23. Li, Z.; Hillmyer, M.; Lodge, T. *Langmuir* **2006,** *22*, 9409-9417.

24. Li, Z.; Hillmyer, M.; Lodge, T. *Macromolecules* **2006,** *39*, 765-771.

25. Honggang, C.; Chen, Z.; Zhong, S.; Wooley, K.; Pochan, D. *Science* **2007,** *317*, 647-650.

26. Li, Z.; Chen, Z.; Honggang, C.; Hales, K.; Qi, K.; Wooley, K.; Pochan, D. *Langmuir* **2005,** *21*, 7533-7539.

27. Li, Z.; Chen, Z.; Honggang, C.; Hales, K.; Qi, K.; Wooley, K.; Pochan, D. *Langmuir* **2007,** *23*, 4689-4694.

28. Chen, Z.; Honggang, C.; Hales, K.; Li, Z.; Qi, K.; Pochan, D.; Wooley, K. *J. Am. Chem. Society* **2005,** *127*, 8592-8593.

29. Ma, J.; Li, X.; Tang, P.; Yang, Y. *J. Phys. Chem. B* **2007,** *111*, 1552-1558.

30. Walther, A.; Matussek, K.; Muller, A. *ACS Nano* **2008,** *2*, 1167-1178.

31. Walther, A.; Dreschsler, M.; Rosenfeldt, S.; Harnau, L.; Ballauff, M.; Abetz, V.; Muller, A. *J. Am. Chem. Soc.* **2009,** *131*, 4720-4728.

32. Li, J.; Ness, J.; Cheung, W. *J. Appl. Polym. Sci.* **1996,** *59*, 1733-1740.

33. Liu, F.; Liu, G. *Macromolecules* **2001,** *34*, 1302-1307.

34. Yan, X.; Liu, G.; Li, H. *Langmuir* **2004,** *20*, 4677-83.

35. WinNuts 1D Version – 19990713.

36. T. W. Greene and P. G. M. Wuts, *Protective Groups in Organic Synthesis*, 3rd ed., Wiley & Sons, New York, **1999**.

37. Zhang, L.; Eisenberg, A. *Polym. Adv. Tech.* **1998,** *9*, 677-699.

38. S. Jain and F. S. Bates, *Science* **2003**, 300, 460.

39. S. Jain and F. S. Bates, *Macromolecules* **2004**, 37, 1511.

40. L. Z. Hong and G. J. Liu, *Macromolecules* Submitted.

41. Z. D. Xu, N. Hadjichristidis, L. J. Fetters and J. W. Mays, *Adv. Polym. Sci.* 1995, **120**, 1.

42. J. W. Hu, G. J. Liu and G. Nijkang, *J. Am. Chem. Soc.* **2008**, 130, 3236.

43. A. D. Dinsmore, M. F. Hsu, M. G. Nikolaides, M. Marquez, A. R. Bausch and D. A. Weitz, *Science* **2002**, 298, 1006.

Chapter 4 – Conclusions

Two triblock copolymers, which produced two different and interesting morphologies, were studied in block selective solvent systems. The first copolymer, PBMA-*b*-PCEMA-*b*-PtBA, self-assembled to produce helical micelles in several solvent mixtures. The second copolymer, PtBA-*b*-PCEMA-*b*-PSGMA, formed hamburger or striped cylinder aggregates, by directed assembly, in THF with (-)-sparteine and 1- or 2-propanol mixtures. The hamburger-like MAs were used as precursors to prepare Janus particles.

Multiple helices were produced by the PBMA-*b*-PCEMA-*b*-PtBA triblock copolymer in dichloromethane (DM)/methanol (MeOH), tetrahydrofuran (THF)/MeOH, and chloroform/MeOH mixtures. DM, THF and chloroform are good solvents for all the blocks of the copolymer, while the solvent composition at which the helical micelles are observed, the PtBA is well solvated, the PCEMA block is collapsed and precipitated from the solvent mixture, while the PBMA block is marginally soluble. This is the first report of the formation of multiple helices as the major product of solution self-assembly. Helical aggregates have been seen before in other block copolymer systems, but they have always been single helices or twisted cylinders. In most cases, the structures have not been well characterized. In our case, TEM, AFM, DLS, and TEM tomography have been used to establish the structure of the helices. The helices were formed mainly to decrease the unfavorable PBMA-to-solvent contact, and were stabilized by the PtBA chains. Due to the reproducible production of these helices in

several solvent mixtures, we believe that this helical structure may be the thermodynamically favoured structure. It remains interesting to examine if this morphology can be reproduced using other analogous triblock copolymers. It may be possible to manipulate this system to form either exclusively double, or triple helices. Other future work may include attempting to fine-tune the conditions in order to produce either entirely right or left-handed helices.

Hamburger-like and striped cylinder MAs were produced by a PtBA-*b*-PCEMA-*b*-PSGMA triblock copolymer in THF, with the addition of (-)-sparteine, a chiral amine (CA) and 1- or 2-propanol. The hamburger-type MAs were then used as precursors to form flattened Janus-type particles by a few simple modification steps. This is the first instance of the use of Hamburger-like or striped cylinder MAs as a precursor for the formation of Janus-type structures. The PtBA-*b*-PCEMA-*b*-PSGMA formed cylindrical MAs in neat 1- or 2-propanol and spherical MAs in mixtures of 1 or 2-propanol and THF. The chiral amine, (-)-sparteine, was used to complex with the carboxylic acid groups of the triblock copolymer in THF which caused the aggregation of the PSGMA block. The addition of 1- or 2-propanol caused the aggregation of the PCEMA block, and led to the formation of hamburger and striped cylinder-like MAs. Similar structures have been seen before, but they have not been extensively characterized. Solubility tests, in addition to TEM, AFM, and ^{1}H NMR experiments were used to establish the structure of the MAs. Our analysis indicated that the PSGMA block complexes with (-)-sparteine to form the core of

these aggregates (hamburger filling), while the PCEMA block collapsed to form the hamburger structure (the bun) around the core, and that the PtBA block remains solubilised, while serving to stabilize the structures. Our belief is that these interesting structures result from amine complexation, along with solvation differences of the polymer blocks. Future work could include trying to reproduce these structures in other solvent systems, and with other complexing agents. It would also be interesting to examine if this morphology can be reproduced using other triblock copolymers. Future work may include producing exclusively hamburger, or striped cylinder-type MAs. It may also be possible to reassemble the Janus-type particles using complexation (amine or other templates). Future studies in this area could include the study of the properties of the Janus particles, including their use to prepare Pickering emulsions.

Appendix A: Polymer Synthesis

PBMA-*b*-PCEMA-*b*-PtBA

PBMA-*b*-PHEMA-TMS-*b*-PtBA prepared by sequential living anionic polymerization in THF at -78 ^{o}C using standard vacuum line techniques. 1,1Diphenyl-3-methylpentyllithium was used as the initiator and lithium chloride was used to decrease the PDI of the resulting polymers. BMA, HEMA-TMS, and tBA were all polymerized for 3 hours. The polymerization was terminated by the addition of several drops of methanol. Stirring the triblock in THF/methanol (75/25) overnight hydrolyzed the TMS groups to yield the PBMA-*b*-PHEMA-*b*-PtBA. The polymer solution was then concentrated and precipitated in hexane.

The HEMA block was then converted to the PCEMA form by reacting with excess (~1.5x) cinnamoyl chloride in dry pyridine at room temperature overnight. The polymer solution was filtered to remove the pyridinium chloride salt and then precipitated on ice to give the PBMA-*b*-PCEMA-*b*-PtBA polymer.

PCEMA-*b*-PtBA

PHEMA-TMS-*b*-PtBA was prepared by sequential anionic polymerization as above. The HEMA group was converted to CEMA via a similar procedure to that above.

PtBA

PtBA was prepared by anionic polymerization as above.

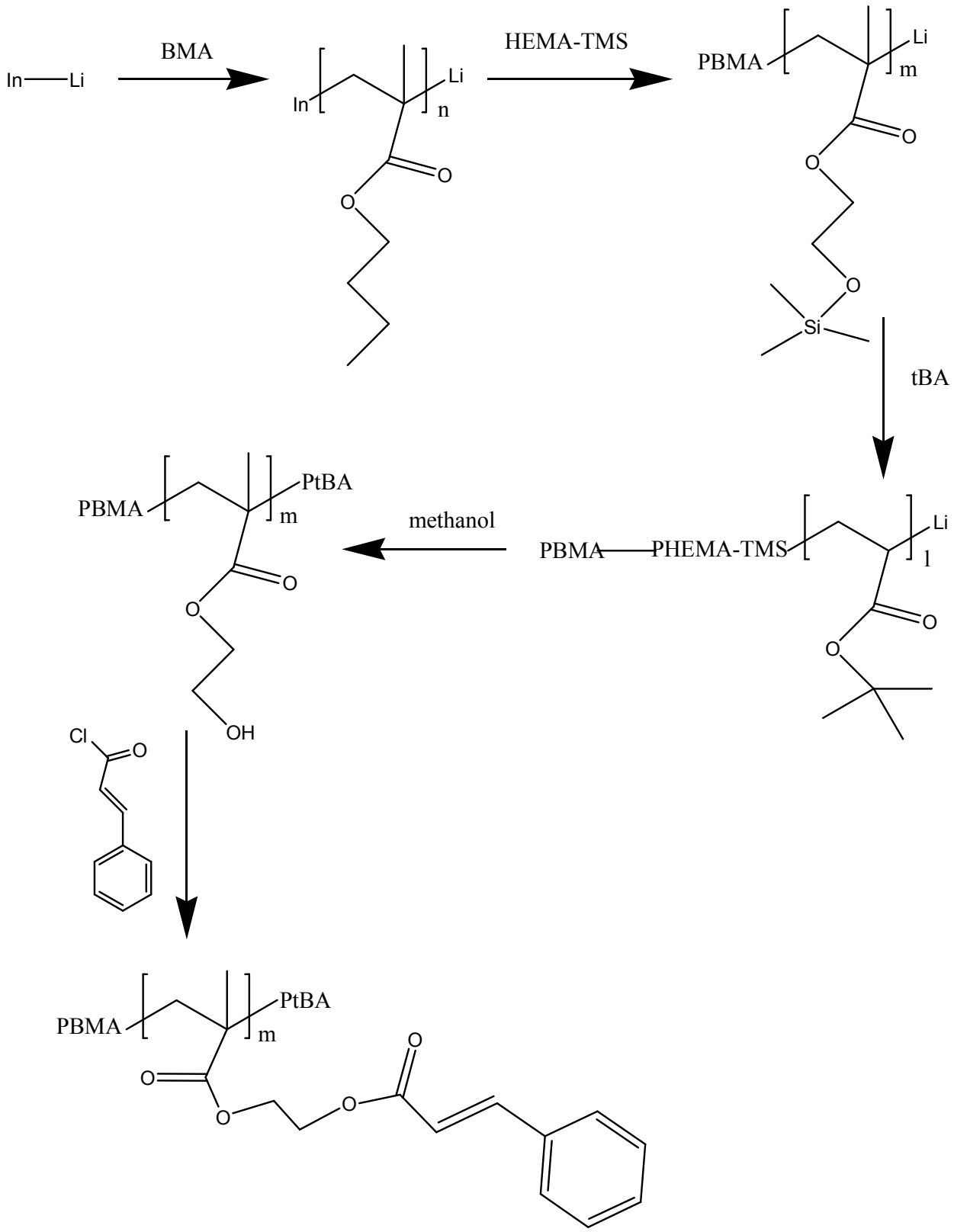

Scheme A.1. Anionic polymerization and other reactions in the synthesis of PBMA-*b*-PCEMA-*b*-PtBA.

PtBA-*b*-PCEMA-*b*-PSGMA

PtBA-*b*-PHEMA-TMS-*b*-PSMA was prepared by sequential anionic polymerization as above. Stirring the triblock in THF/methanol (75/25) overnight hydrolyzed the TMS groups selectively (but not the SMA groups) to yield the PtBA-*b*-PHEMA-*b*-PSMA. The polymer solution was then concentrated and precipitated in hexane.

The HEMA group was converted to CEMA via a similar procedure to that above.

The SMA group was then hydrolyzed in THF with 6M aqueous HCl. The triblock (0.3g) was dissolved in a small amount of THF (20mL). Then 5.0mL of 6M HCl was added and the solution was stirred for 3hours. The solution was then dialyzed (MW cutoff 12-14K) against MeOH (solution change 3 times) to remove the acid and other low molecular weight byproducts. The solution was then concentrated to 10mL and precipitated in diethylether (150mL). The resulting polymer was centrifuged at 3500RPM to recover and dried overnight to yield PtBA-*b*-PHEMA-*b*-PGMA.

The PtBA-*b*-PHEMA-*b*-PGMA, polymer was dissolved in pyridine (5mL) and a 5x molar excess of succinic anhydride was added. The sample was then reacted overnight at room temperature. The polymer was then dialyzed against MeOH overnight (MW cutoff 12-14K) (changed 3 times). The polymer then concentrated to 2mL and precipitated in diethyl ether (100mL). The sample was

then recovered by centrifuge (3500RPM) and then dried overnight under vacuum to yield PtBA-*b*-PHEMA-*b*-PSGMA.

PCEMA

PHEMA-TMS was prepared by anionic polymerization as above. The HEMA group was converted to CEMA via a similar procedure to that above.

PSGMA

PHEMA-TMS was prepared by anionic polymerization as above. The SMA group was converted to SGMA via a similar procedure to that above.

PBMA

PBMA was prepared by anionic polymerization as above.